DIPARTIMENTO DI SANITA' PUBBLICA E MALATTIE INFETTIVE

DOTTORATO DI RICERCA IN MALATTIE INFETTIVE, MICROBIOLOGIA E SANITA' PUBBLICA

XXIX CICLO

Study of the role of the CCL2/CCR2 axis in HIV-1 infection: molecular mechanisms and potential therapeutic approaches

Coordinatore: Prof. Stefano D'Amelio

Relatore interno:

Prof.ssa Miriam Lichtner

(Sapienza, Università di Roma)

Relatore esterno:

Dott.ssa Laura Fantuzzi

(Istituto Superiore di Sanità)

Candidato: Daniela Angela Covino

Anno accademico 2015/2016

Chapter 1

HIV-1 infection: an overview

1.1 Immunopathogenesis of HIV-1 infection

The human immunodeficiency virus type 1 (HIV-1), discovered in the early 1980s, is responsible for the pandemics of the acquired immunodeficiency syndrome (AIDS), representing a public health concern worldwide. The World Health Organization (WHO) estimated that more than 37 million people were living with HIV-1 infection in 2015. Many of these people live in developing countries with sub-Saharan Africa bearing the maximal burden of 25.8 million infected cases. The introduction of highly active antiretroviral therapy (HAART) for the chronic suppression of HIV-1 replication in the mid-1990s represented the major advancement in AIDS research, resulting in a drastic reduction of morbidity and mortality. About 18 million people living with HIV-1 were on antiretroviral treatment in 2015 (http://www.unaids.org/en/resources/fact-sheet). HAART can control HIV-1 replication, reducing plasma viremia below the limit of detection of clinical assays, thus prolonging live, decreasing the risk of transmission and preventing the development of AIDS. However, it is not curative and requires life-long treatment since viremia rebound rapidly following therapy interruption. The operational and logistical challenges involved in delivering lifelong treatment are daunting and the economic costs might be unsustainable. Furthermore, drug resistance and toxicities, as well as persistent immune activation and dysfunctions highlight the urgency of controlling the virus in the absence of HAART or finding a cure (1).

HIV-1 infects cells through the interaction of its gp120 envelope protein with the primary receptor CD4 and a chemokine co-receptor, usually CCR5 in the initial phase of

infection, or CXCR4 in later stages of disease, though often in association with CCR5. This requirement restricts the spectrum of cells that can be infected by HIV-1 essentially to $CD4^+$ T lymphocytes and myeloid cells [monocytes/macrophages, microglia, and myeloid dendritic cells (DCs)] **(Figure 1)**, with the exception of astrocytes that are infected in a CD4/chemokine co-receptor independent manner. Following fusion of the viral envelope with cell membrane, genomic viral RNA enters the target cell and is converted into DNA by reverse transcriptase (RT). The reverse transcription process is initiated in the cytoplasm within the pre-integration complex (PIC) and it is completed in the nucleus where the viral integrase (IN) promotes the integration of linear forms of DNA into the host chromosomes as provirus. Once integrated, the virus remains indefinitely associated with the host cells for their entire life and, depending on the expression of both viral and host cell factors, it can remain silent or become actively transcribed thus producing various forms of mRNA. These latter are translated into viral proteins, that are assembled at the plasma membrane with full length genomic RNAs and released as immature, non-infectious viral particles. Subsequently, the viral protease (PR) catalyses a series of proteolytic cleavages leading to a structural rearrangement of the viral particle into a mature form that is competent to infect a new cell (2).

HIV-1 transmission occurs following the direct exposition to infected blood or secretions in the presence of skin damage or mucosal abrasions (3). In the case of infection acquired through heterosexual and homosexual intercourse, which are among the most common routes of HIV-1 transmission, resident memory T lymphocytes in the vaginal or rectal mucosa are the first cells being infected. At this early point of infection, innate immune activation may contribute to antiviral responses by recruiting granulocytes, macrophages and lymphocytes, thus enlarging the number of cellular targets for infection. Infected cells or free virus then reach the draining lymph nodes, where activated

$CD4^+CCR5^+$ T lymphocytes are encountered and represent targets for further infection. In this process, virus particles are bound by DCs and B lymphocytes, thereby augmenting viral spread by carrying virus to activated T cells (4). In this way the virus can replicate and disseminate to secondary lymphoid tissue throughout the organism, particularly to gut-associated lymphoid tissue (GALT), where activated $CD4^+CCR5^+$ effector memory T cells are present at high levels.

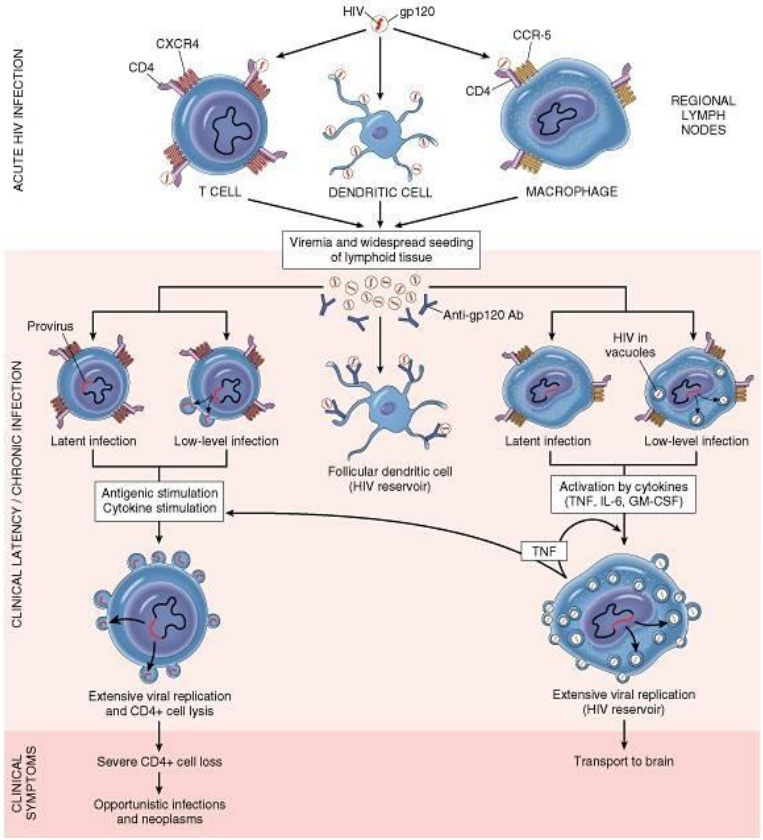

Figure 1. Representation of immune cell targets of HIV-1 and of clinical stages of infection (http://tube.medchrome.com/2010/11/pathogenesis-of-aids-and-replication-of.html).

After 10-12 days from infection, viral RNA is detectable in the blood by Real-time PCR assay. The onset of viremia in plasma is a critical time point of HIV-1 infection because it indicates that infected individual has acquired the potential of transmitting the infection and provides the first chance to diagnose the infection in the blood (3). Then, plasma viremia rapidly increases reaching a peak after 21-28 days from infection, together with depressed peripheral $CD4^+$ T cell numbers. This indicates the "acute HIV-1

infection", during which an estimated 40% to 90% of patients may develop symptoms of acute retroviral syndrome, including influenza-like illness with fever, sore throat, lymphadenopathy and exanthema (https://aidsinfo.nih.gov/guidelines/html/1/adult-and-adolescent-arv-guidelines/20/acute-and-recent--early--hiv-infection). The acute infection is characterized by a selective and dramatic depletion of T cells. When specific immune responses are activated, the number of circulating T cells subsequently return close to normal, whereas the loss of $CD4^+$ T cell number in mucosal tissues is largely irreversible, contributing to the failure of immune defenses and the progression of disease. In particular, the most important effect on T cell homeostasis happens very early in the GALT, which has a massive depletion of activated $CD4^+$ T cells with a minimum recovery after HAART. As a consequence, a profound immunological damage to the gastrointestinal tract occurs followed by local and systemic inflammation (4). Several factors associated with innate and acquired antiviral immunity can influence viral replication and the establishment of a viral set point during acute infection. In particular, $CD8^+$ cytotoxic T lymphocyte (CTL) activity seems to be central in the initial control of virus replication, before the appearance of anti-HIV-1 antibodies (Abs). Neutralizing Abs arise roughly 3 months after transmission, and the period in which Abs are not yet detectable is referred as the serological "window period". Abs specifically bind to HIV-1 antigens, determining the prevention of cell infection or favoring the elimination of infected cells by Antibody Dependent Cellular Cytotoxicity (ADCC) mediated by T lymphocytes and natural killer (NK) cells (3). However, these Abs are characterized by a high frequency of somatic mutations that often take years to develop. Broadly neutralizing Abs do not usually provide benefit to the patient because of the development of viral escape mutations (5). Since the host generates humoral and cellular immune responses that partly control viral replication, the high levels of viremia are normally short-lived. Few weeks after the onset of acute

infection, the viral load decreases reaching a stable viral set point, and most of the infected individuals enter into an "asymptomatic period" characterized by a drop of viremia and absence of symptoms. During this asymptomatic phase, HIV-1 continuously replicates in the body compartments, counteracting antiviral immunity and inducing a state of chronic systemic inflammation. Despite the infection is largely asymptomatic for extended time periods in the majority of patients, a progressive depletion of $CD4^+$ T cells occurs because of increased mortality and reduced replenishment.

Another importan factor is the high viral mutation rate and alteration in cellular tropism, resulting in progression from a pool of CCR5-tropic to dual or rarely dominanlty CXCR4 tropic strains with increased virulence and broader cellular tropism (4).

The continuous viral replication and the chronic activation of immune cells induce the destruction of the lymphoid tissue architecture, favoring HIV-1 spread within local, regional and whole lymphoid environment, resulting in thimic dysfunction, transforming growth factor-β-dependent fibrosis and alterations in lymphoid follicle architecture. HIV-1 infection also profoundly affects blood and tissue B lymphocytes by inducing early class switching in polyclonal B cells, massive B cell apoptosis and loss of germinal centers in lymphoid tissues (4).

The duration of the asymptomatic phase and the progression of disease depend on the host capacity to contain viral replication and to reconstitute the pool of memory T cells. When the host cannot contain virus, the destruction of the lymphoid system proceeds and $CD4^+$ T cell number continues to drop. As a consequence, this late phase of infection (defined as AIDS) is characterized by frequent opportunistic infections, anemia, lymphopenia, fever, respiratory and gastro-intestinal symptoms with severe reduction of body weight. In the absence of treatment, the mean time from initial infection to AIDS-related death is approximately 11 years (3). In HAART treated patients, the predicted

survival can approach that of the general population (6). As a consequence of the increased life expectancy, several disorders that typically affect the aged population now appear in relatively young HIV-1 patients. Chronic inflammation and activation of the immune system observed typically in elderly people contribute to the onset of age associated diseases, defined as 'inflammaging'. The survival of treated individuals depends on several personal characteristics and on the time of therapy initiation. Generally, major causes of morbidity and mortality for these patients are cardiovascular and neurological diseases, renal insufficiency and cancers. The factors underlying the heightened risk of non-AIDS-related diseases are complex and not completely understood. Factors contributing to their development are timing of HAART initiation, differences in drug combinations, co-infections, nutritional status, lifestyle risks, toxicity of antiretroviral treatments and chronic inflammation (7).

1.2 HIV-1 infection of Macrophages

Macrophages are myeloid lineage cells of the innate immune system that are required for multiple functions, from tissue homeostasis and repair to sensing and elimination of microbial pathogens and tumor cells. Based on their anatomical localization and functional phenotype, macrophages can be distinguished in several types (e.g., microglia in the brain, alveolar macrophages in the lung, Kupffer cells in the liver, osteoclasts in the bone) with different life spans. For example, inflammatory macrophages derived from circulating monocytes die after a few days, whereas microglia or alveolar macrophages can live from several weeks up to years (8).

Macrophages play an important role in innate and adaptive immune responses. They express on their surface specific pattern recognition receptors (PRRs) which bind to pathogen associated molecular patterns (PAMPs). Following this interaction, macrophages

engulf pathogens in an internal cytoplasmatic vescicles (phagosome) which then fuse with the lysosome (phagolysosome), thus leading to pathogen destruction. Macrophages can also act as professional antigen presenting cells (APCs), triggering Ab responses through the presentation of pathogen derived peptides via the MHC-II pathway to $CD4^+$ T cells and cross-presentation to CTLs (9).

Along with $CD4^+$ T lymphocytes, macrophage lineage cells play key roles in HIV-1 pathogenesis throughout the course of infection (10) **(Figure 1)**. Macrophage infection by HIV-1 was first described in the 1980s when four different studies provided evidence that these cells can be infected in multiple tissues, particularly in brain and lung (11-14). Additional studies confirmed these initial observations and revealed infection of tissue macrophages at all stages of disease (15-18). Recently, Honeycutt and colleagues demonstrated in a mouse model that HIV-1 can infect and reproduce in macrophages also in the absence of T cells (19). These *in vivo* data are recapitulated *in vitro* by infection of human monocyte-derived macrophages (MDMs) with macrophage-tropic HIV-1 strains. Peculiar features of MDM infection are the high resistance to the viral cytopathic effect and to apoptosis and the long life span even when these cells are exposed to different oxidative stress stimuli (10).

Macrophages contribute to the pathogenesis of HIV-1 infection in several ways. At site of initial infection, resident macrophages are essential to initiate and optimize antiviral responses. However, macrophages can also contribute to the establishment and transmission of infection. These cells can be infected via either cell-free virions or the more efficient cell-to-cell transmission. Furthermore, they can capture and ingest infected $CD4^+$ T cells, and this can lead to efficient macrophage infection (8). Moreover, it was postulated that HIV-1 infected macrophages release virus containing exosomes and microvescices to facilitate and enhance HIV-1 dissemination (8). Interestingly, *in vitro*

infection of MDM leads to the accumulation of infectious particles in vacuolar subcellular structures mostly connected to the plasma membrane, termed virus-containing compartments (VCCs). VCC-associated viruses maintain their infectivity for extended time periods and can be rapidly transferred to contacting $CD4^+$ T cells (20). Finally, viral transmission can also occur when macrophages, similarly to DCs, capture HIV-1 particles, without necessarily resulting in infection, and subsequently transfer them to $CD4^+$ T cells (21).

Macrophage susceptibility to HIV-1 infection is dependent on tissue localization. For example, intestinal macrophages are more resistant to HIV-1 infection than vaginal macrophages (8). The nature, timing, and concentration of microenvironmental stimuli can determine macrophage activation, susceptibility to infection and the type of the elicited immune response. In particular, following exposure to microbial products and cytokines, mononuclear phagocytes can be polarized along the pro-inflammatory (M1) or alternatively activated, anti-inflammatory (M2) pathways. In healthy tissues, M2 activation may represent a default phenotype that serves to maintain a balanced microenvironment in anatomical sites under constant microbial assault. In contrast, M1 macrophages express high levels of classical pro-inflammatory cytokines. In MDM HIV-1 infection, M1 or M2 polarization leads to a restriction of viral replication in comparison to un-polarized cells. In particular, M1 polarization profoundly inhibits HIV-1 replication by decreasing the expression of the primary receptor CD4, increasing the secretion of CCR5-binding chemokines, impairing viral DNA and protein synthesis. M2 polarization shows a less potent, but more durable inhibition of HIV-1 replication, acting at a post-integration step in the virus life cycle (22, 23).

Although $CD4^+$ T cells represent the principal and most studied reservoir for HIV-1, there is accumulating evidence that macrophages can contribute to establish tissue

reservoirs in HIV-1 and simian immunodeficiency virus (SIV) infection (21). In fact, circulating monocytes and tissue macrophages contribute to the initial seeding and establishment of viral infection in anatomical reservoirs, including the brain and the lung. In the central nervous system (CNS), parenchymal microglia as well as meningeal, choroid plexus and perivascular macrophages, express HIV-1 co-receptors and are susceptible to infection. Perivascular macrophages are the major targets of HIV-1 in the brain, and viral DNA can be isolated from these cells throughout infection, indicating that they represent viral reservoirs. In addition, a recent study in SIV-infected rhesus macaques underscores the importance of lung alveolar and interstitial macrophages in local viral infection. Alveolar macrophages are long-life primary viral targets in the lung, whereas interstitial macrophages, which are repeatedly renewed from monocytes, are also infected but die rapidly (24). Alveolar macrophages harbor HIV-1 in untreated viremic patients, suggesting that they may represent important viral reservoirs. Macrophages are widely present also in the GALT. *Ex vivo* analyses of human GALT macrophages revealed that these cells are relatively refractory to HIV-1 infection. However, there is evidence of infection in macrophages proximal to the rectum and from the duodenum, which show increased expression of CCR5 and greater HIV-1 susceptibility compared to colon-resident cells. Moreover, proviral DNA was found in macrophages purified from rectal and ileal tissues. Finally, also urethral macrophages were reported to maintain infection in the face of therapy. Since these data are mostly *in vitro* derived, additional studies are needed to determine whether macrophages can sustain HIV-1 latency and whether they represent a major obstacle in the pursuit of a cure for HIV-1 infection (21).

Aside from their role in HIV-1 spread and persistence, infection of macrophages may directly promote disease, the principal mechanisms being alterations of macrophage functions and activation of inflammatory processes. Monocyte and macrophages isolated

from HIV-1^{+} individuals show defective migratory responses and reduced phagocytic activity. These functional defects, in turn, result in an inefficient control of opportunistic pathogens and further enhancement of immune activation and disease pathogenesis. For example, infected alveolar macrophages have impaired phagocytic activity both in untreated- and HAART-treated patients, resulting in respiratory dysfunction and increased susceptibility to lower respiratory tract infections (21). Furthermore, CNS macrophage and microglial cell activation, mediated directly by infection and indirectly by soluble factors secreted in the brain, increase neuroinflammation. These cells can also produce and release toxins that induce apoptosis of neurons and astrocytes, thus contributing to the neurological dysfunctions associated with infection (8, 24).

1.3 Restriction factors of HIV-1

The host immune system can suppress viral replication acting through several antiviral responses, including the expression of proteins termed restriction factors, which inhibit distinct stages of the viral life cycle providing an early line of defense **(Figure 2)**. HIV-1, in turn, has developed different strategies to counteract some of these restriction factors through the action of accessory proteins (i.e., Vif, Vpu, Vpx/Vpr, Nef) (25). It was through efforts to understand the roles of these proteins in virus replication that host restriction factors and their defense mechanisms were identified (26).

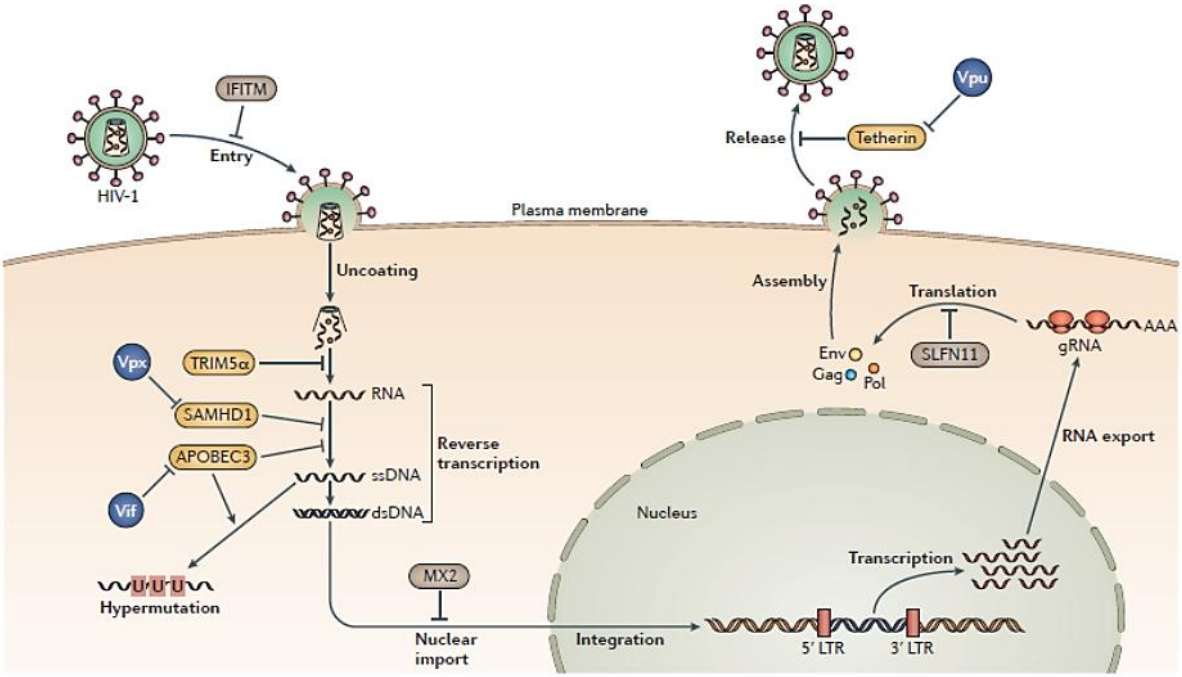

Figure 2. Overview of the restriction factors that target HIV-1 and of their viral antagonists. The picture shows the key mechanisms by which restriction factors directly act upon the retroviral replication cycle and their counteraction by viral accessory proteins *(Doyle T. et al. Nature Review 2015).*

1.3.1 APOBEC3 family

The apolipoprotein B mRNA editing enzyme catalytic polypeptide 3 (APOBEC3, A3) proteins are single-stranded DNA deaminases which potently inhibit lentivirus replication through cytidine deamination of the minus strand of viral DNA, resulting in guanosine-to-adenosine hypermutation of the viral plus strand sequence **(Figure 3)**. Depending on the degree of deamination, the reverse transcripts are either recognized as aberrant by the cell and degraded or become integrated into genomic DNA, but fail to produce infectious progeny. Although cytidine deamination is the primary mechanism of A3 antiviral activity, these proteins can also interfere with reverse transcription by preventing tRNA binding to the primer-binding site and causing termination of minus-strand synthesis (26).

The family includes seven members (A3A, A3B, A3C, A3D, A3F, A3G and A3H), which possess different local sequence preferences for editing substrates. In particular,

A3G preferentially mutates cytidine residues that are preceded by another cytidine, whereas the remaining A3 enzymes display a preference for the mutation of cytidines preceded by a different deoxyribonucleotide, most often thymidine. A3 proteins are widely express in human tissues and in several cell types, mainly in hematopoietic cells (26). Whereas A3G is highly expressed in T and B cells, A3A expression is predominant in myeloid cells (27). The anti-HIV-1 activity of A3 proteins was discovered by studying the function of the viral protein Vif, which is required for HIV-1 replication in non-permissive cells, such as $CD4^+$ T cells and MDMs, but not in permissive T cell lines, where Vif-deleted viruses replicate to high levels. Cell fusion experiments attributed causation to a restriction factor, identified as A3G, which was sufficient to repress the replication of Vif-deficient HIV-1 (28). Vif antagonize the antiviral activity of A3G, as well as that of A3F, A3H and A3D, by binding and recruiting them to a cellular ubiquitin ligase complex, which targets the enzyme for degradation (29). A3 proteins can escape complete inhibition by Vif through several mechanisms, including Vif variants with reduced affinity for specific A3 enzymes, allelic variation in A3 genes or excessive expression of A3 proteins. It was proposed that the inability of Vif to fully prevent deamination by A3 enzymes can provide a benefit to the virus, since nonlethal mutations may contribute to sequence diversification and evolution in terms of immune escape and drug resistance (30).

A3G represents the most studied family member. Its antiviral activity, as well as that of A3F, A3H, and A3D requires that the enzyme is packaged into the virion, and is thus manifested only in the next cycle of infection (29). However, virion packaging of A3 proteins may not be sufficient or necessary for all members. For example, A3A packaged in virions shows little effect on infectivity (26). Conversely, the fusion of this protein to Vpr activates the ability of this deaminase to inhibit infectivity by altering its localization within the virion (31).

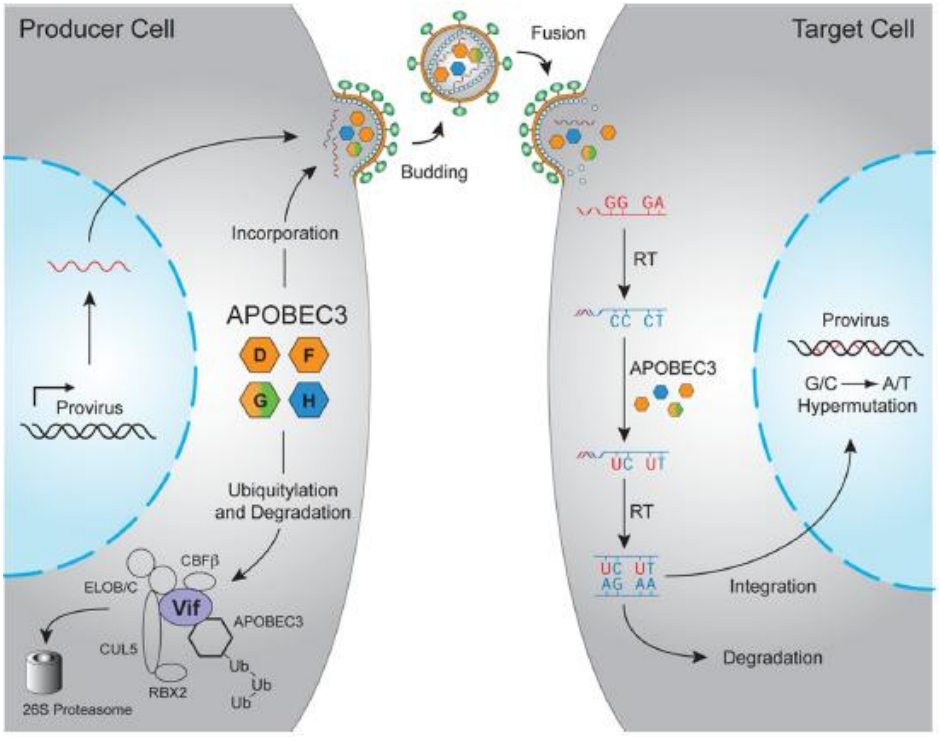

Figure 3. HIV-1 restriction by APOBEC3 proteins. A3D, A3F, A3G and A3H are encapsidated into HIV-1 virions and result in the deamination of cytosines to uracils in viral cDNA upon initiation of reverse transcription in target cells, resulting in a guanine-to-adenine mutation. These proviral cDNAs are subsequently degraded or integrated. HIV-1 Vif overcomes A3 restriction by binding and recruiting A3 proteins to an E3 ubiquitin ligase complex, which targets the enzyme for degradation by the 26S proteasome (*Harris R.S. et al. Journal of Biological Chemistry 2010*).

The role of A3A as inhibitor of HIV-1 replication is controversial. In fact, although some studies indicated that it does not exert an anti-HIV-1 activity in established cell lines in which it is ectopically expressed (32), more recent studies revealed that an anti-HIV-1 activity is explicit only in monocytes/macrophages and DCs in which A3A is naturally expressed. The expression of this protein decreases during monocyte to macrophage differentiation, correlating with an increased susceptibility of these cells to HIV-1 infection (33). The pool of A3A present in primary macrophages, DCs and differentiated THP-1 cells (that mimic macrophages upon differentiation) was shown to be directly capable of inhibiting incoming viruses at the reverse transcription step (34). Moreover, exposure to exogenous type I interferons (IFNs), or to the type I IFN-inducing cytokine interleukin

(IL)-27, was shown to stimulate A3A expression in both macrophages and DCs and to inhibit HIV-1 replication in the former, associated with an increased G-to-A editing of viral DNA, and viral spread to $CD4^+$ T cells in the latter (35-37). Finally, the up-regulated expression of A3A was associated with restriction of HIV-1 replication in M1 polarized macrophages (20, 38, 39).

In addition to counteracting HIV-1, A3A is a potent inhibitor of alpha retroviruses, retrotransposons, HTLV-1, adeno-associated virus, and human papillomavirus (HPV). Increased expression of A3A was found in keratinocytes and skin of precancerous cervical biopsies of HPV^+ patients, and correlated with HPV editing (40). Moreover, IFN-β-induced expression of A3A correlated with the ability to inhibit HPV-16 replication. A3A overexpression was dependent on the presence of the HPV oncoprotein E7, indicating a possible relationship between host response against the virus and cancer development (41). Whether A3A overexpression can lead to DNA damage, thus contributing to increased cancer incidence, is a highly controversial topic (40). In this respect, some studies reported that heterologously expressed A3A is genotoxic as a consequence of its nucleocytoplasmatic localization (42, 43). However, no significant cytotoxicity was found when IFN was used to induce the expression of endogenous A3A in MDMs or THP-1 cells, thus suggesting that monocytic cells use a cytoplasmic retention mechanism to control A3A and avert genotoxicity during innate immune responses (44).

1.3.2 SAMHD1

The protein sterile alpha motif (SAM) histidine/aspartic acid (HD) domain containing 1 (SAMHD1) is a deoxyribonucleoside triphosphate triphosphohydrolase (dNTPase), consisting of an N-terminal SAM domain, a C-terminal HD domain, and an N-terminal consensus nuclear localization sequence (45). SAMHD1 is expressed in the

majority of nucleated cells of hematopoietic origin, including monocytes, tissue-resident macrophages, DCs, T and NK cells as well as at lower levels in B cells (46). SAMDH1 counteracts HIV-1 replication by depleting the cellular dNTP pool available for reverse transcription, as demonstrated in myeloid and $CD4^+$ T cells (47-49). Its antiviral activity can be negatively regulated by phosphorylation (50, 51) **(Figure 4)**. In particular, in proliferating primary T $CD4^+$ cells and macrophages, SAMHD1 can be phosphorylated at Thr592 by specific cyclin-dependent kinases, resulting in loss of antiviral activity but not of dNTPase activity (45). This suggests that dNTPase activity is not sufficient for SAMHD1 antiviral activity. Indeed, SAMHD1 also possesses exonuclease activity on single-stranded DNA or RNA substrates, and this activity may in part account for HIV-1 restriction (52). The antiviral activity of SAMHD1 is counteracted by the viral protein Vpx, encoded by HIV-2 and SIV. Vpx recruits SAMHD1 to a cullin4A-RING E3 ubiquitin ligase complex, which targets the enzyme for proteasomal degradation (26).

In normal conditions, SAMHD1 play an important role in the regulation of cellular dNTP levels, which are critical to the fidelity of DNA synthesis and the stability of the genome, as well as in proper activation of the innate immune response. Mutations in SAMHD1 are associated with chronic lymphocytic leukemia (CLL) and the rare inflammatory disease Aicardi– Goutieres Syndrome (AGS) (25).

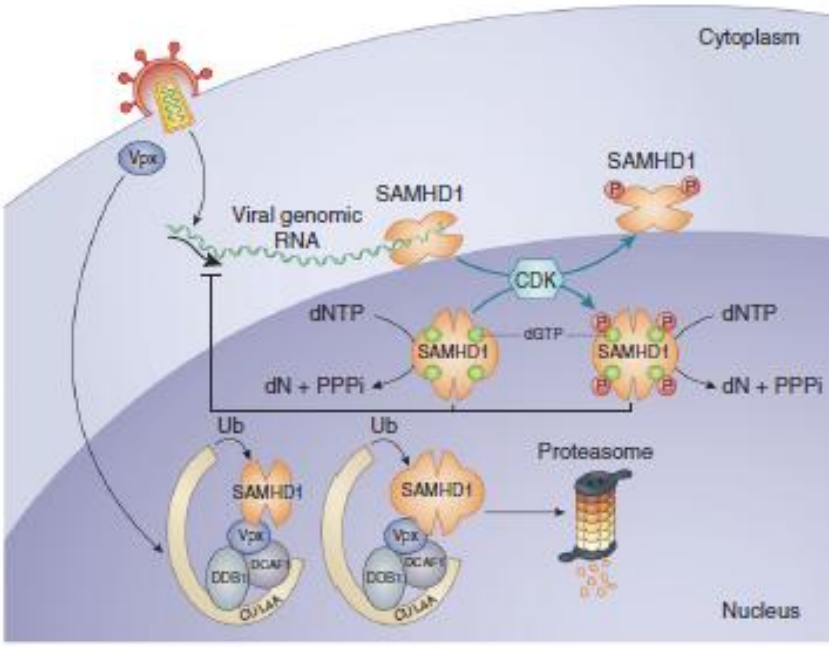

Figure 4. Proposed models for SAMHD1-mediated HIV-1 restriction. HIV-2, SIV or engineered HIV-1 containing Vpx binds to the DCAF1-DDB1-CUL4A E3 ubiquitin ligase complex and to SAMHD1, which is then degraded by proteasomes in the nucleus. If the virus lacks Vpx, SAMHD1 depletes the pool of dNTPs, blocking reverse transcription of the bound tRNA primer. An alternative model calls for SAMHD1 to degrade the viral genomic RNA as it is reverse transcribed in the cytoplasm. This activity is regulated by SAMHD1 phosphorylation *(Simon V. et al. Nature Immunology 2015).*

1.3.3 Mx2

The interferon-inducible myxovirus resistance B protein (MxB or Mx2) is a dynamin-like GTPases highly homologous to the well-known MxA protein (63% identity) that inhibits influenza-like viruses. Both proteins comprise an amino-terminal GTPase domain (G domain) and a carboxy-terminal stalk domain that are connected by a tripartite bundle signaling element. Mx2 exists in two isoforms that are translated as 78 or 76 kDa proteins from alternate AUG start codons of the same mRNA. The longer isoform contains a nuclear localization signal (NLS)-like sequence and localizes preferentially to nuclear pores, whereas the shorter one is cytoplasmic (53). Recently, an anti-HIV-1 activity was reported for Mx2 which is strongest in nondividing cells and depends on the N-terminal sequence containing NLS (54, 55). Mx2 expression is induced by type I IFN in MDMs, primary T cells and myeloid cell lines, conferring resistance to HIV-1 infection. The

current data suggest that Mx2 may target the viral capsid and restrict HIV-1 infection by blocking nuclear complexes or affecting their stability **(Figure 5)** (53). Aside HIV-1, human Mx2 inhibits other primate lentiviruses such as HIV-2 and SIV, but not non-primate viruses (56).

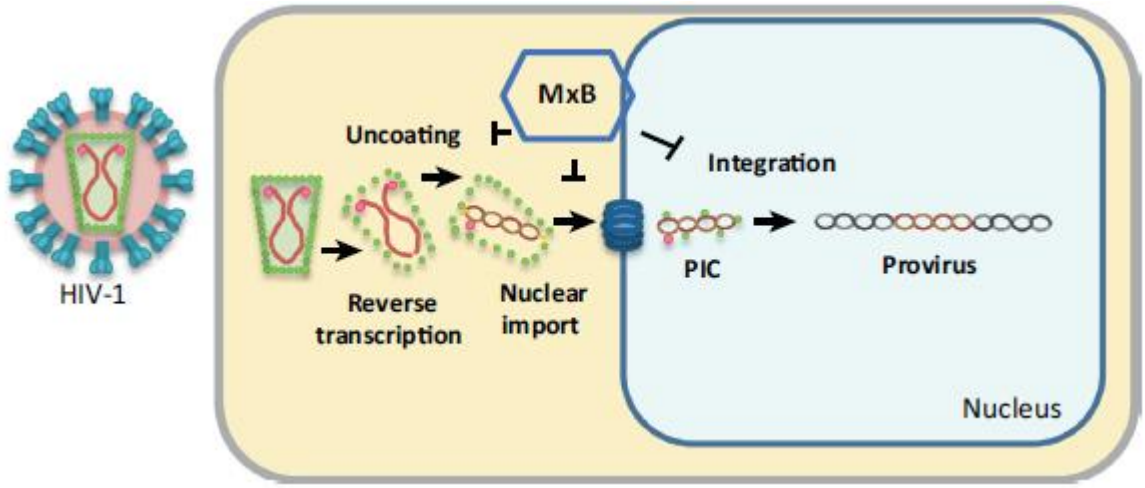

Figure 5. Model of HIV-1 restriction by MxB. MxB inhibits uncoating, nuclear uptake and/or stability, or the integrase activity of the pre-integration complex (PIC), thus preventing chromosomal integration of proviral DNA *(*Adapted from: *Haller O. et al. Trends in Microbiology 2015).*

1.3.4. Other host restriction factors

In addition to the factors described above, other proteins have been reported to exert anti-HIV-1 activity. Member of the tripartif motif family (TRIM), particularly TRIM5, can act at an early stage of the HIV-1 life cycle, binding to the viral capsid and promoting accelerated fragmentation of the viral core thus preventing cDNA synthesis (30). Furthermore, TRIM22 can impair HIV-1 replication by either interfering with viral transcription or posttranslationally modifying host or viral proteins that are required for viral assembly and/or budding (57). Bone marrow stromal cell antigen 2 (BST2), also named Tetherin, inhibits the release of nascent HIV-1 particles and other enveloped viruses by retaining the budding virions at the cell surface. The antiviral activity of this protein can be antagonized by HIV-1 Vpu. Recently, growing evidence is accumulating for the antiviral activity of others IFN-

inducible proteins such as the IFN-induced transmembrane (IFITM) proteins and Schalafen 11 (SLFN11). The former can be incorporated into the viral membrane, thus interfering with membrane fusion, whereas the latter can suppress HIV-1 protein synthesis, thus inhibiting virus production (58).

Chapter 2

HIV-1 infection in the HAART era

2.1 Current antiretroviral therapy

The discovery of HIV-1 as the causative agent of AIDS together with an ever increasing understanding of the virus replication cycle were instrumental in drug discovery focused on targeted inhibition with specific pharmacological agents. In 1987, the RT inhibitor Zidovudine (AZT) was the first drug approved to treat HIV-1 infection. Afterward, a number of other synthetic nucleoside analogues were demonstrated to be effective against the virus. The treatment of HIV-1 infection was revolutionized in the mid-1990s by the development of PI inhibitors and the introduction of drug regimens that combined the different classes of antiretroviral drugs to enhance the overall efficacy and durability of therapy. The advent of combination therapy dramatically suppressed viral replication and reduced the plasma HIV-1 RNA (Viral Load) below the limit of detection of clinical assays (50 RNA copies/mL), thus resulting in reduced morbidity and mortality and partial reconstitution of the immune system (59). Combination therapy decreased the probability of selecting virus clones (from an intrapatient HIV-1 population) bearing multiple mutations and conferring resistance to a three antiretroviral drug regimen, thus changing a certain deadly disease in a chronic manageable one. Antiretroviral drugs approved by Food and Drug Administration (FDA) can be divided into six classes (http://www.fda.gov/ForPatients/Illness/HIVAIDS/Treatment/ucm118915.htm) **(Figure 6)**:

1. Nucleoside reverse transcriptase inhibitors (NRTIs). They are structurally similar to DNA nucleoside bases necessary to complete reverse transcription, but lack the 3'-hydroxyl group on the deoxyribose moiety, thus preventing the formation of the

next 3'-5'-phosphodiester bond with the incoming 5'-nucleoside triphosphates and resulting in termination of the growing viral DNA chain. Chain termination can occur during RNA-dependent or DNA-dependent DNA synthesis, thus inhibiting production of either minus or plus strands of proviral DNA (59). NRTIs are administered as prodrugs, which require host cell entry and phosphorylation by cellular kinases before enacting an antiviral effect. Treatment with NRTIs often results in the emergence of viral strains with reduced drug susceptibility. Resistance to NRTIs is mediated by two mechanisms: ATP-dependent pyrophosphorolysis, which is the removal of NRTIs from the 3' end of the nascent chain and reversal of chain termination, and increased discrimination between the native deoxyribonucleotide substrate and the inhibitor (60). Some NRTI mutations could be associated with decreased RT function and viral replicative fitness (59). At present, approved NRTIs are: abacavir (ABC), didanosine, emtricitabine (FTC), lamivudine (3TC), staduvudine, tenofovir disoproxil fumarate (TDF) and AZT. Fixed-dose combinations of NRTIs are also available, such as FTC/TDF (Truvada) and ABC/3TC (Kivexa). The novel approved prodrug tenofovir alafenamode (TAF) delivers higher intracellular levels of the active metabolite tenofovir diphosphate at a lower dose respect to TDF, thus reducing the risk of TDF-associated toxicity (http://www.salute.gov.it/imgs/C_17_pubblicazioni_2545_allegato.pdf).

2. Non-nucleoside reverse transcriptase inhibitors (NNRTIs). They bind to a hydrophobic pocket close to the RT active site, inducing a conformational change in the enzyme that alters the active site and limits its activity (59). NNRTIs were introduced in 1996 with the approval of nevirapine (NVP) and are part of preferred initial regimens. They are divided in first-generation [e.g., delavirdine, efavirenz (EFV), NVP] and second-generation [e.g., etravirine, rilpivirine (RPV)] drugs,

which display a better resistance profile, an increased genetic barrier to the development of resistance, a convenient dosing schedule, with potential for co-formulation with other antiretroviral drugs. Mutations in the RT gene alter the ability of NNRTIs to bind the enzyme. These drugs have a relatively low genetic barrier to resistance whereby single mutation in the binding site can decrease their ability to bind the enzyme (60).

3. Protease inhibitors (PIs). The approval of PIs in 1996 and the use of ritonavir (RTV) or indinavir (IDV) in combination therapy with two NRTIs dramatically changed the course of the HIV-1 epidemic. PIs function as competitive inhibitors that directly bind to the HIV-1 PR thus preventing cleavage of polypeptides. Resistance to PIs results from mutations both inside and outside the active PR domain, and typically occurs through the development of one or more major mutations, which produce conformational changes in the PR binding site, followed by secondary compensatory mutations that improve enzymatic activity and, in some cases, viral fitness. In fact, mutations at cleavage sites (i.e., gag and pol genes) result in a better substrate for the mutated PR, partially compensating for the resistance-associated loss of viral fitness (60). For more than a decade, RTV was coadministered with other PIs as pharmacokinetic enhancer (RTV-boosted PIs) to increase absorption and prolong the half-life of the coadministered PIs. Cobicistat (COBI or c), a structural analogue of RTV without antiviral activity and with improved physicochemical properties, recently emerged as an alternative boosting agent (61). In addition to RTV and IDV, FDA-approved PIs include atazanavir (ATV), darunavir (DRV), fosamprenavir, lopinavir (LPV)/RTV, nelfinavir (NFV), saquinavir and tipranavir.

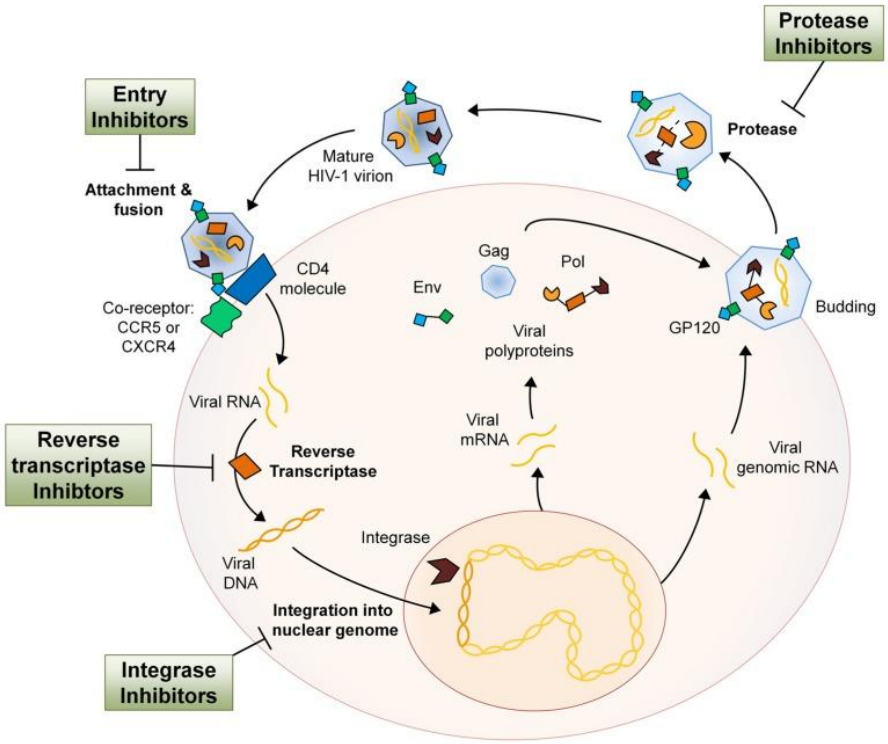

Figure 6. Schematic representation of the different steps of the HIV-1 life cycle targeted by the six classes of antiretroviral drugs currently approved. *(*Adapted from*: Smith R.L. et al. Frontiers in Genetics 2013).*

4. Fusion inhibitors (FIs). FIs act extracellularly to prevent HIV-1 fusion to the target cell. The only approved peptide FI, enfuvirtide (T-20), blocks the second step in the fusion pathway by binding to the HR1 region of glycoprotein 41, thus preventing its conformational change required to complete the final step in the fusion process (59). Mutations that confer resistance to enfuvirtide occur in the HR1 domain, resulting in significant loss of drug binding and activity. However, these mutations result in reduced replication capacity/replicative fitness presumably because they also reduce the overall fusion rate. For their unique mechanism of action, FIs are considered as additional options for therapy in patients who are highly treatment resistant. Their use is limited because of inconvenient administration (subcutaneous injection), adverse effect profile and the production time and costs. The discovery of additional antiretroviral classes and medications with activity against highly

resistant viral strains has further limited their use (http://emedicine.medscape.com/article/1533218-overview#a3).

5. CCR5 antagonists. They are small molecules that antagonize the CCR5 co-receptor. Maraviroc (MVC) was the first drug of this class being approved by FDA in 2007. It binds a hydrophobic transmembrane cavity of CCR5, thus altering the conformation of the second extracellular loop of the receptor and preventing the interaction with the V3 stem loop of gp120. Since MVC binds a host cell protein, the resistance to this drug is unlike that to other antiretroviral drugs (59). However, amino acid substitutions in the V3 loop of gp120 were found *in vitro* and *in vivo* studies which correlated with resistance to this drug. These mutations resulted in increased affinity of the virus for CCR5, enabling gp120 binding to CCR5 also in the presence of MVC. Other mechanisms are faster rate of entry or increased replicative capacity, and tropism switching from CCR5 to CXCR4 or more frequently to CCR5/CXCR4 dual tropism (62). Tropism switching is a concern in the therapeutic administration of this drug because it is typically related to faster disease progression.
6. Integrase strand transfer inhibitors (INSTIs). IN was the most recent HIV-1 enzyme to be successfully targeted for drug development. In 2007 FDA approved raltegravir (RAL), followed by dolutegravir (DTG) and elvitegravir (EVG). These drugs competitively inhibit the strand transfer reaction of proviral DNA to cellular DNA by binding metallic ions in the active site of the enzyme. INSTIs are comprised of a metal-binding pharmacophore, which sequesters the active site magnesium ions, and a hydrophobic group, which interacts with the viral DNA as well as the enzyme in the complex (59). Mutation in the IN gene may occur which are associated with resistance to RAL and EVG. INSTI-based regimens are

recommended as first-line combination HAART in several updated treatment guidelines (http://www.salute.gov.it/imgs/C_17_pubblicazioni_2545_allegato.pdf).

The overall benefits of viral suppression as a result of effective HAART far outweigh the risks associated with the adverse effects of some antiretroviral drugs. However, adverse effects were reported for all these drugs and, in the earlier era of combination therapy, were among the most common reasons for switching or discontinuing therapy and for medication nonadherence. Fortunately, newer drug regimens are associated with fewer serious and intolerable adverse effects than was in the past. The most common side effects are gastrointestinal sequelae (diarrhea, nausea), erithema, rash, fatigue, headache, insomnia and increased risk for respiratory tract infections. More severe complications include hepatic toxicity as well as neuronal and cardiovascular complications. A major adverse effect of NRTIs is mitochondrial toxicity, leading to myopathy, peripheral neuropathy, and hepatic steatosis with lactic acidosis, which can be life-threatening. Although NNRTIs have a lower incidence of adverse effects in comparison to NRTIs, most of them cause some degree of hepatotoxicity and EFV is associated with CNS effects. PIs are important contributors to metabolic complications (dyslipidemia, insulin resistance, lipodystrophy), resulting in an increased risk for cardiovascular events (63). All INSTIs are generally well-tolerated, but they are unable to decrease chronic inflammation.

2.2 Guidelines for the use of antiretroviral drugs

Guidelines regarding initiation of HAART were progressively reviewed over the years. Generally, therapy was initiated based on decreasing CD4 cell count or clinical evidence of AIDS. In 2003, WHO recommended initiating therapy at CD4 count below 200 cells/mm^3. This threshold was increased to 350 and to 500 cells/mm^3 in 2010 and 2013, respectively (http://www.who.int/hiv/pub/guidelines/en/). In recent years, several

studies demonstrated advantages of early initiation of HAART. In particular, in 2015 the Strategic Timing of Antiretroviral Therapy (START) study compared immediate treatment at HIV-1 diagnosis with treatment started at CD4 count of 350 cell/mm^3, demonstrating the beneficial effect of the immediate initiation of HAART regardless of CD4 count. In addition, the TEMPRANO ANRS trial showed that early initiation of therapy reduced the risk of severe HIV-1-related illness by 44% compared to deferred initiation of HAART. The clinical evidence of benefits of earlier treatment initiation led to new guidelines recommending to initiate therapy for all adults at HIV-1 diagnosis regardless of WHO clinical stage and at any CD4 count (https://aidsinfo.nih.gov/guidelines). Furthermore, HIV-1 treatment as prevention (TasP) trials highlighted the benefits of treatment as prevention method to decrease the risk of transmission. In fact, antiretroviral treatment reduces the viral load in the blood, semen, vaginal fluid and rectal fluid to very low levels, which are associated with low risk of transmission. In addition, new recommendations are also made for the use of oral preexposure prophylaxis (PreEP) as an additional prevention choice for people at high risk of HIV-1 infection. As a result of the new guidelines, the target population to be administered HAART will significantly increase (64).

Antiretroviral drug regimens containing at least two and preferably three active drugs from two or more classes are recommended for virologic suppression. Although current HAART is not universal and variations among global and regional guidelines exist for fist-line therapy, initial drug combinations generally consists of two NRTIs, usually ABC/3TC, TAF/FTC, or TDF/FTC, plus a third drug such as an INSTI, an NNRTI, or a Pharmacokinetic-enhanced PI. According to recent guidelines, INRTI-containing regimens are favorite for safety and tolerability (https://aidsinfo.nih.gov/guidelines).

Significant progress was made toward regimen simplification through the combination of active drugs from a single or more than one class into single-tablet regimen

(STR) and optimization of drug profiles that maximize long-term tolerability and safety (64). This allowed many people to take treatment once a day in one pill, contributing to a better therapy adherence which reduces the development of drug resistance. Atripla, which combines two NRTIs and one NNRTI (FCT/TDF/EFV), represented the most used combination in the last years, whereas Eviplera (FTC/TDF/RPV) recently become the most utilized. Combinations of NRTIs and INSTIs are also available, such as Stribild (TFD/FTC/EVG), Triumeq (ABC/3TC/DTG) and Genvoya (TFA/FTC/EVGc) (https://aidsinfo.nih.gov/guidelines/html/1/adult-and-adolescent-treatment-guidelines).

Selection of a regimen is centered on individual patients' needs based on virologic efficacy, potential adverse effects, dosing frequency, resistance test results, comorbid conditions and cost. The therapeutic goals for all patients is maintaining suppression of virus replication while enabling immune recovery and minimizing adverse drug effects. For this reason, a highly individualized approach and a frequent monitoring are essential, and a regimen may be changed due to lack of virologic suppression, drug adverse effects, non-adherence (64). A number of laboratory tests are employed for initial evaluation of patients before and after initiation of HAART. In particular, two markers are routinely used for monitoring, namely viral load and $CD4^+$ T lymphocyte count to assess immune function. In addition, genotypic resistance testing is recommended to guide either selection of the initial HAART regimen or alternative treatments for antiretroviral therapy-experienced patients with suboptimal virologic response or virologic failure (https://aidsinfo.nih.gov/guidelines/html/1/adult-and-adolescent-treatment-guidelines). The optimal threshold for defining viral failure and for switching HAART regimens has not been established. Optimal viral suppression is generally defined as a viral load persistently below the level of detection. However, isolated "blips" (detectable viral RNA with subsequent return to undetectable level) are common and are not usually predictive of

virologic failure. According to DDHS (Department of Health and Human Services) and ACTG (AIDS Clinical Trial Group) guidelines, virologic failure is defined as the inability to achieve or maintain suppression of viral replication to an HIV-1 RNA level <200 copies/mL. In case of virologic failure persistence, regimen should be changed requiring careful review of patient treatment history and resistance testing (https://aidsinfo.nih.gov/guidelines/html/1/adult-and-adolescent-arv-uidelines/15/virologic-failure). Alternative regimens should include combination of 2 NRTIs, such as TAF/FTC, TDF/FTC or ABC/3TC, in combination with EFV, RPV, ATV/c or ATV/r or DRV/c or RAL (https://aidsinfo.nih.gov/guidelines/html/1/adult-and-adolescent-arv-guidelines/11/what-to-start). Depending on the nature and the extent of the resistance, drugs not generally recommended for initial therapy, such as MVC or T-20, could be considered. Additional antiretroviral drugs that are in clinical testing could become valuable options for individuals with multi-class resistance (64).

2.3 DEVELOPMENT of NEW DRUGS

Individuals with long HAART histories may have few remaining options for therapy and the development of new drug is necessary to overcame various challenges. In particular, new drugs mast have higher barriers to resistance and/or new mechanisms of action to overcome resistance, as well as improved availability, safety profile and quality of life. These and other efforts should be made to reach the ambitious aim to end the AIDS epidemic by 2030 launched by the Joint United Nations Programme on HIV-1/AIDS (UNAIDS). They have established a 90-90-90 goal to be achieved by 2020. This goal includes 90% of individuals with HIV-1 globally being diagnosed, on treatment, and virologically suppressed. To reach these goals clinical trials are underway to evaluate the safety and efficacy of alternative formulations of already available drugs as well as new

agents with novel mechanisms of action that will expand upon currently available classes **(Table 1)** (65).

Current trials are evaluating regimen simplification with new coformulated STRs or with long-acting injectable formulations. These options may represent maintenance therapies for individuals with viral loads already suppressed with a three-drugs regimen, or alternative therapies for those unable to tolerate current therapy (65).

Compound name	Medication class	Company
Phase 3		
Darunavir/cobicistat/emtricitabine/tenofovir alafenamide[a]	STR (PI + NRTIs)	Gilead Sciences
Dolutegravir/rilpivirine[a]	STR (INSTI + NNRTI)	ViiV/Janssen
Doravirine (MK-1439)[a]	NNRTI	Merck
Fostemsavir (BMS-663068)[a]	AI	ViiV
GS-9883/emtricitabine/tenofovir alafenamide[a]	STR (INSTI + NRTIs)	Gilead Sciences
Ibalizumab (TMB-355)[a,b]	EI	TaiMed Biologics
Raltegravir once daily[a]	INSTI	Merck
Phase 2b		
BMS-955176[a]	MI	ViiV
Cabotegravir (LA)/Rilpivirine (LA)[a] (IM)	INSTI + NNRTIs	ViiV/Janssen
Cabotegravir[a] (PO)	INSTI	ViiV
Cenicriviroc[a]	CCR5 and CCR2 inhibitor	Takeda/Tobira Therapeutics
PRO-140[a]	EI	CytoDyn
Phase 1		
GS-9620[c]	TL7 agonist	Gilead Sciences

AI attachment inhibitor, *CCR* C-C chemokine receptor, *EI* entry inhibitor, *IM* intramuscular, *INSTI* integrase strand transfer inhibitor, *LA* long-acting, *MI* maturation inhibitor, *NNRTI* non-nucleoside reverse transcriptase inhibitor, *NRTI* nucleoside reverse transcriptase inhibitor, *PO* oral, *PI* protease inhibitor, *STR* single tablet regimen, *TL7* Toll-like receptor

[a] For treatment of HIV

[b] Expanded access available in the US

[c] Being evaluated for HIV eradication

Table 1. The table reports new drugs currently under clinical investigation *(Badowski M.E. Infectious Disease and Thersapy 2016).*

Antiretroviral drugs with new mechanisms of action would broaden treatment options especially for individuals with multi-class resistance. Among these drugs, Fostemsavir is an attachment inhibitor which exerts its action by directly binding to gp120 and causing a conformational change that prevents viral attachment to CD4. In addition,

Ibalizumab is an intravenously administered monoclonal antibody that binds to CD4 causing a post-conformational change that prevents viral fusion and entry. Furthermore, BMS-955176 is a maturation inhibitor that specifically interferes with Gag cleavage (64, 65). Finally, a new class of drugs is represented by chemokine receptor antagonists with dual receptor specificity for CCR5 and CCR2. The main therapeutic advantage of such drugs is their potential anti-inflammatory activity. One of these drugs will be described in the next paragraph.

2.3.1 CENICRIVIROC

Cenicriviroc (CVC; also known as TBR652 and previously TAK-652 from Takeda) is a dual CCR5/CCR2 receptor developed by Tobira Therapeutics which completed phase II of development for the treatment of HIV-1 infection (66, 67). It binds CCR5 blocking HIV-1 entry into host cells, but has also potential anti-inflammatory effect due to CCR2 inhibition, and in this aspect it differs from MVC. In addition, CVC has a long half-life (35-40 hours) and can be taken just once daily, and it does not interfere with the activity of liver enzymes that process other drugs. A double-blind, placebo-controlled, randomized, dose-escalating phase 2a study assessed the antiviral activity, pharmacokinetics/pharmacodynamics (PK/PD), and safety and tolerability of oral once-daily CVC monotherapy for 10 days in HIV-1 infected, antiretroviral treatment–experienced patients. The results of this study demonstrated that the drug is well tolerated with no dose-limiting adverse events and caused significant reductions in HIV-1 RNA at all tested doses (25, 50, 75, 100, and 150 mg), which persisted for up to two weeks after treatment discontinuation. In addition, CCL2 increased significantly by day 10 in the 50 mg and 150 mg dose groups, suggesting a strong CCR2 blockade (67). As a consequence of these positive results, Tobira Therapeutics conducted a phase 2b randomized, double-

blind, double-dummy, dose finding study of CVC in comparison to EFV, both in combination with Truvada, in treatment-naive HIV-1 infected subjects with CCR5 virus (Study 652-2-202,NCT01338883) (https://clinicaltrials.gov/ct2/results?term=NCT01338883&Search=Search).

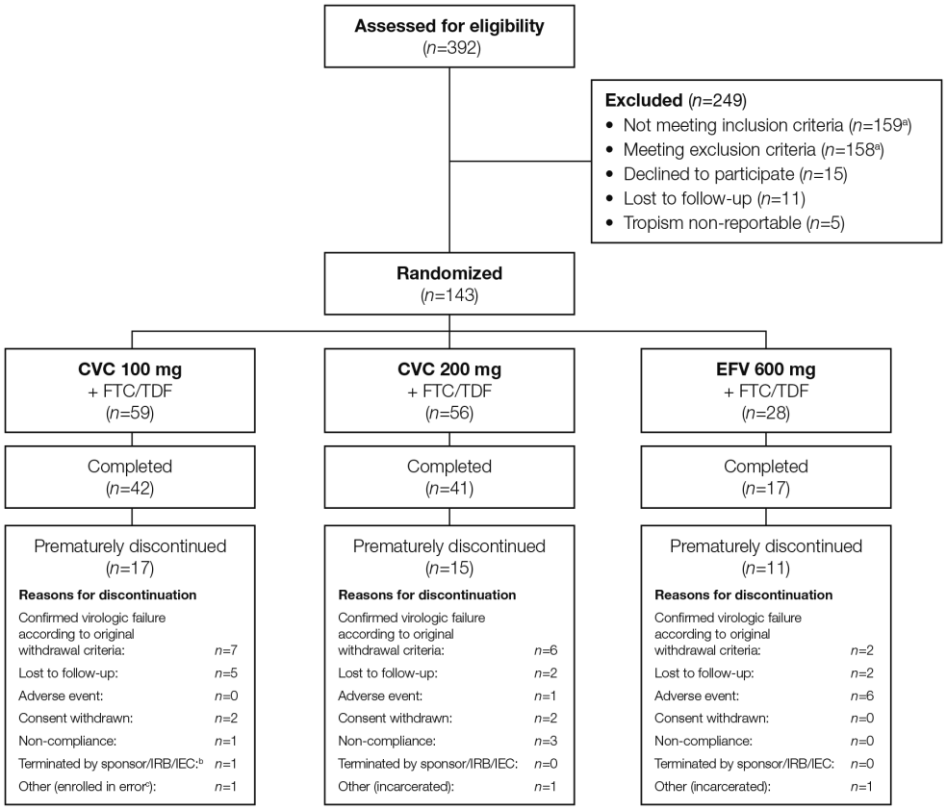

Figure 7. Schematic representation of Study 202 design and participants *(Thomson M. et al. AIDS 2016).*

The 143 participants included in the trial were stratified 2:2:1 to CVC 100 mg (n=59; men 92%), CVC 200 mg (n=56; men, 100%) and EFV 600 mg (n=28; men, 89%). Of these patients 42, 41 and 17 completed the study, respectively **(Figure 7)**. Virologic success was obtained in 76, 73, 71 % (week 24) and 68, 64, 50 % (week 48) of study participants receiving CVC 100, CVC 200, and EFV, respectively. Mean $CD4^+$ T cell counts and $CD4^+/CD8^+$ ratio increased from baseline in all arms. No significant differences were observed between treatment groups in the number of adverse events (68). Total and

low-density lipoprotein (LDL) cholesterol decreased with CVC and no meaningful change in high-density lipoprotein (HDL) cholesterol was found, whereas there were increased levels of LDL and HDL in the EFV arm. Concerning the expression of biomarker of inflammation and immune activation, CVC lead to a dose-dependent, compensatory increase in CCL2 because of CCR2 blockade, whereas no change was observed with EFV. During the first 12 weeks, soluble CD14 (sCD14) (a marker of monocyte activation) levels decreased and remained below baseline in the CVC arms throughout the study, whereas in the EFV arm sCD14 levels increased and remained above baseline values. No significant differences across the arms were observed for other inflammatory (hs-CRP, fibrinogen, IL-6, and D-dimer) or immune activation (total CD38 and HLA-DR expression on $CD4^+$ and $CD8^+$ T cells) biomarkers (68). Data of efficacy and favorable safety supported the selection of CVC 200 mg for phase 3 studies.

2.4 HIV-1 cure: is it achievable?

Despite the extraordinary success of HAART to increase the life expectancy of HIV-1-infected individuals, several factors hinder the achievement of a cure. In particular, the virus persists in cellular and anatomical reservoirs for the lifetime of the individuals receiving therapy. The magnitude of this viral reservoir is strongly associated with the residual levels of immune activation, suggesting that HIV-1 persistence and residual inflammation are interdependent and represent the major challenges to achieve a cure (69). A variety of new compounds, including latency reversal agents (LRAs) or immune-based drugs, are under investigation with the final aim to eliminate or control viral persistence.

2.4.1 Latent reservoirs as obstacles for an HIV-1 cure

The first indication that true eradication could be difficult to reach came in 1997 when three independent studies reported the persistence of latently infected resting $CD4^+$ T lymphocytes carrying replication competent virus in treated patients who maintained their plasma viremia below the limit of detection for years (70-72). After 20 years, resting memory $CD4^+$ T cells are still considered as the major HIV-1 reservoir. Two models were proposed to explain latent infection in resting memory cells. The pre-activation latency model relies on the supposition that HIV-1 can directly infect a subset of resting $CD4^+$ T cells, while the post-activation latency model proposes that activated antigen-specific $CD4^+$ memory T cells become preferentially infected yet avoid cell death and then revert to a resting state (73). The frequency of resting $CD4^+$ T cells that become latently infected varies widely between individuals and depends also on the infected memory T cell subset. In particular, long-lived central memory T cells represent the major source of persistent HIV-1 in most patients. In addition to the memory T cell subsets, some effector T cells, such as $CD4^+$ T helper cells, were shown to harbor replication-competent virus in individuals on long-term effective HAART. Recently, T follicular helper cells, a subset of $CD4^+$ T cells enriched in lymph node germinal centers, were identified as a prime anatomic niche, inaccessible to CTLs, for HIV-1 persistence during antiviral therapy (74, 75). Furthermore, HIV-1 reservoirs can be also found in other anatomical reservoir, such as lung, genital tract, and lymphoid tissues, particularly the GALT (75). While latent HIV-1 persists primarily in $CD4^+$ T cells in the peripheral blood, other cell types, such as γδ T lymphocytes, macrophages, follicular DCs and NK cells, also contribute to HIV-1 persistence in tissues (76) **(Figure 8)**. Despite the role of myeloid cells remains controversial, as discussed in Chapter 1, numerous studies suggest that macrophages, microglia and astrocytes in the CNS could potentially establish HIV-1 reservoirs (24).

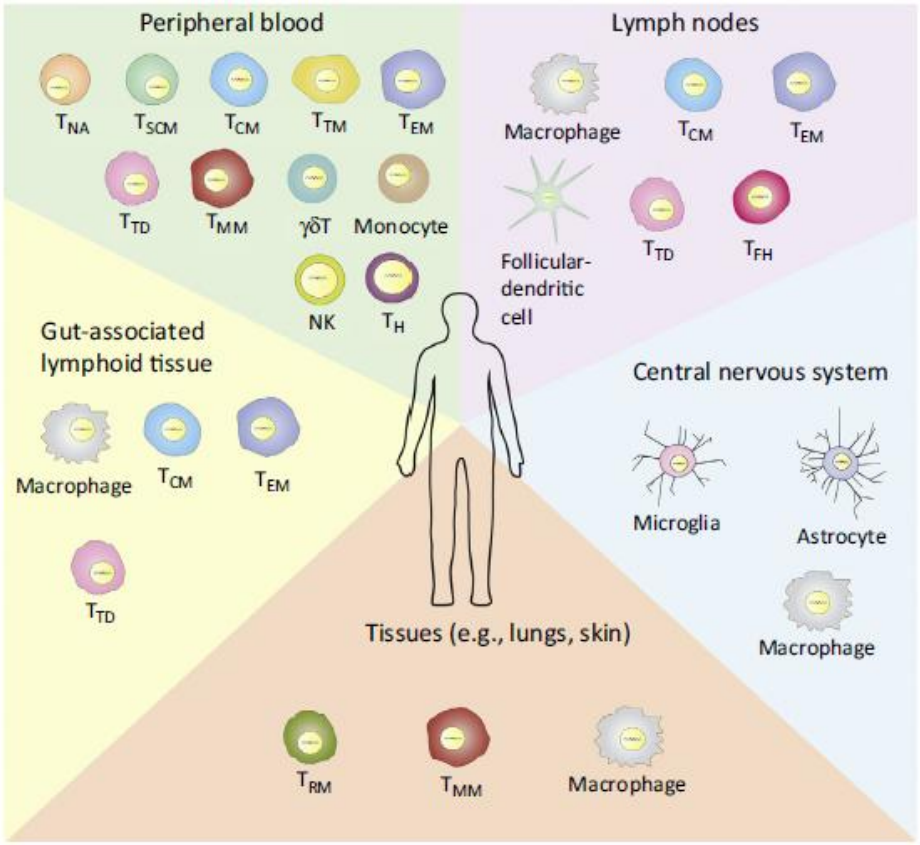

Figure 8. Tissues and cellular reservoirs of HIV-1. In addition to the $CD4^+$ memory T cell subsets found in the peripheral blood, lymph nodes, gut-associated lymphoid tissue, and the central nervous system are significant anatomic sanctuaries of latent HIV-1 infection. Additional tissues, such as the lungs and skin, may also contain cells harboring latent HIV-1. Abbreviations: T_H, $CD4^+$ helper T cells; NK, natural killer cells *(Barton K. et al Trends in Microbiology 2016).*

Latently infected cells contain a stable form of integrated viral DNA that is replication competent but transcriptionally silent. Viral quiescence was initially thought to derive principally from the quiescent cellular state of host T cells. Studies of viral transcriptional regulation showed that several specific cellular mechanisms, such as epigenetic transcriptional silencing, availability or deficiency of key host factors, and transcriptional interference are involved in maintaining latently infected cells in a nonproductive state (77).

While it is well established that longevity of latently infected cells allows for persistence of the reservoir over time, the question of whether ongoing viral replication or cell proliferation is maintaining the HIV-1 reservoir is controversial (76). Studies of

HAART intensification with INSTIs demonstrated increased generation of 2-LTR circles, suggesting that HIV-1 integration was blocked and that there existed a steady-state in which there was ongoing viral replication. The observation of reduction of immune activation after intensification and viral evolution during HAART agree with this theory, suggesting that ongoing viral replication contribute to HIV-1 persistence. However, these findings were not reproduced in all INSTI intensification studies. Additionally, the lack of effect of HAART intensification on low-level viremia and several phylogenetic studies showing lack of viral evolution along with the evidence of expanding populations of identical sequences over time during long-term suppressive HAART, suggest that homeostatic proliferation of latently infected cells may alternatively, or additionally, contribute to the maintenance of the HIV-1 reservoir (76).

Several approaches to reverse latency are currently being investigated. The most studied approach is based on the hypothesis that inducing viral expression from latently infected cells would cause a reduction of the overall viral load through the death of infected cells due to virus-induced cytophatic effects and/or host immunological mechanisms. This approach, named "shock and kill", is based on the administration of LRAs to patients on HAART to induce an increase in both cell-associated and plasma HIV-1 RNA levels. Such drugs include: 1) histone deacetylase inhibitors (HDACIs); 2) disulfiram, postulated to involve nuclear factor κB (NF-κB) activation; 3) bromodomain-containing protein 4 (BRD4) inhibitor JQ1, which elicits effects through positive transcription elongation factor (P- TEFb); 4) protein kinase C (PKC) activators such as ingenol, prostratin, 1,2-diacylglycerol analogues 15 and bryostatin-1 (78). HDACIs are the most advanced LRAs in current clinical testing. However, these drugs have no apparent effect on the frequency of latently infected cells probably because current approaches are insufficiently potent to block complex signaling networks *in vivo* that maintain memory

cells in a resting state and for the lack of efficient activation of CTLs to ensure clearance of infected cells (79).

Two additional strategies are being evaluated to achieve a cure. The first approach, called "sterilizing cure", aims to completely eliminate all traces of HIV-1 in an infected individual, leading to a permanent virologic remission in the absence of HAART. This approach is based on the Berlin patient who was HIV-1 positive and subsequently diagnosed with acute myeloid leukemia. He received two cycles of bone-marrow transplantation from an HLA-matched donor who was homozygote for CCR5Δ32, which genotype is associated with the lack of CCR5 cell-surface expression. Repeated rounds of chemotherapy followed by stem cell transplantation, as well as the development of graft-versus-host disease, contributed to the elimination of infected cells in this patient. However, despite intense efforts to recapitulate this situation by gene therapy strategies to generate an immune system resistant to HIV-1, this outcome has not yet reproduced (76, 80).

The second approach, called "functional cure" or "sustained virologic remission", is defined as a long-term host-mediated control of viral replication and remission of the symptoms of HIV-1 infection in the absence of antiretroviral therapy, even if replication-competent viruses remain in the body. This approach is based on a rare population of HIV-1^+ individuals, defined elite controllers, who maintain an undetectable viral load and high CD4 counts without having to take antiretroviral therapy, suggesting that complete eradication of reservoirs may not be necessary to achieve sustained virologic remission. The strategies for a functional cure that are being pursued include early HAART initiation and immunological approaches to eliminate infected $CD4^+$ T cells or to reinforce anti-HIV-1 immune responses **(Figure 9)**.

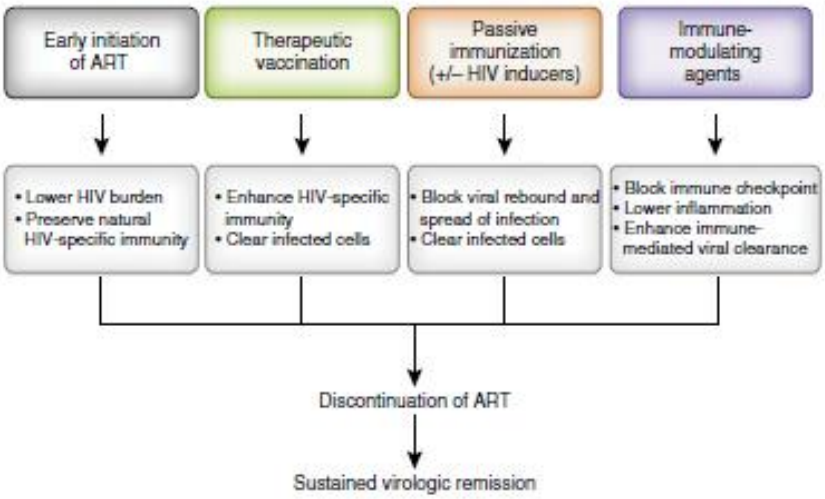

Figure 9. Representation of different approaches to achieve sustained virologic remission in infected individuals *(Chun T.W. et al. Nature Immunology 2016).*

Administration of antiretroviral therapy in very early acute infection substantially reduces the reservoir and increases virological control after HAART discontinuation, but does not block reservoir establishment. Thus, early initiation of HAART alone may not be sufficient to achieve sustained virologic remission for prolonged time in a majority of individuals; however, it could succeed in combination with other curative strategies, such as therapeutic vaccines and other immunotherapies (81) **(Figure 9)**.

2.4.2 Chronic immune activation and residual inflammation as a consequence and a driver of viral persistence

Systemic chronic immune activation is considered today as the driving force of HIV-1 pathogenesis (82). Immune activation in HIV-1 infection covers a large range of events involved in active molecular and cellular processes, such as cell activation, proliferation and death and secretion of soluble mediators (83). In particular, a strong correlation between the expression of T cell activation markers, such as CD38 and HLA-DR, and the progression of disease was found either in untreated or HAART-treated HIV-1^+ individuals. As a consequence of persistent activation, the expression of negative

regulators of T cell activation, such as programmed death-1 (PD-1) and cytotoxic T-lymphocyte antigen-4 (CTLA-4), increased to limit cell proliferation and effector functions. During infection, T cells also acquire a senescent profile characterized by downregulation of the co-activation molecules CD28 and CD27 and decreased capacity to divide in response to IL-2, leading to programmed cell death. Like T cells, also B and NK cells, as well as monocyte/macrophages and DC, are activated and display increased or dysregulated activity (84, 85).

Given the complexity of the interaction between HIV-1 and the host immune system, various factors may partecipate to chronic immune activation. The first aetiological factor is HIV-1 infection per se. Indeed, HIV-1 production not only provides alloantigens that trigger the immune system directly, but viral compontents also bind to PRRs, such as Toll-like receptors 7 and 9, and stimulate immune activation (85). In addition, viral particles, as well as viral proteins, activates target cells by signaling through CD4 and coreceptors (82). However, HIV-1 replication is neither sufficient nor necessary to induce pathological levels of immune activation. Indeed, the markers of immune activation and inflammation are still significantly higher in HAART-treated-HIV-1 patients with undetectable viral load than in uninfected individuals. Interestingly, HIV-1^+ patients who spontaneously control viral replication tend also to show a more favorable immunological profile and a reduced immune activation compared to HIV-1^+ non controllers. How these individuals are able to more effectively control immune activation than others is a key open question. Another factor contributing to chronic immune activation is represented by opportunistic infections and environmental pathogens. In fact, most HIV-1^+ individuals contain other chronic viral infections, such as human cytomegalovirus (HCMV), Epstein-Barr virus (EBV), and hepatitis C virus (HCV) (82,85).

Another aspect trigerring immune activation and dysregulation is the loss of $CD4^+$ T cells, particularly of specific $CD4^+$ T cells subsets. The majority of $CD4^+$ T cells in the body is contained in the GALT, where the massive depletion of $CD4^+$ T cells during the early phase of infection is associated with the disruption of tight junctions and the compromised integrity of the mucosal intestinal barrier, which lead to local inflammation and increased permeability of the gut epithelium (86). This favors the translocation of microbial products from the intestinal lumen to the systemic circulation and the consequent activation of various immune cells, leading to the production of pro-inflammatory factors, such as tumor necrosis factor (TNF)-α, IL-6, IL-1β and type I IFN. Indeed, a close relationship exists between high levels of some microbial translocation markers, such as, lipopolysaccaride (LPS) and sCD14, in plasma of HIV-1^+ individuals, and immune activation (84). In addition, a close association was found between the depletion of Th17 in the GALT and microbial translocation. These cells produce the cytokines IL-17 and IL-22 which are involved in intestinal epithelial barrier homeostasis as well as in mucosal defense. The preservation of Th17 avoid microbial translocation, chronic immune activation, and correlates with effective $CD4^+$ T cell restoration in gut associated lymphoid tissue of HIV-1^+ patients on HAART. Conversely, the depletion of Th17 is associated with an inceased number of regolatory T cells (Treg), resulting in the production of the anti-inflammatory cytokine IL-10 and TGF-β, and a decrease of the Th17/Treg ratio. The role of Treg cells in HIV-1 infection is still intensively debated. In fact, they could be "harmful" due to the suppression of HIV-1-specific immune responses, but could also be "beneficial" through the inhibition of chronic immune activation and consequent control of viral replication (87).

Overall, these factors contribute to create a vicious cycle in which infection stimulates immune activation and immune activation contribute to viral persistance.

Residual HIV-1 replication in anatomical santuaries may induce activation of resident cells which could reactivate latenlty infected cells and attract uninfected cells to sustain inflammation and residual replication (69, 84). The result of this strict correlation between immune activation and viral persistence, in which each one is either cause or consequence of the other, is the establishment of a chronic inflammatory state that stimulates potent and sustained immunoregulatory responses while preventing the generation of optimal HIV-1-specific immune responses, thus contributing to the development of AIDS and non-AIDS patological conditions **(Figure 10)**.

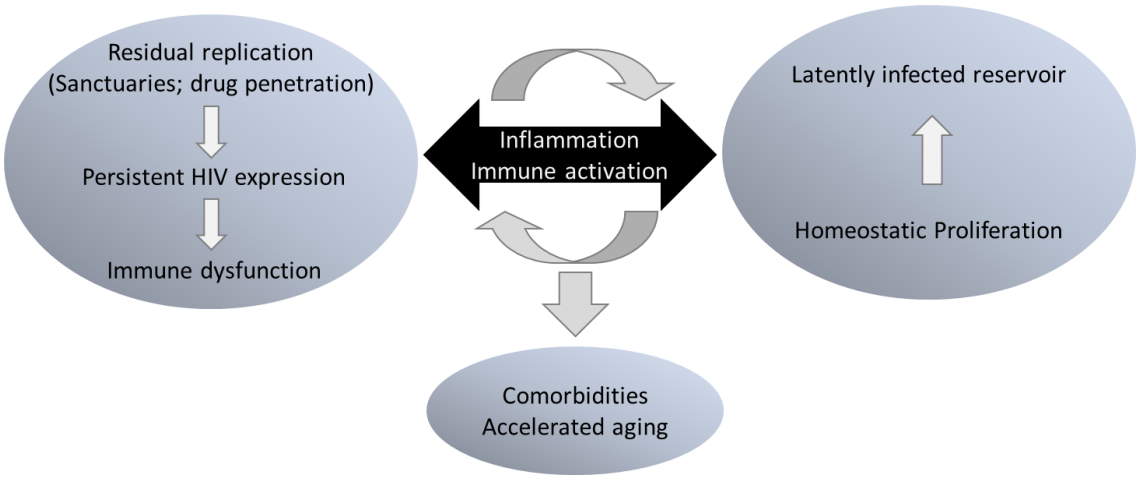

Figure 10. Role of inflammation and immune activation in HIV-1 persistence. Anatomical and cellular sanctuaries may favor residual levels of replication in tissues during HAART. Local inflammation could reactivate more latently infected cells and attract more uninfected cells into lymphoid tissue to sustain inflammation and residual replication. Chronic inflammation and immune dysfunction contribute to the development of comorbidities and accelerated aging.

In recent years, immune-modulating agents are emerging as new therapeutic approaches with the aim to directly target immune responses (78, 80, 88). One approach aims to expand HIV-1-specific $CD8^+$ T lymphocyte responses with the goal of improving virus-specific immune responses, thus accelerating the decay of the reservoir during HAART or ameliorating the control of viral rebound after therapy interruption. This concept has led to the development of several viral and non-viral vector vaccines, which

are being evaluated. Broadly neutralizing HIV-1 specific monoclonal Abs represent another strategy being explored. They target the viral reservoir and would clear virally infected cells via ADCC or Ab-dependent cell-mediated viral inhibition. An additional approach is direct neutralization of free virions that reduce chronic antigen stimulation and augment the functionality of virus-specific T cell responses, resulting in improved virologic control. However, a potential limit of this approach is the limited accessibility of Abs to certain anatomic reservoir sites (80). Another strategy to increase host immune control involves the blockade of immune checkpoint molecules, such as PD-1 and CTLA-4, which are expressed at high levels in activated T cells. Another approach being investigated is the use of Toll-like receptor (TLR) agonists or cytokines. TLR agonists may act as enhancers of anti-HIV-1 responses and as indirect LRAs, promoting reactivation of viral transcription in T cells. Actually, GS-9620, a TLR7 agonist, originally developed for the treatment of chronic viral hepatitis, is in phase I trial for HIV-1 infection (78). Treatment based on cytokines which play a role in modulating T cell proliferation, such as IL-7, IL-2, IL15 and IL-21, seems to improve $CD4^+$ T cell count. However, these cytokines also contribute to tissue inflammation and immune activation, thus increasing the number of potential viral target cells susceptible to infection. An ideal immune modifying regimen would reverse HIV-1 latency in a specific manner while preventing the negative consequences of T cell activation and proliferation. The use of immunosuppressive agents may reduce the number of activated $CD4^+$ cells. Some of these drugs, such as the mammalian target of rapamycin (mTOR) inhibitor Sirolimus (rapamycin) and the JAK/STAT inhibitor Ruxolitinib, are being evaluated (69, 78). Finally, probiotic supplementation is a new potential approach to limit the effects derived from compromised mucosal intestinal integrity and microbial translocations (82).

Chapter 3

The CCL2/CCR2 axis in the pathogenesis of HIV-1 infection

3.1 CCL2 and its receptor CCR2

CCL2, also known as monocyte chemotactic protein-1 (MCP-1), is the first discovered member of the human CC chemokine family (89). The human CCL2 gene is located on chromosome 17 and encodes for a 99 amino acid residue precursor protein with a hydrophobic signal peptide of 23 amino acids, whereas the mature peptide is composed of 76 amino acids and has a molecular weight of 13 kDa (90). CCL2 is produced by many types of cells, including endothelial, epithelial, fibroblast, smooth muscle, monocytic, astrocytic, microglial and mesangial cells and DCs, either constitutively or after induction by a variety of mediators, comprising growth factors and oxidative stress cytokines [i.e., PDGF, IL-1, IL-4, TNF-α, vascular endothelial growth factor (VEGF), LPS, IFN-γ, type I IFN and vitamin D] (91-93). The biological activity of CCL2 is mediated through the interaction with CCR2, one of the eleven CC-chemokine receptors characterized by seven trans-membrane domains and coupled to a guanosine triphosphate (GTP)-binding protein. Unlike CCL2, CCR2 expression is relatively restricted to certain cell types, mainly monocytes, NK and T cells, although it can be induced in other cell types under inflammatory conditions. Two alternatively spliced forms of CCR2 have been identified, namely CCR2A and CCR2B, which differ in their C-terminal tails and are differentially expressed on different cell types. CCR2A is the main isoform expressed by mononuclear and vascular muscle cells, whereas the CCR2B isoform is predominantly expressed by monocytes and activated NK cells. The two isoforms may activate different signaling pathways thus exerting different actions (91). CCL2 is a potent chemoattractor of

leukocytes and controls the recruitment of these cells to sites of infection and inflammation (90). As a consequence, it is involved in the pathogenesis of various chronic inflammatory conditions associated with monocyte/macrophage infiltration, such as multiple sclerosis, rheumatoid arthritis, nephropathies, diabetes, inflammatory bowel disease, bone remodeling, atherosclerosis and CNS inflammatory processes. It is also involved in cancer pathogenesis contributing to tumor growth and progression due to its pro-angiogenic properties and conversely stimulating host antitumor responses due to its ability to attract and activate lymphocytes. Finally, CCL2 is involved in the pathogenesis of infections with either bacterial or viral pathogens, such as rhinovirus, respiratory syncytial virus, HCMV, SIV, and HIV-1 (94).

3.2 Multiple roles of the CCL2/CCR2 axis in HIV-1 infection

Accumulating evidence suggests an important role of the CCL2/CCR2 axis in the pathogenesis of HIV-1 infection and in disease progression (95, 96). Several studies demonstrated that the expression of CCL2 and CCR2 is increased during HIV-1 infection. In particular, *in vitro* studies reported increased levels of CCL2/CCR2 transcripts and/or proteins following infection or exposure to viral proteins (i.e., gp120, Nef, matrix protein p17 and Tat) in different types of cells [i.e., monocytes, macrophages, peripheral blood mononuclear cells (PBMCs), astrocytes, hepatic stellate cells, human retinal pigment epithelial (HRPE) cells and mucosal tissues] **(Figure 11)** (96). In MDMs, either HIV-1 infection or exposure to gp120 resulted in CCL2 secretion increase (97-99). In some studies, this enhanced expression was linked to biological effects. For example, increased CCR2 and CCL2 expression correlated with transmigration of PBMCs, monocytes and microglia cells, whereas the induction of CCL2 release in HRPE cells was associated with the impairment of retinal pigment epithelial barrier function (100, 101). In addition, CCL2

can recruit new cells to the site of infection, thus enlarging the number of new targets for the virus.

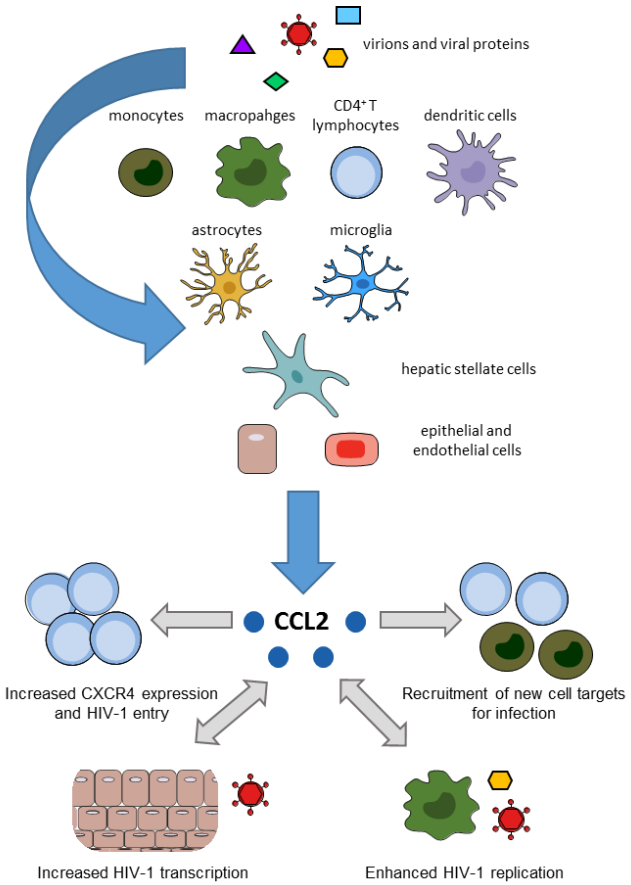

Figure 11. Model for CCL2-driven mechanisms of enhanced HIV-1 replication. Exposure to HIV-1 or viral proteins upregulate CCL2 expression in several types of cells, particularly monocytes/macrophages, astrocytes and epithelial cells. The resulting high levels of CCL2 affect HIV-1 replication in different ways. It recruits new cell targets for infection and increases CXCR4 expression on resting $CD4^+$ T lymphocytes rendering them susceptible to infection with X4 viruses. In macrophages, CCL2 enhances HIV-1 replication whereas in ectocervical tissue cells increases HIV-1 transcription. Overall, these effects enhance viral replication and may contribute to increasing viral load *in vivo* in HIV-1 infected individuals *(*Adapted from*: Covino D.A. et al. Current Drug Targets 2016).*

CCL2 can also directly affect viral replication, with different mechanisms depending on the cell type. In particular, the effect of CCL2 addition on viral replication was investigated in cultures established from $CD8^+$ T cell depleted-PBMCs of HIV-1^+ individuals that were either co-cultivated with allogeneic T cell blasts (ATCB) of uninfected individuals or directly stimulated by mitogen plus IL-2. CCL2 enhanced HIV-1 production in most patient cultures or co-cultures that were characterized by secreting

relatively low levels of this chemokine. In addition, during co-cultivation with CD8-depleted PBMCs of infected individuals, the depletion of $CD14^+$ monocytes from ATCB resulted in the downregulation of virus replication, whereas the addition of CCL2 increases HIV-1 production (102). In resting $CD4^+$ T cells, exposure to CCL2 resulted in a CCR2-dependent up-regulation of CXCR4 expression, which increased the ability of these cells to be chemoattracted by gp120 and rendered them more susceptible to X4 HIV-1 infection (103). In macrophages, CCL2 neutralization resulted in a potent inhibition of p24 Gag release with respect to control cells, in the intracellular accumulation of this viral antigen and in marked changes in cytoskeleton organization (99). Finally, CCL2 neutralization in HIV-1 infected ectocervical tissues explants from post-menopausal women resulted in decreased viral transcription (104). Overall, these results suggest that CCL2 may represent a key factor enhancing HIV-1 spreading, particularly in anatomical sites where infection of macrophages is dominant and in late stages of the disease when also X4 viruses are present.

Increased levels of CCL2 were also found *in vivo* in plasma, cerebrospinal fluid (CSF), cervical-vaginal lavages (CVLs) and renal and mucosal tissues of infected individuals (96). Increased amounts of CCL2 in blood and CVLs were associated with high viral loads and increased risk of HIV-1 acquisition as well as with low $CD4^+$ T cell counts (95, 105-111). The dysregulated expression of CCL2 and CCR2 in patients also contributes to HIV-1-related complications, mostly as a consequence of their role in leukocyte recruitment and in sustaining inflammation **(Figure 12)**. Indeed, a deregulated CCL2 production plays a key role in HIV-1-infected leukocyte infiltration into the CNS and is associated with a wide spectrum of HIV-1-related neurological complications. CCL2 was suggested to be responsible for the increased transmigration across the blood-brain barrier

(BBB) of leukocytes, particularly monocytes, macrophages and neuronal cells, such as astrocytes and microglia, leading to BBB disruption and neuronal degeneration (112, 113).

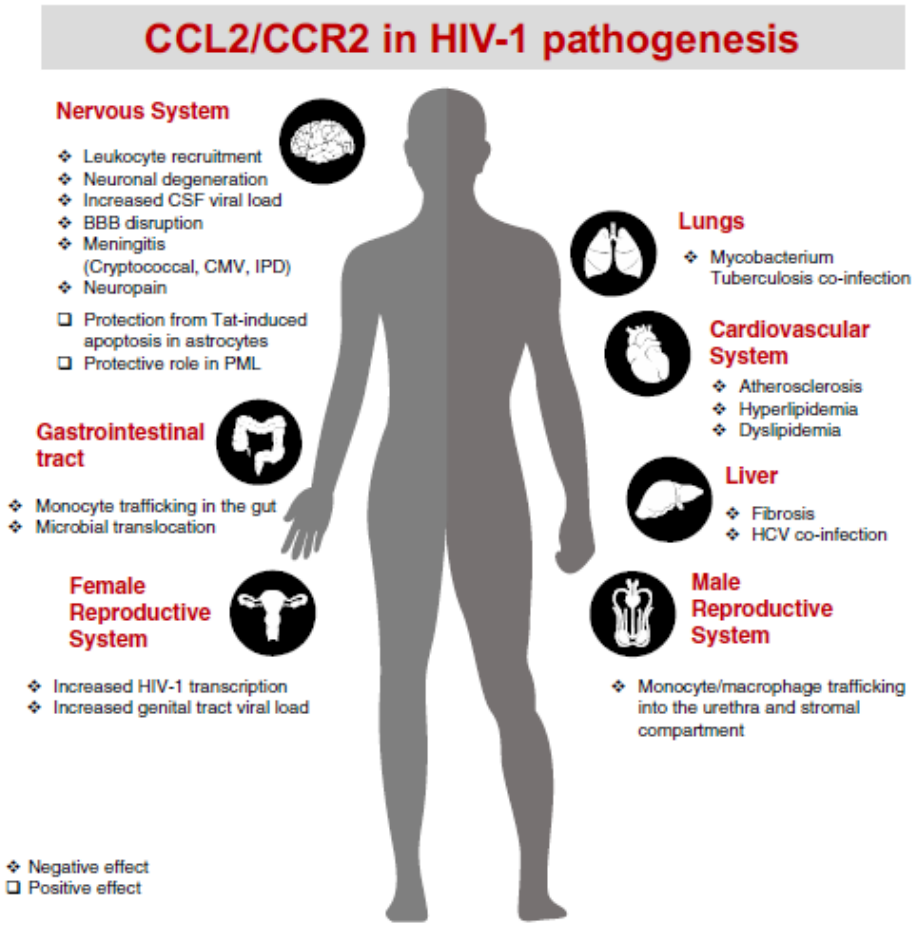

Figure 12. Schematic representation of the CCL2/CCR2 involvement in HIV-1 infection related disorders. The figure summarizes the CCL2/CCR2 driven effects in the diseases associated to HIV-1 infection in different organs/tissues (*Covino D.A. et al. Current Drug Targets 2016).*

Furthermore, CCR2 expression is increased on $CD14^{+}CD16^{+}$ monocytes in individuals with HIV-1-associated neurocognitive disorders (HANDs) compared to infected people with normal cognition, and CCR2 expression was proposed as a novel peripheral blood biomarker of HANDs (114). CCL2 is also strongly elevated in the CSF of patients with encephalitis associated with opportunistic infections such as CMV and Cryptococcus (115-118). High CCL2 levels were also detected in the broncho alveolar lavage and pleural fluids of patients coinfected with mycobacterium tuberculosis (119). In

addition, CCL2 is involved both in the initiation of liver inflammation and in keeping chronic injury following HCV infection that is common in people who are at risk or living with HIV-1 (120). Moreover, high CCL2 plasma levels can contribute to cardiovascular and metabolic dysfunctions that are common in HIV-1-infected patients (96). Finally, high CCL2 levels were found in jejunal biopsies and duodenal mucosa of patients, and contribute to leukocyte trafficking in the GALT leading to the accumulation of activated macrophages that promote microbial translocation (121).

Overall, increased expression of CCL2/CCR2 seems to be associated with enhanced viral replication as well as with at least some of the HIV-1–related disorders. Interestingly, associations between CCL2 and CCR2 allelic polymorphisms, affecting their expression or function, and AIDS progression were reported. In particular, the CCL2-2518 A/G polymorphism was associated with faster progression to AIDS and HAD. Moreover, the CCR2-V64I polymorphism was associated with a protective role against HIV-1 infection and a slower disease progression. However, not all the studies performed were concordant with the correlation between CCL2/CCR2 polymorphisms and the progression of HIV-1 pathogenesis (96).

Chapter 4

Hypothesis and Aim

The hypothesis beyond this work is that CCL2 is an endogenous negative regulator of host restriction factor expression, thus acting as a host determinant of HIV-1 pathogenesis and representing a potential target for new HIV-1 therapeutic interventions. This hypothesis stems from data, either from our or other groups, showing that, during the course of monocyte differentiation into macrophages, CCL2 expression may be correlated with A3 expression and susceptibility to HIV-1 infection. Indeed, as depicted below, monocytes express low levels of CCL2, high levels of A3 enzymes and are resistant to HIV-1 infection, whereas macrophages express high amounts of CCL2, low levels of A3 proteins, and are susceptible to infection (33, 99, 122).

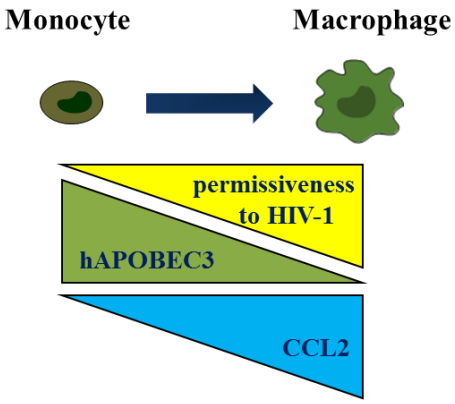

On this basis, this study aimed to: i) determine the step(s) of the HIV-1 life cycle affected by CCL2; ii) define the role of CCL2 in the regulation of host restriction factor expression and function; iii) evaluate the effect of blocking the CCR2/CCL2 axis *in vivo* in HIV-1 infected patients. To achieve this goal, we used two different approaches: i) *in vitro* studies in MDMs assessing the effect of CCL2 neutralization by specific Abs; ii) *ex vivo* studies in PBMCs from patients enrolled in study 202 evaluating the effect of CVC.

The figure below summarizes the overall experimental scheme of this thesis work:

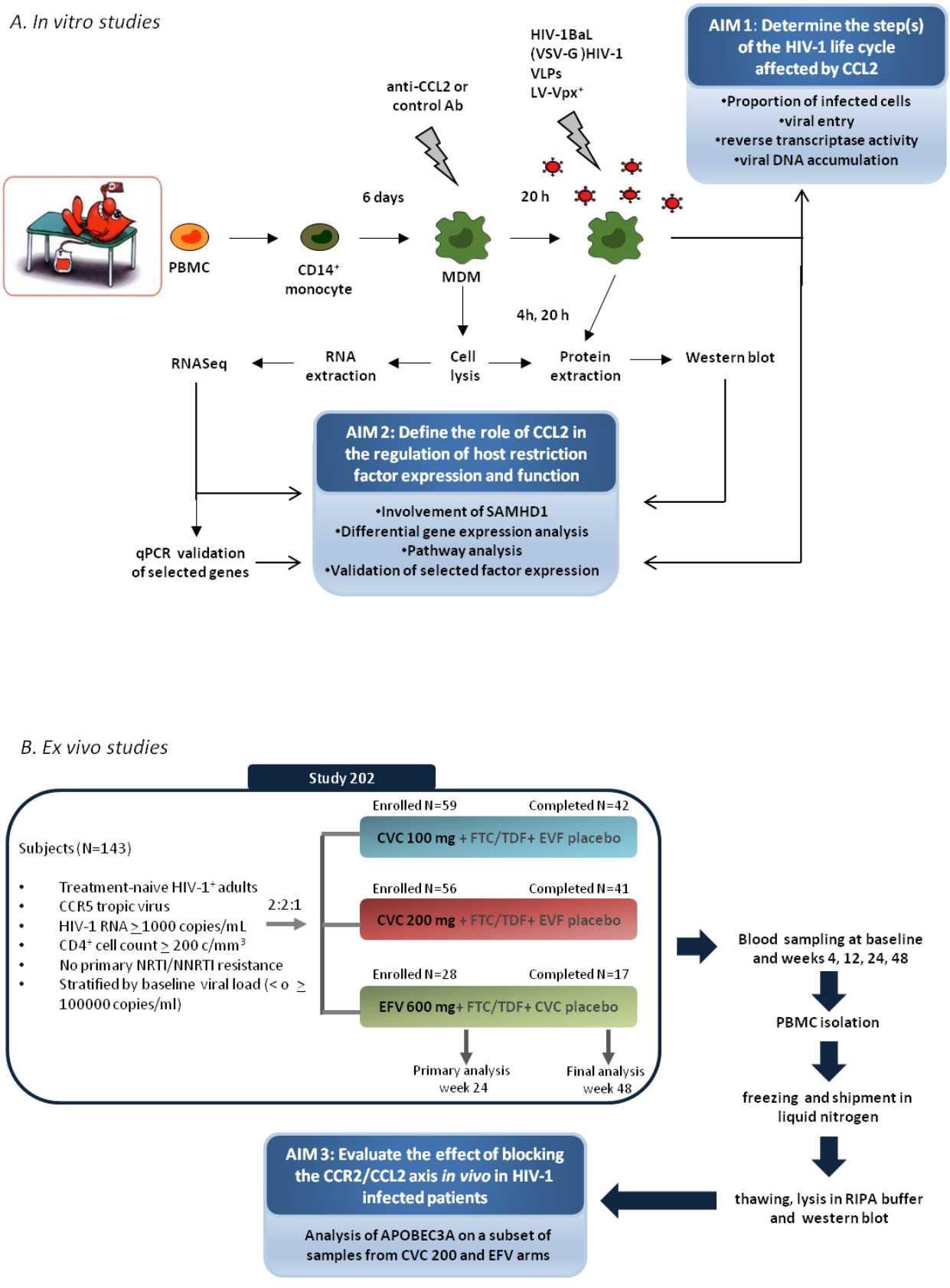

Chapter 5

Material and Methods

5.1 Ethics statements

Healthy donor Buffy coats were obtained from Centro Trasfusionale - University of Rome "Sapienza" not specifically for this study. Informed consent was not asked because data were analyzed anonymously. Data from healthy donors were treated by Centro Trasfusionale according to the Italian law on personal data management "Codice in materia di protezione dei dati personali" (Testo unico D.L. June 30, 2003 n. 196).

PBMC samples of HIV-1^+ patients enrolled in Study 202 (trial registration: NCT0133888) were obtained from Tobira Therapeutics following the establishment of Confidential Disclosure and Material Transfer Agreements between the Istituto Superiore di Sanità and Tobira Therapeutics. Study 202 was conducted in accordance with the Declaration of Helsinki. CVC is an investigational drug that has not yet been approved by FDA.

5.2 Human subjects

Antiretroviral treatment naïve HIV-1 infected adults ($\geq$ 18 years of age) with CCR5 tropic virus, plasma HIV-1 RNA level of at least 1000 copies/ml, and $CD4^+$ cell count of at least 200 cells/ul were enrolled in Study 202. Tropism was determined by phenotypic and genotypic assay. HIV-1 patients were treated with two doses of CVC (200 and 100 mg) or EFV 600 mg, all in combination with Truvada. PBMC samples, isolated from the peripheral blood of Study 202 participants collected at baseline and after 4, 12, 24, and 48 weeks of treatment, were frozen, shipped and maintained in liquid nitrogen. Samples from 17 and 15 patients of the CVC 200 and EFV arms, respectively, were used for this study.

Only for a fraction of these patients (e.g., 9 and 5 patients of CVC 200 and EFV arms, respectively), samples of all time points were available.

5.3 Monocytes isolation and differentiation to MDMs

Monocytes were isolated from the peripheral blood of healthy donors by Ficoll-Paque density centrifugation followed by immunomagnetic selection using $CD14^+$ microbeads (MACS monocyte isolation kit, Miltenyi Biotec) according to manufacturer's instructions. This procedure yields a 95-98% pure population of monocytes. Freshly isolated monocytes were seeded in 48-well cluster plates at $1x\ 10^6$ cells per well in 1 ml of endotoxin-free IMDM (Lonza) supplemented with 2 mM L-glutamine, 2 mM penicillin/streptomycin and 10% FBS (Hyclone) without the addiction of growth factors. After 6 days, the medium was replaced with 0.5 ml fresh medium and cells were treated with rabbit polyclonal Ab directed against CCL2 as well as control Ab (Peptrotech) at the doses and times indicated. In same experiments, cells were treated with recombinant IFN-α (Schering-Plough).

5.4 Viruses infection

5.4.1 Productive infection

For productive infection, cells were infected with the Vif^+ CCR5-dependent HIV-1BaL strain (3000 TCID50 per well; Advanced Biotechnologies). After 2 h, cells were washed and maintained in complete medium either in the presence or in the absence of anti-CCL2 or control Ab. Medium was replaced with fresh medium every 7 days. Abs were added twice a week. In some experiments, infected MDM were treated with dNTPs (Pharmacia) once a week.

5.4.2 Single cycle infection

HIV-1 preparations pseudotyped with VSV-G were obtained from the supernatants of 293 T cells 48 h after cotransfection with a vector expressing VSV-G under the control of CMV immediate early promoter and a vector expressing pdeltaEnvNL4-3 HIV-1 in a molar ratio 1:5. Cotransfection was performed using Lipofectamine 2000 (Invitrogen). Supernatants were clarified and concentrated by ultracentrifugation as previously described (123). VSV-G pseudotyped HIV-1 preparations were titrated in terms of HIV-1 CAp24 content using quantitative enzyme-linked immunosorbent assay (ELISA; Innogenetics). Infection with pseudotyped HIV-1 derivatives was achieved by spinoculation at 400 × g for 30 min at room temperature using 250 ng CAp24 equivalent of (VSV-G) HIV-1 per 10^5 cells. Virus adsorption was prolonged for an additional 3 h at 37°C and the cells were washed and re-fed with complete medium. Cells were analyzed 3 days post-infection. Some cultures were treated with AZT obtained from the National Institutes of Health AIDS Research and reference reagent Program.

5.4.3 HIV-1 based Viral Like Particles (VLPs)

For VLP preparations, 293/RGP cells (124) were cotransfected by using Lipofectamine 2000 with the immediate-early CMV promoter vector expressing NefG3C-GFP alone or in combination with vectors expressing VSV-G or R5 Env HIV-1 from the Ada isolate. After 6 h, cells were induced with 5 mM sodium butyrate (Sigma-Aldrich) and 2 μM of Ponasterone A (Sigma-Aldrich) for 24 h. Supernatants were then replaced with fresh medium containing the inducers. VLP-containing supernatants were harvested from 48 to 72 h later, clarified, and concentrated by ultracentrifugation on 20% sucrose cushion at 100,000 g for 2 h at 4°C. VLP preparations were titrated by measuring the HIV-1 CAp24 contents by ELISA. For MDM challenge, VLPs (1 μg of CAp24 equivalent per 10^5

cells) were absorbed by spinoculation at 150 g for 30 min at room temperature or at 4°C. Afterwards, the cell cultures were re-fed by adding fresh medium, and incubated at 37 or 4°C. After 2 or 4 h, the cells were treated for 15 min with trypsin at 37 or 4°C, fixed, and analyzed by flow cytometry. Some cultures were treated with soluble LDLR (R&D Systems) or T20 obtained from the National Institutes of Health AIDS Research and Reference Reagent Program.

5.4.4 HIV-1 based lentiviral vector (LV) containing SIV-Vpx (LV/Vpx)

For lentivirus preparations a total of 12 μg of plasmid DNA were used for each plate in a ratio 6:4:2 (transfer vector: packaging vector: VSV-G vector). The plasmids pCMVdR8.2, the VSV-G envelope expressing pMD.G plasmid and the pTY2-CMV-GFP-W transfer vector have been already described (125, 126). For construction of SIV-Vpx expressing plasmid, Vpx derived from the SIVMAC251 strain was modified (127) and 10 μg of this plasmid were included in the transfection. 293 T cells were transiently transfected with the calcium phosphate-based protocol using the Calcium Phosphate-based Profection Mammalian Transfection System (Promega Corporation) and the supernatants were clarified and concentrated by ultracentrifugation as previously described (128). Lentiviral titres were normalized by RT (129). Infection was achieved by spinoculation at 400 g x g for 30 min at room temperature using 2 $x10^6$ TU of LV/Vpx per 10^6 cells. Virus adsorption was prolonged for an additional 3 h at 37^o C and the cells were washed and re-fed with complete medium. Cells were analyzed 3 days post-infection.

5.5 Evaluation of CCL2 release

The levels of CCL2 released in culture supernatants were measured by ELISA kits (R& D Systems; detection limit 5 pg/ml). Supernatants were collected, centrifuged to remove cell debris, and frozen before CCL2 determination.

5.6 Flow cytometry analysis

For intracellular p24 Gag detection, MDMs were detached by using 0.05% trypsin-EDTA solution, fixed and permeabilized by using Fixation and Permeabilitation Buffers (eBioscience). Cells were then labeled with a Phycoerythrin-conjugated monoclonal Ab specific for p24 Gag (KC57-R01, Coulter Clone) and washed with Permeabilization Buffer. The background fluorescence was determined by labelling uninfected cells.

To evaluate the fraction of GFP^+ cells in MDMs challenged with VLPs or LV/Vpx, cells were treated with trypsin and fixed with paraformaldehyde 2%.

Samples were acquired with a FACS Calibur flow cytometer by using Cell Quest (Becton Dickinson) and data analyzed by FlowJo (Tree Star, Inc.) or the Cell Quest software.

5.7 Analysis of HIV-1 DNA synthesis during early phase of transcription by polymerase chain reaction

A semi-quantitative PCR assay was used to estimate the extent of reverse transcription at three replicative steps: R-U5, initial minus strand synthesis; R-PB, initial plus strand synthesis up to the PB region; and R-gag, complete minus-strand synthesis. The primers used to amplify these products were M667/AA55 (R-U5) producing a 140 bp amplicon, M667/BB301(R-PB) producing a 156 bp amplicon, and M667/M661 (R-gag) producing a 200 bp amplicon (M667, 5′-GGCTAACTAGGGAACCCACTG3′; AA55, 5′-CTGCTAGAGATTTTCCACACTGAC-3′; BB301, 5′-

CCCTGTTCGGGCGCCACTG-3′; M661, 5′-CCTGCGTCGAGAGAGCTCCTCTGG-3′). DNA load for each PCR amplification was normalized by Real-Time PCR quantitative amplification of RNase P gene using TaqMan RNase P Detection Reagents Kit (Applied Biosystems) according to manufacturer's instructions. Quantization of HIV-1 DNA during PCR amplification was performed by analyzing a standard curve of serial dilutions of HIV plasmid pHxb2 ranging from 1 to $1x10^5$ copies. PCR conditions were: 95°C, 3 min; 95°C, 30 s; 60°C, 30 s; 72°C, 30 s, for 35 cycles.

The quantitative analysis of HIV-1 intermediate reverse-transcript products was performed by SYBR Green real-time PCR of minus-strand strong-stop DNA using M667/AA55 primers and of 1st template switching of RT using M667/BB301 primers. A standard curve was generated using serial dilution ranging from 10,000 to 1 copy of pHxb2 plasmid containing the full length sequence of HIV. Each primer was used at a final concentration of 200 nM. The PCR parameters were as follows: 20 sec at 95°C followed by 40 cycles at 95°C for 15 sec and 60°C for 1 min. Fluorescent product was detected at the last step of each cycle. After amplification a melting curve was generated. All samples and HIV-1 negative controls were run in duplicate.

5.8 Quantification of HIV-1 DNA by real-time polymerase chain reaction

Total DNA was extracted from frozen MDM samples using the QIAamp DNA Blood Mini kit (Qiagen) according to the manufacturer's instructions; in each extraction uninfected cells were included as negative control. The concentration of the extracted DNA was determined by Real-Time PCR quantitative amplification of RNase P gene using TaqMan RNase P Detection Reagents Kit.

Total HIV-1 DNA amount was determined using primers and probe that recognize the HIV-1 gag gene (22). Standard curve was generated using the genomic DNA from the 8E5 cell line, a T lymphoblastoid cell line that contains a single defective copy of HIV-1 genome per cell.

Integrated HIV DNA was quantified by a two-step Alu-gag PCR assay. The first PCR was performed in triplicate for each sample, using two primers annealing to Alu sequences (AluFw 5′ -GCCTCCCAAAGTGCTGGG ATTACAG-3′ ; AluS 5′ -TCCCAGCTACTGGGGAGGCT GAGG-3′ ; final concentration: 100nM each) and one primer annealing to gag gene (HIV-gag Rev nt 1505– 1486: 5 ′ -GTTCCTGCTATGTCACTTCC-3 ′ ; final concentration: 600nM). Samples were amplified in triplicate also with the HIV-gag Rev primer alone (gag-only PCRs) in order to establish whether the level of integration is detectable (see below). Standard curve was generated using serial dilutions of genomic DNA extracted from a standard cell line prepared as previously described (130). The number of HIV proviruses per cell of the standard cell line was calculated with the same procedure used to calculate total HIV-1 DNA and then adjusting the result by the number of assayed cells calculated by RnaseP gene quantification. The standard curve ranged from 10,000 to 1 integrated HIV-1 copies per well. To keep the number of Alu DNA sites constant in each reaction, uninfected PBMC genomic DNA was added to each sample (including standards and controls) to reach the concentration of 70 ng of genomic DNA per well. The parameters for the first PCR were as follows: 10 min at 95°C followed by 25 cycles at 95°C for 15 sec, 50°C for 15 sec and 72°C for 3 min and 30 sec and finally 5 min at 72°C. The second Real-time PCR step detects HIV specific products by using primers annealing to the R and U5 regions within the HIV LTR: RU5 R forward (5′ -TTAAGCCTCAATAAAGCTTGCC-3 ′), RU5 U5 reverse (5′ -GTTCGGGCGCCACTGCTAGA-3′) and RU5 Probe (5′ -

CCAGAGTCACACAACAGACGGGCACA-3′); this Real-time PCR was performed on 5 ul from each replicate of both Alu-gag and gag-only PCRs of standard curve and unknown samples. The PCR parameters were as follows: 3 min at 95°C followed by 45 cycles at 95°C for 3 sec and 60°C for 30 sec. Student's t-test was performed to determine whether Cts derived from the Alu-gag PCRs were significantly lower than those from the gag-only reactions. If Alu-gag Cts are statistically lower than gag-only Cts ($p < 0.05$) for the same sample, HIV-1 integrated copies can be calculated with reference to the standard curve. Otherwise, the level of integration is to be considered below the limit of detection of the assay (130).

The 2-LTR DNA circles were quantified by SYBR Green real-time PCR and amplified from extracted DNA with 25 nM forward primers HIV-F (5′ -TGTGCCCGTC TGTTGTGTGACT-3 ′) and 25 nM reverse primer HIV-1R1 (5 ′ - TGGTGCTACAAGCTAGTACCAGT-3′) spanning the LTR–LTR junction (modified protocol from Reigadas S et al.) (131). A plasmid containing the 2-LTR junction sequence was used to generate the standard curve (ranging from 10,000 to 1 copy) for 2-LTR DNA circles quantification; each curve point was obtained diluting the plasmid DNA in 50 ng of genomic DNA from HIV negative donors PBMCs. The PCR parameters were as follows: 20 sec at 95°C followed by 45 cycles at 95°C for 3 sec and 62°C for 1 min. Fluorescent product was detected at the last step of each cycle. After amplification a melting curve was generated. All samples and HIV-1 negative controls were run in triplicate. Rnase-P, HIV-1 gag and HIV-1 2LTR standard curves had slopes between −3.15 and −3.6 and the coefficients of correlation was >0.987. HIV-1 DNA load and HIV-1 2-LTR circles load were normalized to the amount of cellular DNA by quantification of RNAseP copies and were expressed as number of copies/10^6 cells. The limit of detection was 2 copies/10^6 cells for total HIV-1 DNA and 200 copies/10^6 cells for HIV-1 2-LTR circles. The ABI Prism

7500 FAST Real-time PCR System (Applied Biosystem) was used for PCR amplification, acquisition and data analysis.

5.9 Quantification of host restriction factors by real-time polymerase chain-reaction

Total RNA was isolated with RNeasy Plus Micro kit (Qiagen) according to the manufacturer's instructions and was quantified by NanoDrop ND-1000 Spectrophotometer. RNA was retrotranscribed into cDNA by using poly d(N)6 (GE Healthcare) and Real-time PCR was performed on an ABI-Prism 7000 PCR cycler (Applied Biosystems, Foster City, CA) using the TaqMan universal master mix (Applied Biosystems) according to the manufacturer's instructions. Validated PCR primers and TaqMan MGB probe (6FAM-labeled) for A3A (Hs00377444; AppliedBiosystem) and Mx2 (Hs.PT.58.21491026; Integrated DNA Technologies) were used. As endogenous control, primers and TaqMan probe for the human β-actin (ACTB RNA; Hs99999903_m1; Applied Biosystems) were used. Thermal cycler conditions were as follows: 2 min at 55°C, 10 min at 95 C, followed by 40 cycles of denaturation (15 sec at 95°C) and combined annealing/extension (1 min at 60°C). Relative quantification was performed using the comparative Ct method: arithmetic formulas were used to calculate relative expression levels, and compare with a calibrator (untreated MDMs). The amount of target, normalized to endogenous housekeeping gene (ACTB) and relative to the calibrator, is then given by $2^{-\Delta\Delta Ct}$, where $\Delta\Delta Ct = \Delta Ct(\text{target}) - \Delta Ct(\text{calibrator})$, and ΔCt is the Ct of the target gene subtracted from the Ct of the housekeeping gene. The equation thus represents the normalized expression of the target gene in the unknown sample, relative to the normalized expression of the calibrator sample.

5.10 RNA sequencing and differential expression analysis

RNA samples were collected individually from three donors and subjected to poly (A) selection followed by reverse transcription. RNAseq libraries were created with the Illumina Truseq RNA sample pre kit and sequenced using the Illumina Hiseq 2500 platform. Samples were sequenced 3 times in multiplexed lanes and reads of the same sample from the 3 runs were pooled together. Tophat (132) (Version 2.0.6) together with bowtie (version 0.12.8) were used to align reads to human genome GRCh37/hg19 with Ensembl 75 gene annotation. Only uniquely mapped reads were used to count reads aligned to each gene. The reads were quantified by htseq-count (133) (version 0.5.3p9) with Ensembl 75 gene sets. Gene differential expression analysis was performed using DESeq2 (134) (version 1.4.5). Genes which had no reads across all samples were discarded. Genes with and with more than a two-fold change in expression and an adjusted p-value of less than 0.1 were classified as significantly differentially expressed. The **D**atabase for **A**nnotation, **V**isualization and **I**ntegrated **D**iscovery (DAVID) was used to perform pathway analysis of genes upregulated at 20 h and downregulated at 4h, whereas the **G**ene **O**ntology en**RI**chment ana**L**ysis and visua**L**iz**A**tion tool (GOrilla) was used for the analysis of genes upregulated at 4 h.

5.11 Western blot analysis of host restriction factors

Whole cell extracts were prepared by lysing cells in RIPA buffer [150 mM NaCl, 50 mM Tris-Cl (pH 7.5), 1% Nonidet P-40, 0.5% sodium deoxycholate, and 0.1% sodium-dodecyl sulfate (SDS)] containing a cocktail of protease (Roche) and phosphatase inhibitors (Sigma-Aldrich). Protein concentration was determined using the Bradford reagent (Bio-Rad) and a standard curve obtained with bovine serum albumin (Bio-Rad). Cell lysates (10 μg per lane) were fractionated on 8-12% SDS-PAGE and electroblotted to

nitrocellulose filters (Protran BA 85, Schleicher & Schuell). Membranes were incubated with 4% fat-free milk dissolved in PBS-T (PBS 1X, 0.05%) to block non-specific binding and then probed with the following Abs: anti-human A3A (rabbit polyclonal D23, Santa Cruz Biotechnology), anti-human SAMHD1 (rabbit polyclonal 366–380, Sigma-Aldrich), anti-human Mx2 (goat polyclonal N17, Santa Cruz Biotechnology), and anti-actin (mouse monoclonal Abs-5, BD Biosciences) as gel loading control. The anti p-SAMHD1 T592 Ab was kindly provided by Alexandra Cribier (51). Blots were then incubated with appropriate secondary Abs conjugated with horseradish peroxidase (Santa Cruz Biotechnology) followed by ECL Western blot detection Reagent (Amersham) or SuperSignal West Femto Substrate (Pierce) according to the manufacturer's instructions. Levels of A3A and Mx2 proteins were quantified using a GS-800 Calibrated Densitometer (Bio-Rad Laboratories).
For western blot analysis of patient PBMC samples, protein concentration was determined as previously described reading in triplicate each sample. Cell lysates (20 μg per lane) were fractionated on 12% SDS-PAGE and A3A and actin expression was detected by Chemidoc XRS (Biorad). To develop a more quantitative western blot, a standard curve was generated using a dose-scale concentration (20-10-5 ug) of protein extracts derived from healthy donor PBMCs. This standard curve was used to assess the best Ab dilutions and was included in the blots of all the patients analyzed.

5.12 Statistical analysis

Results were reported as means ± SE or SEM. Comparison between two groups was performed using paired, two-tailed t test. One-way and Two-way analysis of variance (ANOVA) followed by Dunnett or Bonferroni's Multiple Comparison Test, respectively, was used for the statistical analysis of PBMC samples from Study 202. Differences were considered significant at $p<0.05$ (*$p < 0.05$; ** $p < 0.01$; *** $p < 0.001$). Statistical

analysis was performed by using Microsoft Office Excel 2007 software or GraphPad Prism 5.0.

Chapter 6

Results

6.1 Effect of CCL2 neutralization on the different steps of the HIV-1 life cycle in MDMs

6.1.1 Neutralization of CCL2 decreases the proportion of HIV-1 infected MDMs

Our group previously demonstrated that CCL2 neutralization reduced the release of p24 Gag in HIV-1 infected MDMs (99). To investigate the mechanisms by which CCL2 blocking inhibits HIV-1 replication in these cells, we assessed whether neutralization of this chemokine affected the total number of infected cells. To this aim, MDM cultures established from 22 donors were treated with anti-CCL2 or control Ab for 20 h and then challenged with HIV-1_{BaL}. The proportion of infected cells was determined 14 days post-infection by flow cytometry after staining for intracellular p24 Gag. We found a great variability in the percentage of p24 Gag^+ cells among donors **(Figure 13A)**. However, treatment with anti-CCL2 Ab strongly reduced the percentage of p24 Gag^+ cells in all the donors analyzed, whereas only an occasional effect of the control Ab was observed. As shown in **Figure 13B**, the exposure to anti-CCL2 Ab reduced the faction of p24 Gag^+ cells to 0.23 ± 0.04 (mean ± SE) fold compared to control Ab treatment ($p < 0.001$). Measurement of CCL2 release in Ab treated cultures showed that the anti-CCL2 Ab effectively neutralized the chemokine produced by MDMs in these experimental conditions **(Figure 13C)**.

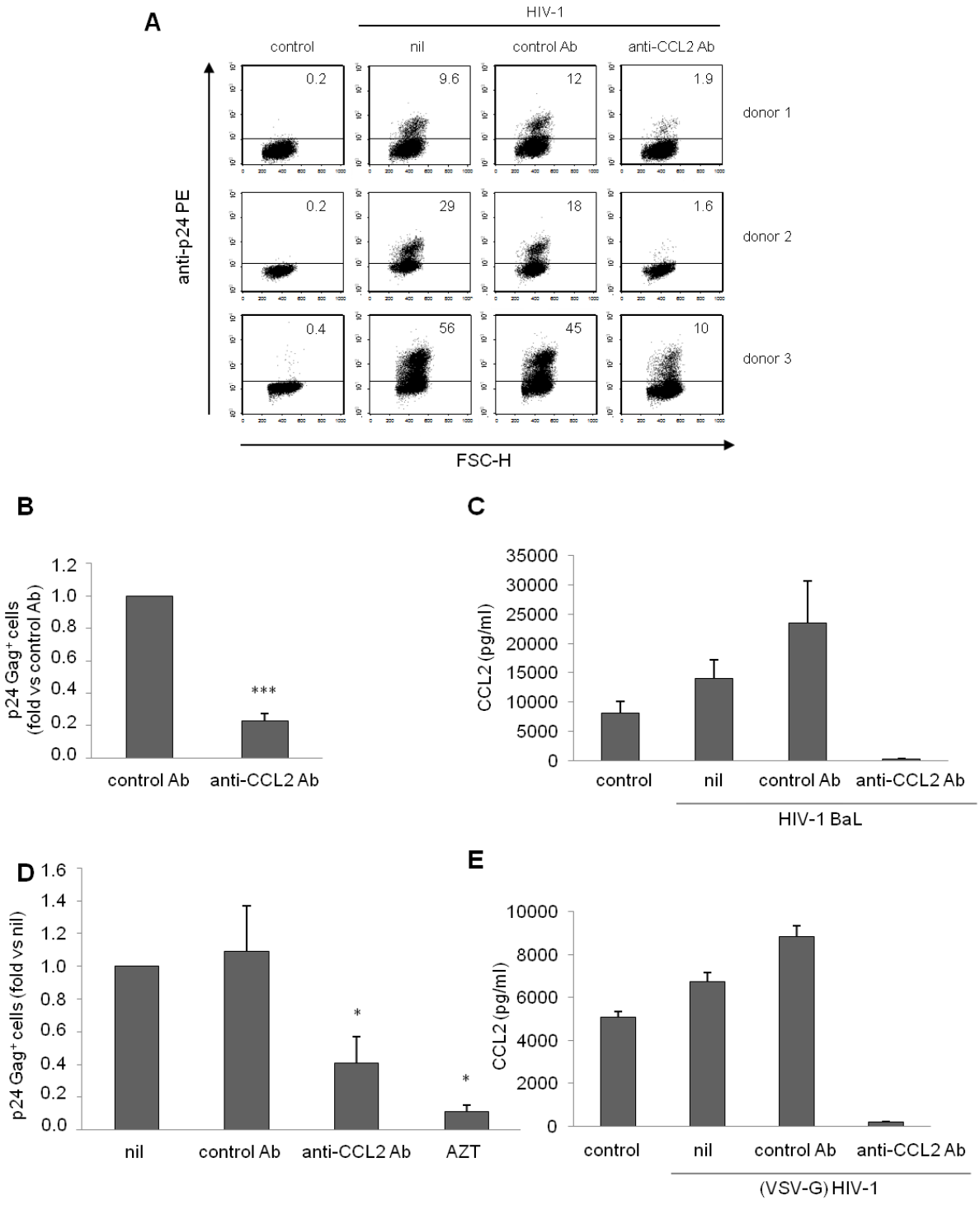

Figure 13. Neutralization of endogenous CCL2 reduces the proportion of HIV-1 infected MDMs. MDMs were treated with anti-CCL2 or control Ab (2.5 μg/ml) for 20 h, and then challenged with HIV-1_{BaL} (3000 $TCID_{50}$ per well) (A-C) or (VSV-G) HIV-1 (250 ng CAp24 equivalent per 10^5 cells) (D, E). Intracellular HIV-1 p24 Gag expression and CCL2 release were evaluated 14 (A-C) or 3 (D, E) days post-infection by flow cytometry or ELISA, respectively. In D, some cultures were treated with AZT (10 μM). In A, the results from 3 representative donors out of 22 tested are shown. In B, data represent mean values (+ SE) of the results obtained with all the donors analyzed. ***$p < 0.001$ (anti-CCL2 Ab vs. control Ab). In C, data represent mean values (+SE) of the results obtained with 6 donors. In D, data represent mean values (+SE) of the results obtained with MDMs from 4 different donors. *$p < 0.05$ (anti-CCL2 Ab or AZT vs. nil). In E, the results from 1 representative donor out of 2 tested are shown.

To investigate whether CCL2 blocking also inhibited a single cycle infection, we used a recombinant virus, mutated in the *env* gene and pseudotyped with VSV-G, which enters macrophages through a CD4/CCR5-independent pathway and completes only a single round of infection (135). MDMs were treated with anti-CCL2 or control Ab for 20 h, challenged with (VSV-G) HIV-1 and the percentage of p24 Gag^+ cells was measured 3 days post-infection. Treatment with anti-CCL2 Ab reduced the percentage of p24 Gag^+ MDMs to 0.41 $\pm$ 0.16 (mean + SE) fold with respect to untreated cells ($p < 0.05$) **(Figure 13D)**. To ensure that the detected fraction of infected cells was not biased by cell membrane-attached p24 Gag, we performed control experiments in the presence of AZT. As expected, a strong reduction in the fraction of p24 Gag^+ cells was observed in the presence of this drug. Measurement of CCL2 release in Ab treated cultures showed that the anti-CCL2 Ab effectively neutralized the chemokine produced by MDMs also in these conditions **(Figure 13E)**.

6.1.2 CCL2 neutralization does not affect HIV-1 entry and RT activity in MDMs

To evaluate whether the inhibitory effect of CCL2 blocking on HIV-1 replication could be due to reduced viral entry, we used VLPs pseudotyped with either VSV-G or R5 HIV-1 Env from the Ada strain (VSV-G –VLPs and Ada VLPs, respectively). MDMs were exposed for 20 h to anti-CCL2 or control Ab, then challenged with VLPs and the percentage of GFP^+ cells was measured after 2 and 4 h of incubation at 37°C. Control experiments were performed by incubating cells at 4°C. About 50% of MDMs were GFP^+ following 2 h of incubation with VSV-G-VLPs, whereas viral entry driven by Ada-VLPs was less efficient and rendered fluorescent about 10% of the cells **(Figure 14A)**. Treatment with anti-CCL2 or control Ab did not modify entry of either VSV-G-VLPs or Ada-VLPs.

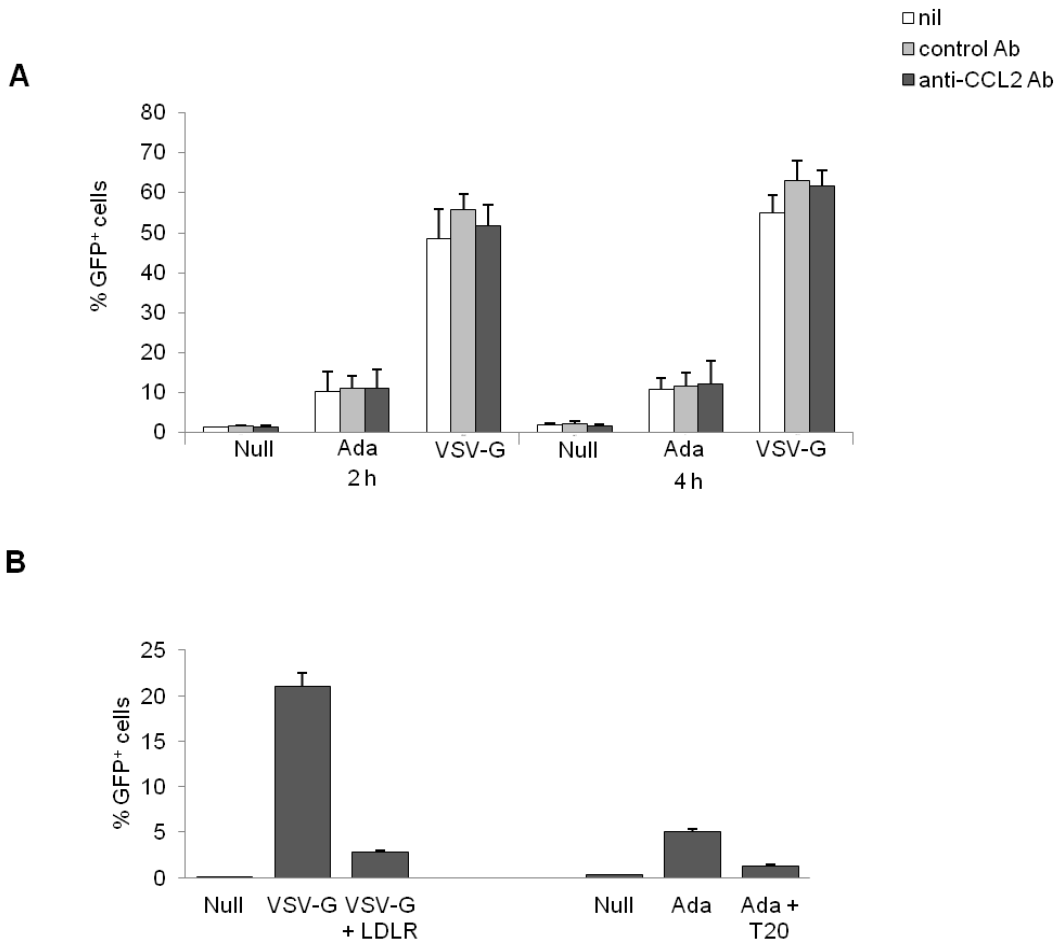

Figure 14. Endogenous CCL2 neutralization does not affect HIV-1 entry in MDMs. (A) MDMs were treated with anti-CCL2 or control Ab (2.5 μg/ml) for 20 h and then challenged with Null-VLPs, VSV-G-VLPs or Ada-VLPs (1 μg of CAp24 equivalent per 10^5 cells). After 2 and 4 h, the percentage of GFP^+ cells was assessed by flow cytometry. Data represent mean values (+SE) of the results obtained with MDMs from 4 different donors. (B) MDMs were treated as in A and then challenged with VSV-G-VLPs or Ada-VLPs either in the presence or in the absence of soluble LDLR (5 μg/ml) or T20 (1 μg/ml). The results obtained with 1 out of 2 different donors analyzed are shown.

Control experiments were performed in the presence of soluble LDLR or T20 to block fusion of VSV-G-VLPs or Ada-VLPs, respectively (136, 137). As shown in **Figure 14B**, a strong reduction in the fraction of GFP^+ cells was observed in these conditions, thus confirming that the fluorescence detected in target cells relied on authentic viral fusion events.

We then assessed whether CCL2 neutralization affected early post-entry events of the HIV-1 life cycle, particularly RT activity. To this aim, we evaluated HIV-1 DNA

synthesis by semi-quantitative PCR at 24 h post-infection. The primers used in this assay amplify different regions of the HIV-1 genome to estimate the extent of reverse transcription at three replicative steps that occur in subsequent order during reverse transcription: R-U5, initial minus strand synthesis; R-PB, initial plus-strand synthesis up to the PB region; and R-gag, complete minus-strand synthesis (138). The results of these experiments indicated that the presence of anti-CCL2 Ab did not influence HIV-1 DNA synthesis in the infected

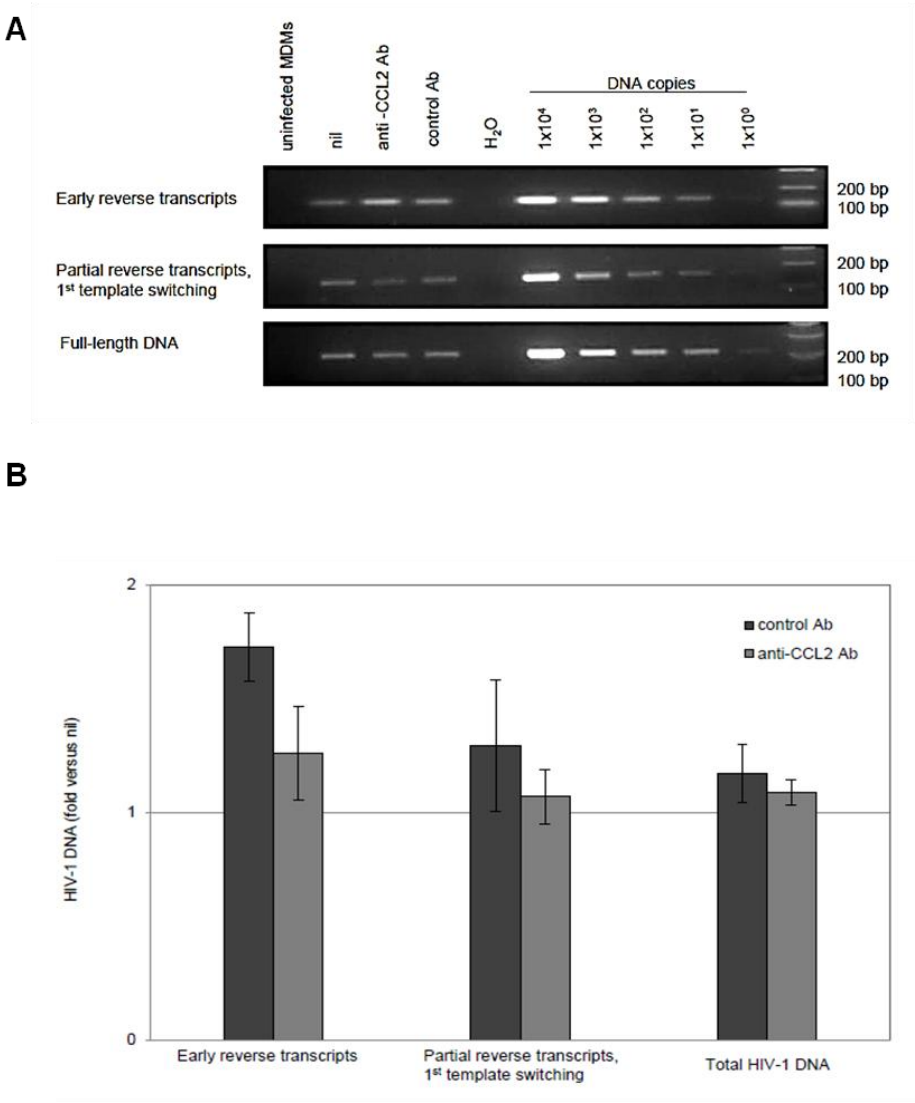

Figure 15. Endogenous CCL2 neutralization does not affect HIV-1 DNA intermediates synthesis in MDMs. MDMs were treated with anti-CCL2 or control Ab (2.5 μg/ml) for 20 h and then infected with HIV-1_{BaL} (3000 $TCID_{50}$ per well). Total DNA was extracted 24 h after infection and the levels of HIV-1 DNA intermediates (early, partial reverse and full-length transcripts) were assessed by semi-quantitative PCR (A) or quantitative Real-Time PCR (B). The results from 1 representative donor out of 2 tested are shown.

cells early post-infection **(Figure 15A)**. These results were confirmed by further evaluation of the HIV-1 DNA intermediates by a quantitative PCR Real-Time assay **(Figure 15B)**. Overall, these results demonstrate that CCL2 blocking does not interfere with both entry and RT activity.

6.1.3 Neutralization of CCL2 impairs HIV-1 DNA accumulation in MDMs

To further investigate the mechanisms underlying the anti-HIV-1 effect mediated by CCL2 blocking, we quantified the levels of viral DNA that accumulated at different time points post-infection. MDMs exposed to anti-CCL2 or control Ab for 20 h were challenged with HIV-1_{BaL} and total viral DNA was quantified 4 and 7 days post-infection. As shown in **Figure 16A**, CCL2 neutralization strongly influenced the kinetics of HIV-1 DNA accumulation. In fact, a marked increase of total viral DNA was observed in both untreated and control Ab treated cells at 7 vs 4 days post-infection, whereas in anti-CCL2 Ab treated MDMs the levels of HIV-1 DNA at 7 days post-infection were similar to those found 4 days after infection.

We next examined the concentration-dependency of the effect of anti-CCL2 Ab on HIV-1 DNA levels after 7 days of infection. The treatment with anti-CCL2 Ab decreases viral DNA in a concentration dependent manner and this reduction was statistically significant at all the concentrations tested [0.08 ± 0.03 (mean ± SE), 0.12 ± 0.04 (mean ± SE) and 0.37 ± 0.07 (mean ± SE) at the concentrations of 2.5 ($p < 0.001$), 1.25 ($p < 0.01$) and 0.625 ($p < 0.05$) μg/ml, respectively] **(Figure 16B)**. We also investigated the effect of CCL2 neutralization on the accumulation of different intracellular forms of viral DNA. HIV-1 genome is preferentially integrated into host DNA, but multiple forms of unintegrated viral DNA exist, including linear cDNA and circular forms.

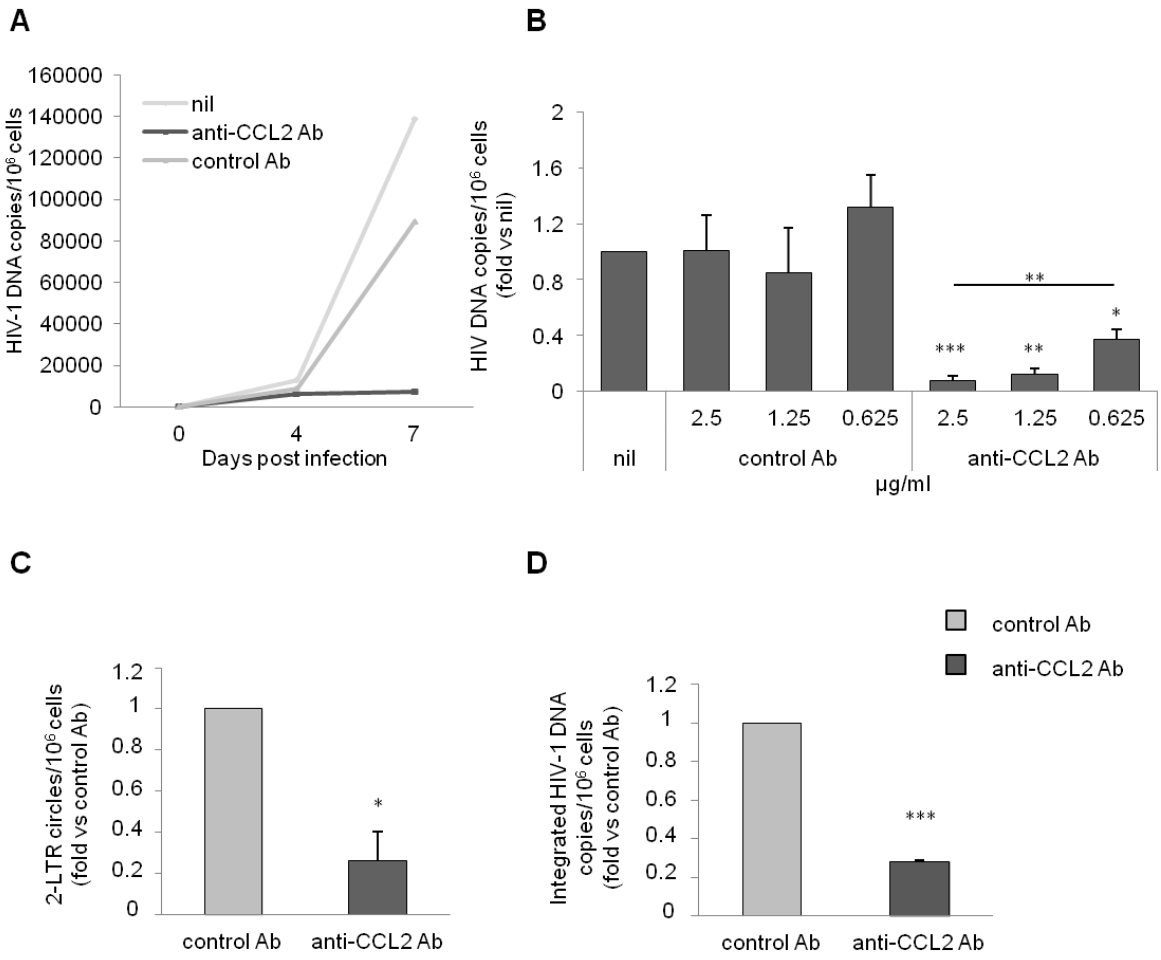

Figure 16. Neutralization of endogenous CCL2 impairs HIV-1 DNA accumulation in MDMs. (A) MDMs were treated with anti-CCL2 or control Ab (2.5 µg/ml) for 20 h and then infected with HIV-1 $_{BaL}$ (3000 $TCID_{50}$ per well). Total DNA was extracted 4 and 7 days after infection and the amount of total HIV-1 DNA (copies/10^6 cells) was determined by qPCR. The results from 1 representative donor out of 4 tested are shown. (B). MDMs were treated with different concentrations of anti-CCL2 or control Ab (2.5, 1.25 and 0.625 µg/ml) for 20 h and then infected as in A. Total DNA was extracted 7 days after infection and the amount of total HIV-1 DNA was determined by qPCR. (C, D) MDMs were treated and infected as in A. Total DNA was extracted 7 days after infection and the amounts of HIV-1 2-LTR circles (C) and integrated HIV-1 DNA (D) were determined by qPCR. Data represent mean values (+SE) of the results obtained with 3 (B and D) and 4 (C) different donors. *$p < 0.05$; **$p < 0.01$; ***$p < 0.001$.

These latter can be classified as 1-LTR and 2-LTR based on the number of LTR (139). The presence of anti-CCL2 Ab significantly reduced the amount of (2-LTR) DNA circles [0.26 ± 0.14 (mean ± SE) fold vs. control Ab; $p < 0.05$] **(Figure 16C)** and of integrated proviral DNA [0.28 ± 0.007 (mean ± SE) fold vs. control Ab; $p < 0.001$] **(Figure 16D)**.

Overall, these data indicate that CCL2 neutralization significantly impairs HIV-1 DNA accumulation.

6.2 Effect of CCL2 neutralization on host restriction factor expression and function in MDMs

6.2.1 SAMHD1 expression and function is not involved in the CCL2 blocking mediated inhibition of viral replication in MDMs

Searching for cellular correlates of the post-entry restriction of HIV-1 replication mediated by CCL2 blocking in MDMs, we first focused our attention on SAMHD1, a host factor that restricts HIV-1 replication in myeloid cells by either depleting dNTPs levels below those required for optimal synthesis of viral DNA or degrading HIV-1 RNA (45). Therefore, we assessed the effect of CCL2 neutralization on SAMHD1 expression and phosphorylation, which may potentially regulate the RNase activity of this enzyme. As shown in **Figure 17A**, neither SAMHD1 constitutive expression nor its phosphorylation were affected by anti-CCL2 Ab treatment in uninfected MDMs. Similarly, SAMHD1 protein expression was not affected by CCL2 blocking in HIV-1-infected MDMs **(Figure 17B)**. These findings strongly suggest that the mechanism of inhibition of HIV-1 replication induced by anti-CCL2 Ab do not involve modulation of SAMHD1 expression or phosphorylation. We further investigated whether SAMHD1 dNTPase activity could be regulated by CCL2 blocking. To this aim, we evaluated the effect of dNTPs supply in our experimental conditions. MDMs exposed for 20 h to anti-CCL2 or control Ab were infected with HIV-1_{BaL} either in the absence or in the presence of dNTPs and the percentage of p24 Gag^+ cells was assessed 14 days post-infection. As shown in **Figure 17C**, the percentage of p24 Gag^+ cells was similarly reduced by anti-CCL2 Ab both in the

absence and in the presence of exogenous dNTPs, thus suggesting that SAMHD1 dNTPase activity is not involved in the restriction of HIV-1 replication mediated by CCL2 blocking.

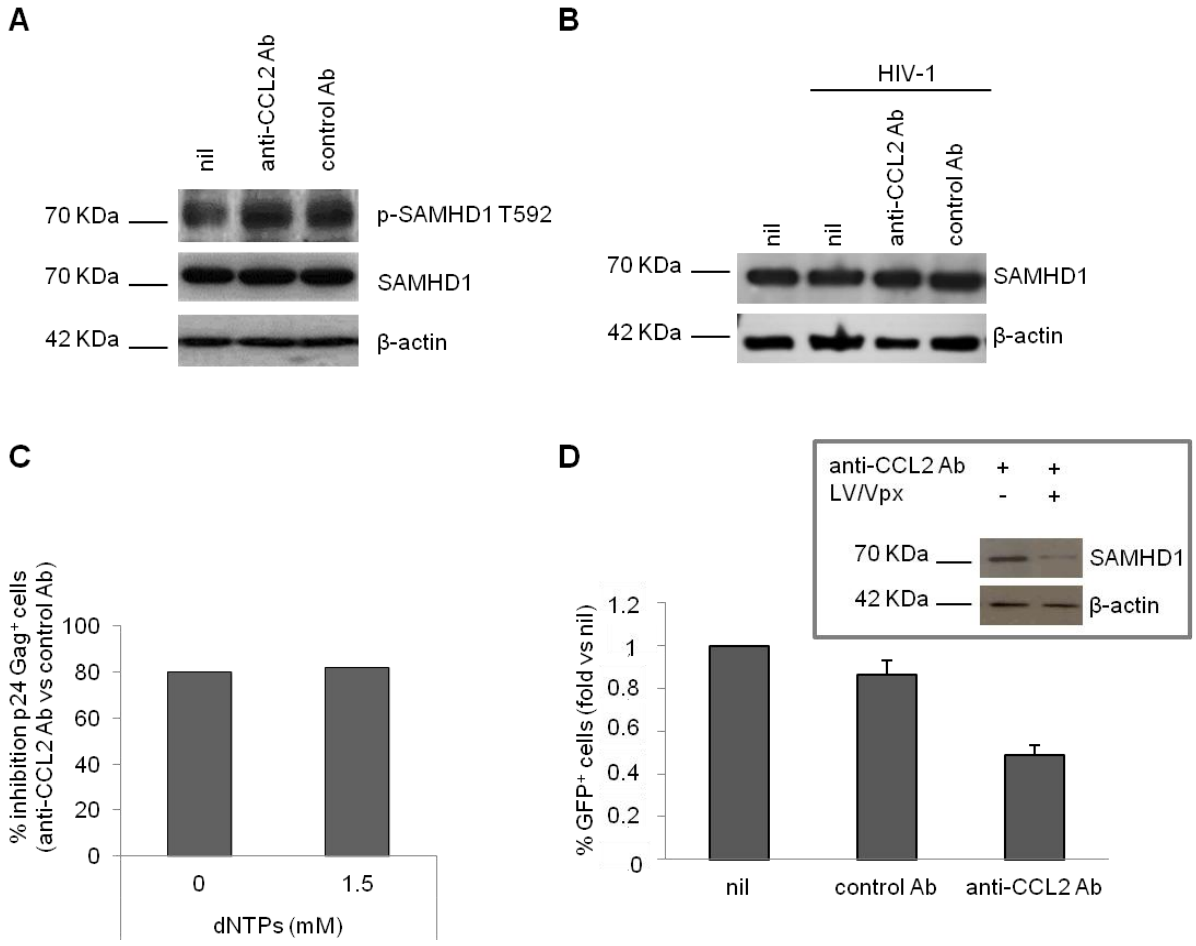

Figure 17. SAMHD1 expression and function is not involved in the CCL2 blocking mediated inhibition of HIV-1 replication in MDMs. (A) MDMs were treated with anti-CCL2 or control Ab (2.5 μg/ml) for 20 h. Cells were then lysed and SAMHD1 protein expression and phosphorylation were detected by western blot. B) MDM were treated as in A and then infected with HIV-1_{BaL} (3000 $TCID_{50}$ per well). Cells were lysed 14 days after infection and SAMHD1 protein expression in whole cell extracts was detected by western blot. (C) MDMs were treated as in A and infected as in B in the absence or in the presence of dNTPs (1.5 mM). After 14 days, cells were recovered and p24 Gag expression was evaluated by flow cytometry. (D) MDMs were treated as in A and then challenged with LV/Vpx expressing GFP (2×10^6 TU per 10^6 cells). The proportion of GFP^+ cells was determined 3 days post-infection by flow cytometry. The effect of Vpx on SAMHD1 protein expression is shown in the inset. In western blot experiments, actin was used as house-keeping gel loading control. In A, B and C the result from a single representative experiment out of 4 independently performed is shown. In D, data represent mean values (+SE) of the results obtained with 4 different donors.

Finally, we assessed the effect of SAMHD1 knock-down on the CCL2 neutralization-mediated anti-HIV-1 activity. To this aim, since it was shown that SIV-Vpx induces proteasomal degradation of SAMHD1 (47, 48), we used a LV/Vpx to knock-down SAMHD1 and then compare LV/Vpx infected MDM treated with anti-CCL2 or control Ab. MDMs treated for 20 h with anti-CCL2 or control Ab were challenged with LV/Vpx and the proportion of GFP^+ cells was determined 3 days post-infection by flow cytometry. As shown in **Figure 17D**, a significant reduction in the fraction of GFP^+ cells was observed in the cultures treated with anti-CCL2 Ab. As expected, the presence of Vpx strongly reduced SAMHD1 protein expression **(Figure 17D inset)**, thus confirming that the observed inhibition is SAMHD1 independent. Collectively, these data demonstrate that neither altered SAMHD1 expression nor its function account for the CCL2 neutralization-dependent restriction of HIV-1 replication in MDMs.

6.2.2 Transcriptome analysis of the effect of CCL2 neutralization on global gene expression in MDMs

To further investigate the molecular mechanisms involved in viral restriction mediated by CCL2 blocking in MDMs, we analyzed the effect of CCL2 neutralization on global gene expression by RNAseq. To this aim, MDMs from three donors were exposed to anti-CCL2 or control Ab for 4 and 20 h and total RNA was isolated, subjected to poly (A) selection followed by reverse transcription, generation of cDNA libraries, and sequencing on an Illumina Hiseq 2500 platform. We performed differential expression analysis using DESeq2 (134). Genes with logFC $\geq$ 1 (upregulated) or logFC $\leq$ -1 (downregulated) and adjusted p-value < 0.1 were classified as significantly differentially expressed. We found that anti-CCL2 Ab treatment resulted in the differential expression of 1915 and 311 genes at 4 and 20 h, respectively, compared to untreated cells. Of these

genes, 1103 and 194 were upregulated, whereas 812 and 117 were downregulated at 4 and 20 h, respectively.

We then compared the transcriptional program induced by CCL2 neutralization (e.g. differentially expressed genes in anti-CCL2 Ab-treated MDMs respect to unstimulated MDMs) with that induced by control Ab (e.g. differentially expressed genes in control Ab-treated MDMs respect to unstimulated MDMs) at 4 and 20 h. We found that the majority of the differentially expressed genes were specifically modulated by anti-CCL2 Ab at either 4 or 20 h of treatment, whereas only a minor fraction of genes were modulated also

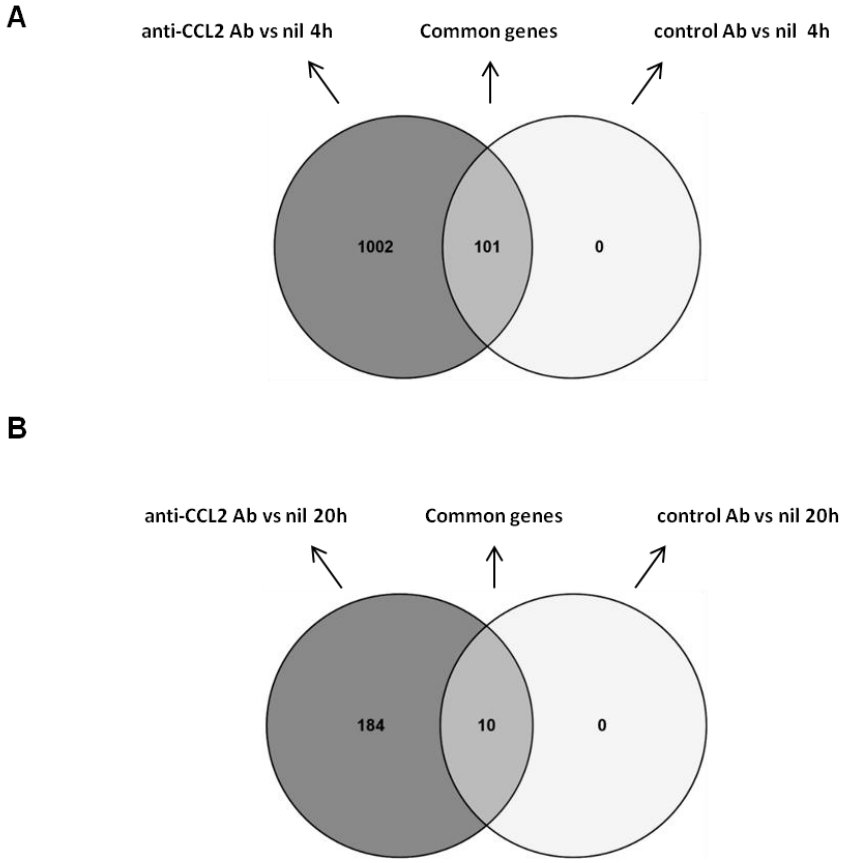

Figure 18. Comparison of the upregulated genes induced by anti-CCL2 and control Ab. Venn diagrams of the gene lists from "anti-CCL2 Ab vs nil" respect to "control Ab vs nil" at 4h (A) and 20 h (B).

by control Ab. Indeed, only 101 and 10 genes were upregulated either by anti-CCL2 or control Ab at 4 h **(Figure 18A)** and 20 h **(Figure 18B)**, respectively, whereas 4 **(Figure**

19A) and null **(Figure 19B)** genes were downregulated at 4 and 20 h, respectively. A complete list of the genes specifically modulated by anti-CCL2 Ab treatment is reported in the Appendix **(Tables I-II)**. We finally compared the transcriptional program induced by CCL2 neutralization at 4 h with that induced at 20 h, and we found that the majority of the genes were differentially modulated at the early time of treatment, whereas some were differentially modulated at both times or only at 20 h **(Figure 20)**.

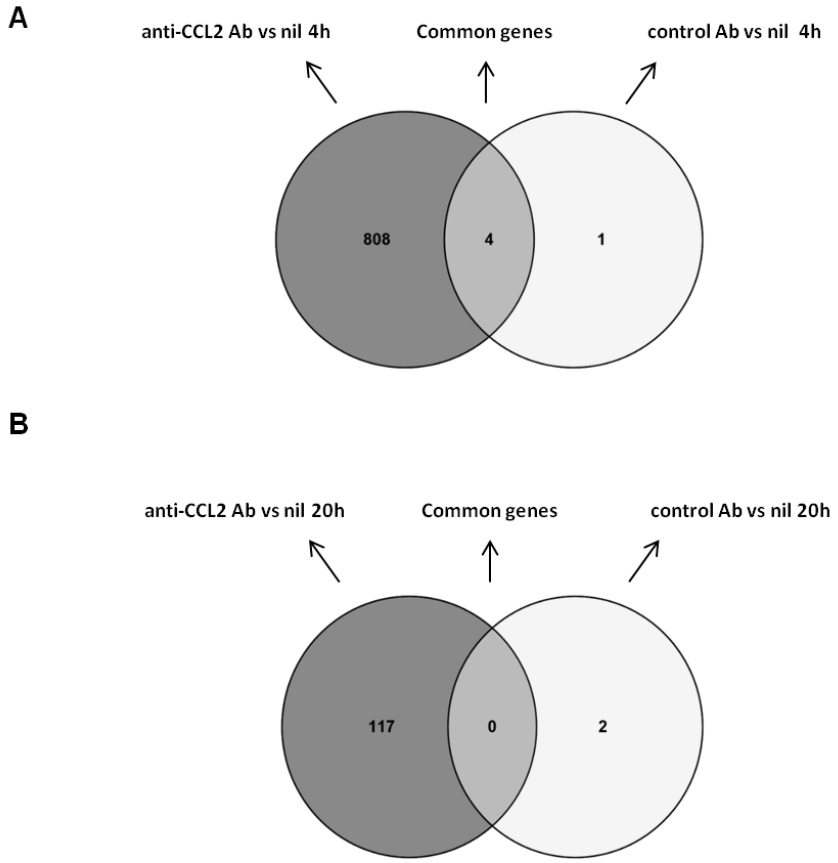

Figure 19. Comparison of the downregulated genes induced by anti-CCL2 and control Ab. Venn diagrams of the gene lists from "anti-CCL2 Ab vs nil" respect to "control Ab vs nil" at 4h (A) and 20 h (B).

Indeed, 979 and 780 genes were upmodulated and downmodulated, respectively, by anti-CCL2 Ab at 4 h, whereas 70 and 85 genes were upmodulated and downregulated, respectively, by anti-CCL2 Ab at 20 h. Finally, 124 and 32 genes were upmodulated and downregulated, respectively, by anti-CCL2 Ab at either 4 or 20 h.

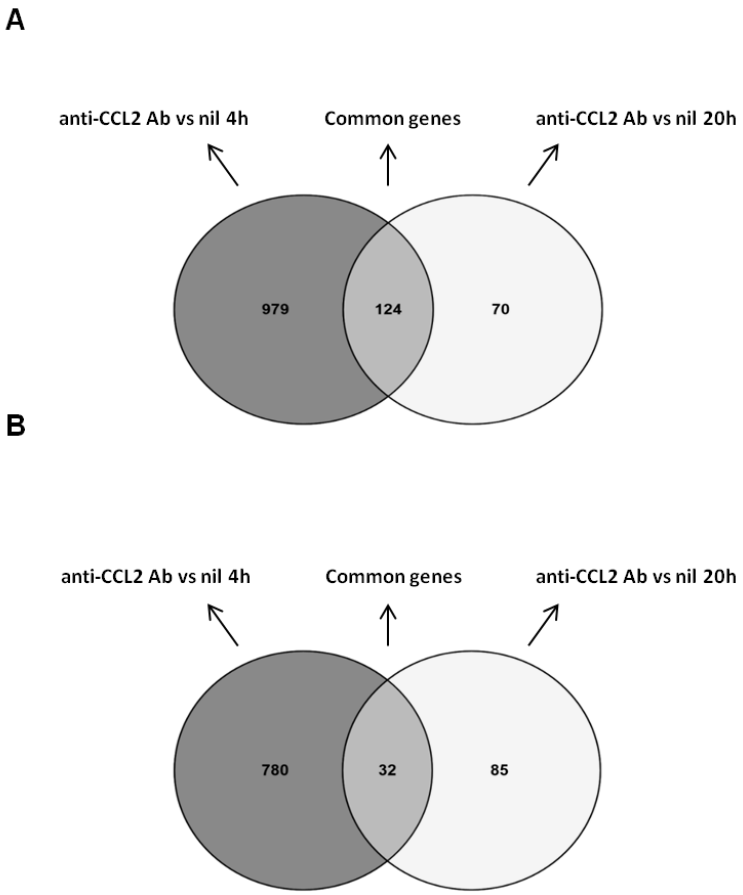

Figure 20. Comparison of the gene program induced by anti-CCL2 Ab at 4 and 20 h. Venn diagrams of the upregulated (A) and downregulated (B) gene lists from "anti-CCL2 Ab vs nil" at 4h respect to "anti-CCL2 Ab vs nil" at 20h.

In order to gain further insight into the specific categories of genes whose expression is changed upon treatment with anti-CCL2 Ab, we performed annotation and pathway analysis for genes upregulated at 4 and 20 h or downregulated at 4 h **(Appendix - Table III-V)**. We were unable to obtain categories for genes downregulated at 20 h because this list was not enriched for specific functions. We found that several of the upregulated genes were included in categories involved in immune responses. In particular, 86, 71 and 108 of the genes upregulated at 4 h were annotated with the GO biological terms defense response (GO:006952; FDR = 1.93E-2), immune response (GO:006955; FDR = 4.8E-2), immune system process (GO:0002376; FDR = 5.15E-2), respectively **(Table 2)**, whereas 33, 21 and 20 of the genes upregulated at 20 h were annotated with the GO

biological terms innate immune response (FDR = 1.71E-04) and the UP_KEYWORDS Innate Immunity (FDR = 1.37E-10) and Immunity (FDR = 4.52E-17), respectively **(Table 3)**.

Table 2. Genes upregulated at 4 h annotated in the categories involved in immune responses

GO:0006952: defense response	TNFRSF9, IFIT2, IFIT1, IFIT3, XCL2, FN1, OASL, CXCL9, SPP1, TNFRSF10A, CLEC5A, INHBA, PMAIP1, REL, ABL2, PML, GBP5, IFNGR2, IFI44L, IL36RN, KCNN4, IRG1, CD97, SLAMF1 ,P2RX7, VGF, TNIP1, CCL5,IL2RA, SLAMF7, ZC3HAV1, CCL7, CD40, CCL1, MATK, IL36B, CXCL11, CXCL5, **APOBEC3A,** IFIH1, SERPINE1, B4GALT1, IFIT5, FYN, CCL24, DDX58, CCL20, BATF2, IL6, CCR5, DDIT4, CLEC4E, NFKBID, LTA, ISG20, PTGER2, GZMB, ISG15, **MX2**, MX1, TNIP2 ,PTGS2, EIF2AK2, TAP1, OAS2, CEBPB, CCL4L2, RSAD2, MAPK8IP2, TRIM56, GBP1 ,RASGRP1 ,BCL3, IRF1, TNFRSF18, BCL2, ADORA2A, HERC5, SRC, GAL, S1PR3, IL27, TNFRSF10D, CXCL3
GO:0006955: immune response	TNFRSF9, EBI3, CXCL9, LIF, CLEC5A ,TNFRSF10A, GEM, REL, ABL2, JAG1, LCP2, PML, IL36RN, CD97, SLAMF1, AQP9, IL2RA, IL1RN, SLAMF7 ,ZC3HAV1, CD40, MATK, IL36B ,CXCL11, **APOBEC3A**, CXCL5, IFIH1, CCL24, FYN, IFIT5, IL7, DDX58, CCL20, TINAGL1, IL6, ALCAM, CD276, CCR5, LTB, CLEC4E, LTA, IL1R2, GZMB, RGCC, **MX2**, MX1, TNFSF14, TNFSF10, EIF2AK2, TAP1, CEBPB, TNFSF15, OTUD7B, ZP3, SERPINB9,CSF2, RIPK2,P OU2F2, GBP2, RASGRP1, BCL3, TNFRSF18, BCL2, HERC5 ,SRC, LAMP3,PDCD1, IL27, TNFRSF10D, CXCL3, IL36G
GO:0002376: immune system process	CCL24, CCL7, CCL20, CCL1, CCL4L2, TNFRSF9, FN1,FLT1,EBI3, CXCL9, LIF, CLEC5A, GEM, PMAIP1, ABL2, REL, LCP2, IDO1, PML, IFI44L, IRG1, CD97, MMP1, MYO10, P2RX7, TNIP1, AQP9,CCL5, IL2RA, SLAMF7, IL1RN, ZC3HAV1, CD44, CCL7, CD40, CCL1, SLC7A5, CXCL11, **APOBEC3A**, BCAR1, CXCL5, B4GALT1, CCL24, IL7, DDX58, CCL20, IL6, CD80, CD276, IL1R2, ISG20, GZMB, COL1A1, **MX2**, MX1, TAP1,CEBPB, CCL4L2, ITGB3, OTUD7B, ZP3, POU2F2, RASGRP1, IRF1, EDN1, PDCD1,BATF3, IFIT2, IFIT1, IFIT3, XCL2, SBNO2, OASL, JAG1, TBX21, ABCB4, IL36RN, KCNN4, SLAMF1, MATK, IL36B, CYP7B1, IFIH1, FYN, TINAGL1, ALCAM, BATF2, DDIT4, CLEC4E, LTA, RGCC, ISG15, TNIP2, TNFSF14, TNFSF10, RSAD2, TNFSF15, SERPINB9, CSF2, RIPK2, CAV1, AMPD3, GBP2, GBP1, CLCF1, BCL3, TNFRSF18, SRC, LAMP3, IL27, TNFRSF10D, CXCL3, IL36G

Table 3. Genes upregulated at 20 h annotated in the categories involved in immune responses

UP_KEYWORDS : Immunity	IFIH1, C3, FFAR2, CSF1, S100A9, CLU, RSAD2, C1R, C1S, ALCAM, **APOBEC3A**, ISG15, LILRA3, TAP2, DDX60, TAP1, **MX2**, GBP5, LYN, IDO1, CD40, DCSTAMP, S100A12, LILRB1, DDX58, IFIT3, KCNN4, OASL, IRF7, C1RL, EIF2AK2, CLEC5A, GBP1
UP_KEYWORDS : Innate Immunity	IFIH1, LYN, C3, CSF1, CLU, S100A9, RSAD2, C1R, C1S, S100A12, DDX58, IFIT3, **APOBEC3A**, OASL, ISG15, DDX60, IRF7, C1RL, EIF2AK2, **MX2**, CLEC5A
GO:0045087: innate immune response	IFIH1, LYN, CSF1, CLU, S100A9, C1R, COLEC12, C1S, S100A12, DDX58, **APOBEC3A**, CYBB, DDX60, IRF7, C1RL, EIF2AK2, PTX3, **MX2**, CLEC5A, MATK

6.2.3 Neutralization of CCL2 modulates the expression of the host-restriction factors A3A and Mx2 in MDMs

Among the genes whose expression was upregulated upon CCL2 neutralization we found several genes involved in antiviral responses, particularly some HIV-1 restriction factors. We concentrated our attention on Mx2 and A3A, since their mechanisms of action in viral inhibition may account for the post-entry restriction of HIV-1 replication mediated by CCL2 blocking in MDMs. Our data demonstrate that Mx2 and A3A expression is induced either at 4 (FC = 4.27 and 3.90, respectively) or 20 h (FC = 2.35 and 2.25, respectively) of anti-CCL2 Ab treatment **(Table 4)**.

		Host restriction factors	
	GENE	APOBEC3A	Mx2
4h	FC	3.90	4.27
	p	2.04E-06	5.7E-13
20h	FC	2.25	2.35
	p	0.00159	0.00015

Table 4. CCL2 neutralization induces A3A and Mx2 expression in MDMs.

We thus performed qPCR and western blot experiments to confirm the RNA transcriptome analysis at either the transcriptional or protein level in MDMs obtained from additional donors. We found that treatment with anti-CCL2 Ab for 20 h increased Mx2 transcripts at similar levels to those found in RNAseq studies, although at considerably lower level than that elicited by IFN-α, which is a well known inducer of Mx2 expression **(Figure 21A)**. However, the expression of the Mx2 protein was not modified by CCL2 neutralization, whereas it was induced by IFN-α **(Figure 21B-C)**.

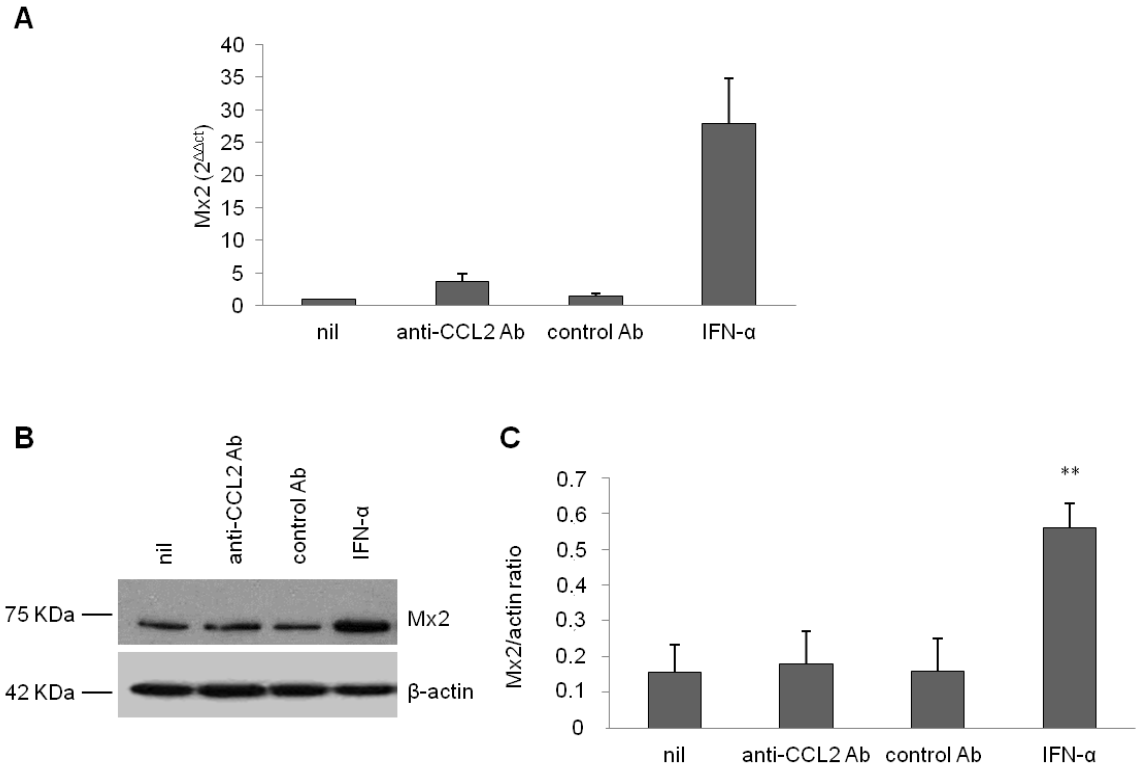

Figure 21. Validation of the differential expression profile of Mx2 in MDMs. MDMs were treated with anti-CCL2 or control Ab (2.5 μg/ml) or IFN-α (1000 U/ml) for 20 h. (A) Total RNA was extracted and Mx2 expression was analyzed by qPCR and expressed as $2^{\Delta\Delta Ct}$ values. The result from a single representative experiment of 3 independently performed is shown. (B) Cells were lysed and Mx2 protein expression in whole cell extracts was detected by western blot. The result from a representative donor out of 6 analyzed is shown. (C) Densitometric analyses of Mx2 expression performed on immunoblotting of MDM extracts from the 6 different donors analyzed. The graph shows the ratio of Mx2 to actin OD determined by densitometry. **p < 0.01 (IFN-α vs. nil).

Furthermore, exposure to anti-CCL2 Ab strongly increased A3A transcripts at both 4 and 20 h of treatment **(Figure 22A)**, as well as A3A protein expression at the latter time **(Figure 22B)**. As reported by other groups (36,140), we detected two isoforms of A3A by western blot analysis in MDMs, with some variability in their constitutive expression among donors. CCL2 neutralization significantly increased A3A expression of both isoforms respect to untreated or control Ab-treated conditions. Interestingly, A3A expression levels induced by CCL2 blocking were comparable to those of freshly isolated monocytes **(Figure 22B-C)**, where high levels of A3A were associated with resistance to HIV-1 infection (33).

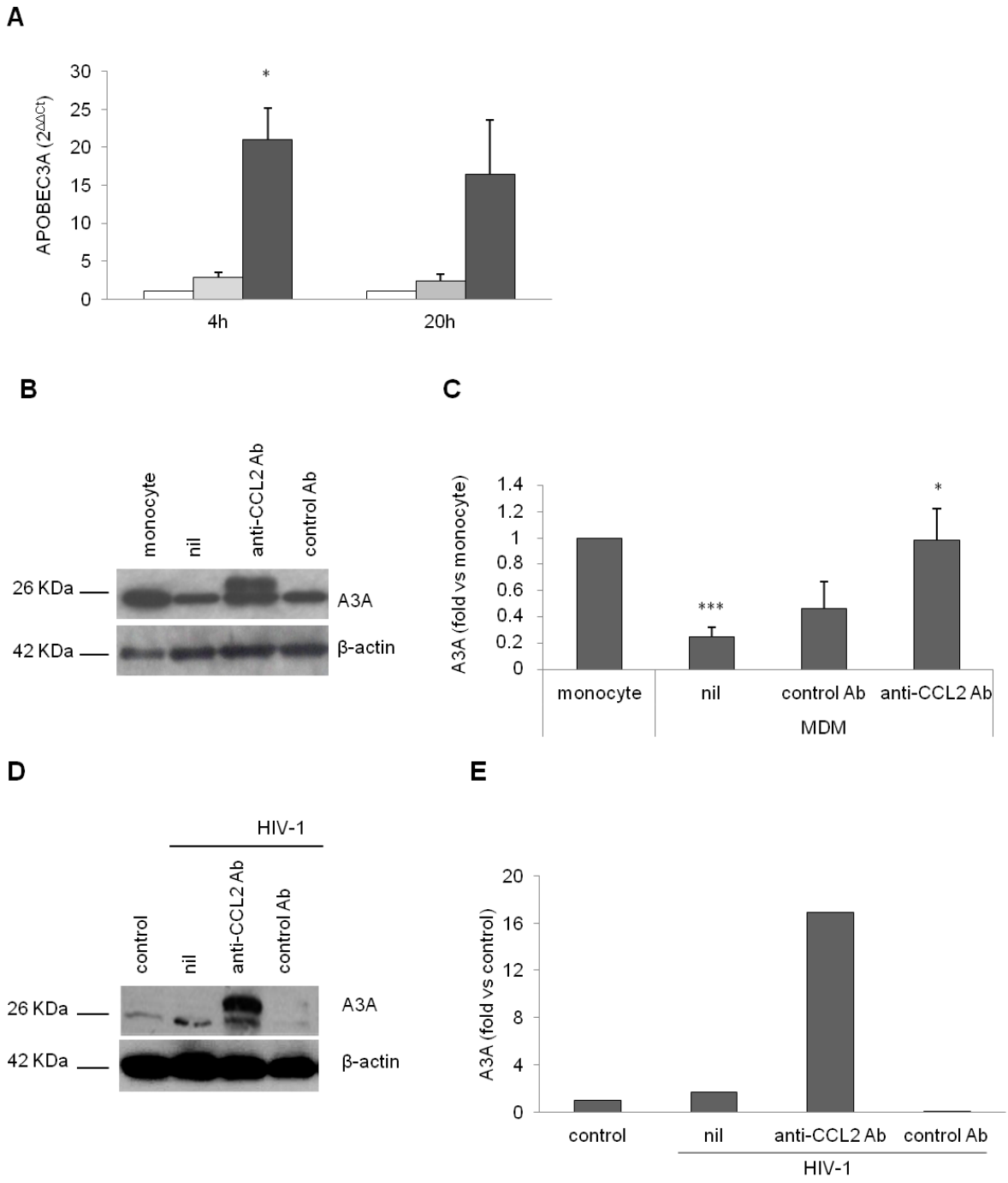

Figure 22. Validation of the differential expression profile of A3A in MDMs. (A) MDMs were treated with anti-CCL2 or control Ab (2.5 μg/ml) for 4 and 20 h. Total RNA was extracted and A3A expression was analyzed by qPCR and expressed as $2^{\Delta\Delta Ct}$ values. Data represent mean values (+SE) of the results obtained with 3 donors. (B-C) MDMs were treated for 20h, and A3A protein expression was detected by western blot and compared to that of freshly isolated monocytes from the same donor. In B, the result from 1 representative donor of 5 analyzed is shown. In C, the ratio of A3A to actin was determined by densitometry, and graph shows the mean of the fold relative to monocytes (+SE) of the 5 donors tested. *p< 0.05 (anti-CCL2 Ab vs. nil); ***p< 0.001 (nil vs. monocyte). (D-E) MDMs were treated as in B and then infected with HIV-1_{BaL}. After 14 days, A3A protein expression was detected by western blot. In E, the ratio of A3A to actin protein was determined by densitometry, and graph shows the fold relative to control. The results from one representative experiment of 4 independently performed are shown.

We also investigated the effect of CCL2 neutralization on A3A expression in HIV-1 infected MDMs, and we found a high increase in the expression of this enzyme at day 14 post-infection **(Figure 22D-E)**.

6.3 Effect of blocking the CCL2/CCR2 axis *in vivo* in HIV-1 infected patients on A3A expression

The results we obtained in the MDM model suggested a potential association between A3A expression and the restriction of HIV-1 replication mediated by CCL2 neutralization. To investigate whether the inhibition of the CCL2/CCR2 axis *in vivo* in the context of HIV-1 infection may elicit a similar effect, we assessed the consequence of i*n vivo* treatment with CVC on A3A expression by analyzing the expression of this protein in a subset of the HIV-1-infected patients enrolled in Study 202 (68).

In particular, we compared A3A expression in PBMCs of patients of the CVC 200 arm to that of patients of the EFV arm. Frozen PBMCs samples, collected before and at weeks 4, 12, 24, and 48 of CVC 200 (17 patients) or EFV (15 patients) treatment, were lysed in RIPA buffer to extract total proteins, and A3A expression was assessed by western blot and normalized to actin by densitometric analysis. As shown in **Figure 23**, we found a significant increase of A3A expression at week 48 respect to baseline in the CVC 200 arm ($p = 0.02$), but not in the EFV arm. To compare the difference of A3A expression between the CVC 200 and EFV arms, we considered only the patients for which a complete longitudinal assessment of A3A expression was possible (e.g., 9 and 5 patients of CVC and EFV arms, respectively). Notably, as shown in **Figure 24**, A3A expression at week 48 was significantly different between the CVC and EFV arms ($p < 0.05$).

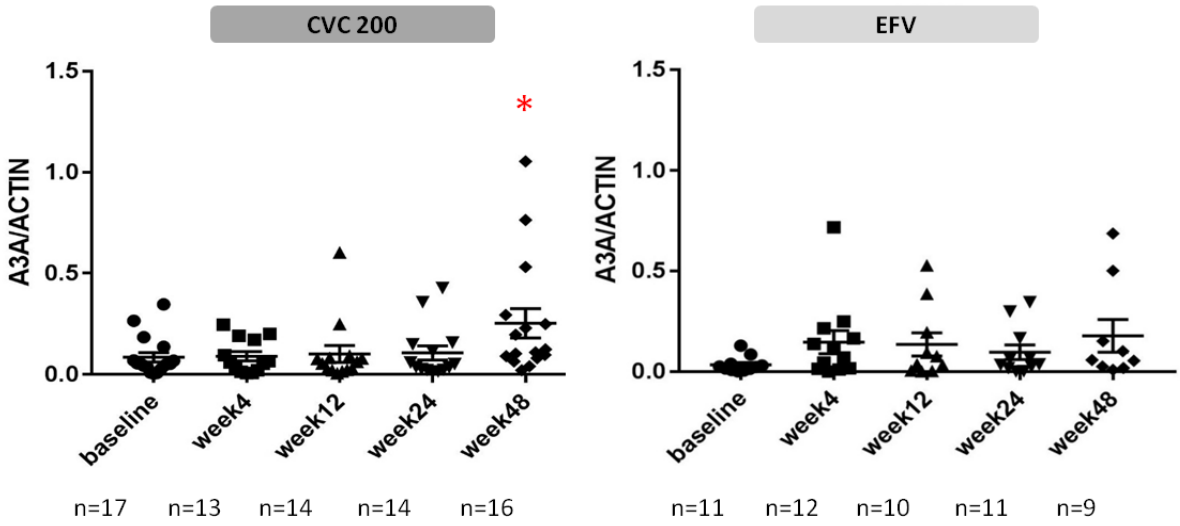

Figure 23. Effect of CVC 200 and EFV *in vivo* treatment on A3A expression. PBMCs from patients of Study 202 CVC 200 (n=17) and EFV (n=15) treatment groups were thawed, lysed and A3A protein expression was detected by western blot and normalized to actin by densitometric analysis. The dot plots show the ratios of A3A to actin OD determined by densitometry for each time point of the patients analyzed. *p < 0.01 (week 48 vs baseline).

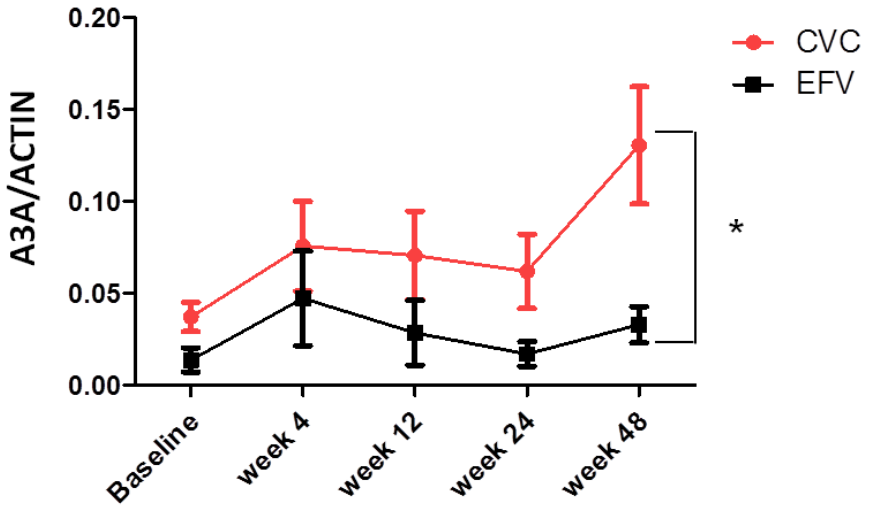

Figure 24. Mean A3A expression in CVC 200 and EFV treatment groups. PBMCs from patients of Study 202 CVC 200 (n=9) and EFV (n=5) treatment groups were thawed, lysed and A3A protein expression was detected by western blot and densitometric analyses. The graph shows the mean values of the ratios of A3A to actin OD determined by densitometry for each time point of the patients analyzed. *p < 0.05 (CVC 200 vs EFV).

Chapter 7

Discussion

CCL2 is a potent pro-inflammatory chemokine whose expression is rapidly induced following HIV-1 infection and which represents a triggering factor of chronic inflammation and tissue damage in infected individuals (95). Growing evidence suggests that CCL2 plays a key role in the pathogenesis of HIV-1 infection. Either HIV-1 infection or exposure to viral products can induce the expression of this chemokine and of its receptor CCR2 in different types of cells, and high levels of CCL2/CCR2 are indeed found in HIV-1^{+} individuals. The CCL2/CCR2 axis is tightly linked to the high level of immune activation and inflammation that is the hallmark of HIV-1 infection even in patients undergoing antiretroviral therapy (95, 96). In addition, more direct effects of CCL2 on viral replication are becoming apparent. Thus, modulation of CCL2/CCR2-driven effects may have significant impact on HIV-1 disease progression (96). Our group previously found that CCL2 expression increases during monocyte differentiation to macrophages and it is further up-modulated by HIV-1 infection (99, 122); conversely, endogenously released CCL2 promoted HIV-1 replication. Consistently, infection of MDMs with HIV-1 in the presence of anti-CCL2 Ab resulted in a potent inhibition of p24 Gag release, in the intracellular accumulation of this viral antigen and in remarkable changes in cell morphology. Thus, CCL2 may act as an autocrine factor that promotes virion production likely by affecting the macrophage cytoskeleton (99).

In this study we demonstrate that additional early post-entry steps of the HIV-1 life cycle are also impaired following CCL2 blocking. In fact, we found that neutralization of

CCL2 strongly decreases the proportion of p24 Gag^+ cells during the course of either a productive infection with R5 HIV-1_{BaL} or a single cycle infection with (VSV-G) HIV-1. Our data also demonstrate that the inhibitory effect of CCL2 blocking on HIV-1 replication does not involve HIV-1 entry or RT activity. Indeed, neither HIV-1 based VLP entrance nor immediate products of reverse transcription are affected by treatment with anti-CCL2 Ab. Conversely, CCL2 blocking strongly impairs the accumulation of viral DNA, both total, integrated and 2-LTR circles.

In order to investigate the molecular mechanisms underlying the post-entry restriction of HIV-1 replication mediated by CCL2 blocking in MDMs, we concentrated our attention on host restriction factors that can prevent the progression of HIV-1 replication acting after reverse transcription. In particular, we assessed the potential involvement of SAMHD1, which is highly expressed in macrophages and which acts prior to integration, possibly by preventing the accumulation of viral DNA (25, 45). Our data demonstrate that neither altered SAMHD1 expression nor function likely account for the restriction of HIV-1 replication mediated by CCL2 neutralization. Although SAMHD1 was shown to reduce the pool of dNTPs thus inhibiting the reverse transcription step especially in myeloid cells, a recent study suggested that this factor moderately restricts a macrophage-tropic HIV-1 strain in MDMs, whereas it potently inhibits HIV-1 replication in undifferentiated monocytes (141). In accordance with this report, it was shown that SAMHD1 is not a major effector of the early type I IFN-mediated block toward HIV-1 in these cells (142, 143).

In this study we also performed a genome wide transcriptional analysis of anti-CCL2 Ab-treated MDMs in order to obtain a global characterization of the consequences of CCL2 neutralization and gain further insights into cellular factors potentially involved in viral restriction in our experimental model. RNAseq data show that the host restriction

factors Mx2 and A3A are among the genes whose expression is differentially modulated by CCL2 neutralization. Interestingly, these factors exert their antiviral activity acting on viral DNA accumulation. In particular, Mx2 possibly restrict HIV-1 replication by inhibiting nuclear accumulation and integration of viral reverse transcripts, whereas A3A induces hypermutation of HIV-1 DNA, thus impairing viral DNA accumulation (40, 53). CCL2 blocking up-modulates transcript levels of both factors, and this effect is confirmed by quantitative real-time PCR. However, Mx2 protein expression is not increased following treatment with anti-CCL2 Ab. Conversely, CCL2 neutralization results in a strong induction of A3A protein expression to levels comparable to those of freshly isolated monocytes. The expression of A3A was previously shown to decrease during monocyte differentiation to macrophage, and this was associated with an increased susceptibility of these cells to HIV-1 infection (33). Interestingly, the trend of CCL2 expression in these cells is opposite to that of A3A expression, thus suggesting that CCL2 may act as a negative regulator of the expression of this restriction factor in macrophages.

Although controversial data exist on the anti-HIV-1 activity of A3A, several studies suggested that this factor restricts viral replication in cells where it is naturally expressed, i.e. myeloid cells (35-39). Indeed, the pool of A3A present in primary macrophages, DCs and differentiated THP-1 cells is directly capable of inhibiting incoming viruses at the reverse transcription step (34). Furthermore, additional studies pointed to an upregulated expression of A3A as the causal factor of the restriction of HIV-1 replication elicited by different conditions in myeloid cells. In particular, exposure to exogenous type I IFNs, or to the type I IFN-inducing cytokine IL-27, was shown to stimulate A3A expression in both macrophages and DCs and to inhibit HIV-1 replication in the former and viral spread to $CD4^+$ T cells in the latter (35, 37). In macrophages, treatment with IFN-α induced not only A3A expression but also its activity, resulting in an increased G-to-A editing and reduced

accumulation of viral DNA (36). In addition, treatment with 17β-estradiol was shown to inhibit the early phase of HIV-1 infection in macrophages in an IFN-α-dependent manner and to induce A3A expression (144). Finally, the restriction of HIV-1 replication in M1 polarized macrophages was associated with the increase of A3A expression (38, 39). Overall, these studies demonstrate that inhibition of HIV-1 DNA accumulation in myeloid cells correlates with increased A3A expression and/or activity in different experimental conditions. In keeping with these results, our data further support a close association between induction of A3A expression and restriction of viral DNA accumulation mediated by CCL2 neutralization. Unfortunately, our efforts to deplete A3A protein in anti-CCL2 Ab-treated MDMs using RNA interference were not successful, due to several technical biases (data not shown) and as already experienced by other groups in different experimental settings (36, 38). Thus, we cannot formally prove the involvement of this protein in the observed inhibition of viral replication. Future work will assess whether the CCL2 blocking-mediated inhibition of HIV-1 replication in MDMs is associated or not with an increased G-to-A editing of viral DNA and/or with others mechanisms of HIV-1 restriction.

Concerning the molecular mechanisms underlying the induction of A3A expression, only few studies investigated the role of signalling pathways in A3 expression, and most of them regarded A3G. In particular, the JAK/STAT and MAPK pathways were shown to be involved in the IL-2- and IL-15-mediated induction of A3G expression in $CD4^+$ T cells (145). JAK/STAT signalling was also implicated in the IL-27-mediated, type I IFN-dependent, induction of A3A and A3G expression in macrophages (37). Moreover, IFN-α was shown to induce A3G in a STAT1-dependent manner in hepatic cell lines and in liver tissues of chronic HBV patients with a complete response to IFN-α treatment, but not in those who did not respond to therapy (146). Conversely, a different study reported

that STAT2, but not STAT1, is necessary for the IFN-α induction of A3G in liver cell lines (147). Finally, PKC was shown to differentially regulate IFN-α- and LPS-mediated induction of A3A, A3G and A3F transcripts in PBMCs. In particular, inhibition of PKC suppressed IFN-mediated induction of these factors, whereas it enhanced LPS-mediated expression of A3A and A3G (148). Interestingly, our transcriptomic analysis shows that several genes coding for signalling proteins are upmodulated following CCL2 neutralization in MDMs. In particular, STAT1 is upregulated both at 4 (FC = 3.19) and 20 (FC = 4.4) h of anti-CCL2 Ab treatment. Future work is required to define whether the CCL2 blocking-mediated induction of A3A in MDM is mediated or not by STAT1.

Our data also suggest that, in addition to A3A, other factors may be involved in the restriction of HIV-1 replication elicited by CCL2 blocking. Indeed, the RNAseq data show that other genes involved in immune and antiviral responses are upmodulated in MDMs exposed to anti-CCL2 Ab. Among these genes, IFN-stimulated genes (ISGs) are of particular interest, since they mediate the antiviral effector functions of IFNs. We found an increased expression of IFITM1 (FC = 2.47) at 4 h of anti-CCL2 Ab treatment and of ISG15 at both 4 (FC = 4.47) and 20 (F C= 4.33) h. The former is a member of IFITM family, which comprise small transmembrane proteins that inhibit entry and replication of several viruses. IFITM1 is emerging as an important barrier to HIV-1 transmission (149). Although the exact inhibitory mechanisms of its antiviral activity are still unclear, it is thought that IFITM1 interferes with the fusion of viral and cellular membranes by altering their lipid composition and decreasing fluidity (149). ISG15 is one of the most upregulated genes upon type I IFN treatment or pathogen infection. It forms conjugates with a diverse pool of target proteins in a process termed ISGylation, which provides a series of enzymatic reactions similar to the ubiquitin conjugation pathway resulting in post-translational modifications that affect the function of target proteins. ISG15 can be also

found in an unconjugated form both inside the cell and released into the extracellular environment following IFN stimulation. Either unconjugated ISG15 or ISGylation may act to block HIV-1 budding (150). Interestingly, a significant impairment of the type I IFN response, among which a decreased ISG15 expression, was found in the latently HIV-1-infected U1 and OM10.1 cell lines in comparison to their respective uninfected parental U937 and HL60 cell lines (151). Intriguingly, in keeping with our results, it was shown that SIV-infected astrocytes produce CCL2 that binds to CCR2 on macrophages resulting in the suppression of specific IFN-stimulated genes (152). Although the mechanisms of the antiviral effect mediated by IFITM1 and ISG15 are not associated with an impairment of viral DNA accumulation, they may contribute to further strengthen the restriction of HIV-1 replication mediated by CCL2 blocking.

Additional insight concerning the potential mechanisms underlying HIV-1 restriction by CCL2 blocking derived from the analysis of the genes whose expression was dowmodulated by anti-CCL2 Ab treatment. Of note, CXCR4 expression decreases at either 4 (FC = 0.4) or 20 h (FC = 0.5) of anti-CCL2 Ab treatment. In keeping with this, a previous study performed in resting $CD4^+$ T lymphocytes demonstrated that exposure to CCL2 resulted in a CCR2-dependent upregulation of CXCR4 expression, rendering them more permissive to CXCR4-tropic HIV-1 infection (103). These results suggest that CCL2 has the capacity to render a large population of leukocytes more susceptible to HIV-1 in the course of infection, and this effect might be particularly relevant in late stages of the disease when both X4 viruses and high levels of CCL2 are present. This effect may ultimately contribute to the switch from CCR5- to CXCR4-using viruses which is associated with a worse prognosis.

To further investigate the role of the CCL2/CCR2 axis in the regulation of A3A expression, we took advantage of PBMC samples from HIV-1^+ patients enrolled in Study

202. In particular, we performed a longitudinal *ex vivo* evaluation of the effect of CVC on A3A expression. Our results demonstrate a significant increase of A3A protein levels at 48 weeks of treatment respect to baseline in the CVC 200 arm, but not in the EFV treatment group. Notably, the increase of A3A expression in CVC-treated patients is statistically significant also when compared to the EFV arm. Whether this increased A3A expression may correlate with the virological and immunological outcomes of CVC *in vivo* treatment still remain to be determined, and will be the subject of future investigation. Several studies showed a positive correlation of hypermutation and A3 levels, particularly A3G, with $CD4^+$ T cell count and a negative correlation with viral load (153-156). A3G was found to be significantly increased in PBMCs and cervical tissues of HIV-1-exposed uninfected individuals compared to healthy control or infected individuals (153, 157). Higher levels of A3G were also observed in LTNPs when compared to HIV-1-uninfected subjects and normal progressors (154). However, not all the studies were concordant with these associations (158, 159), and A3G levels were found to be higher in HIV-1^- compared to HIV-1^+ individuals, suggesting that A3G transcription may be rapidly downregulated upon infection (158, 159). Interestingly, A3A baseline expression in PBMC from HIV-1 infected patients was found to significantly correlate with viral load decline observed following 3 weeks of treatment with pegylated IFN-α-2a (Peg IFN-α-2a) (160).

Another open question is whether increased A3A expression following CVC *in vivo* treatment is really due to CCL2/CCR2 blockade. In fact, since CVC is also a potent CCR5 antagonist, additional experiments are needed to assess the effective role of CCR2 inhibition in the regulation of A3A expression. In this study, we did not investigate the role of CCR2 in the CCL2 neutralization-mediated modulation of A3A expression in the MDM model. A previous study from our group demonstrated that monocyte differentiation to macrophage resulted in a decrease of CCR2, particularly the b isoform, at the plasma

membrane, which was associated with a reduction of the biological response of MDMs to CCL2 in terms of calcium flux and migration (122). Thus, MDMs may not be the best experimental model to investigate the role of CCR2 in the regulation of A3A expression. Concerning the observed effects of CCL2 neutralization in these cells, we hypothesize that low levels of CCR2 expression could mediate the observed phenotype. Furthermore, both increased CCR2 expression and enhanced response to CCL2 were described in HIV-1-infected leukocytes by other groups (100). Thus, enhanced CCR2 expression in HIV-1-infected macrophages might also occur and mediate the observed effects on viral replication and A3A expression.

Chronic inflammation is considered nowadays a driving force of immune dysfunction and AIDS progression. A residual chronic immune activation persists even in HIV-1 infected patients in which viral replication is inhibited by antiretroviral therapy. In fact, persistent latently infected cells contribute to the continuous activation of immune cells, establishing a dangerous vicious cycle between viral persistence and immune activation which contributes to the development of pathological conditions and hinders a complete remission (69, 84). Although virologic success and CD4 count increase were similar across CVC and EFV arms, a significant decrease of total cholesterol level and of the monocyte activation biomarker sCD14 was observed only in the CVC arm, suggesting the potential anti-inflammatory effects of this drug. Thus, the increased expression of A3A in the CVC treatment group suggests that decreasing inflammation may represent a mechanism to boost host defence against HIV-1 (69, 84).

The CCL2/CCR2 axis is tightly linked to the high level of immune activation and inflammation and to several virus-associated disorders in HIV-1^{+} individuals. In addition, our data suggest that CCL2 is exploited by HIV-1 to boost its replication by rendering target cells more susceptible to viral replication, particularly by inhibiting the expression of

innate viral antagonists in macrophages (99). Further investigation exploring the molecular mechanisms by which CCL2/CCR2 affect HIV-1 replication and pathogenesis may help to define the precise contribution of this chemokine/chemokine receptor pair in these processes, thus opening the way for the investigational treatment of HIV-1-associated co-morbidities with drugs interfering with CCL2/CCR2. These drugs may represent interesting therapeutic options that could be exploited in HIV-1 infected subjects to control viral replication as well as the associated immune activation and inflammation, thus hopefully resulting in further improving quality of care and life expectancy of patients in the post-HAART era.

Chapter 8

Appendix

Table I. Genes modulated by anti-CCL2 Ab at 4h in MDMs

Up-regulated		**Down-regulated**	
GeneSymbol	FC	Gene Symbol	FC
C11orf96	2412.84	KIF26B	0.00
TM4SF1	683.66	PGF	0.00
SHANK3	520.48	DEPTOR	0.02
NKX3-1	517.78	FFAR4	0.03
SERPIND1	374.44	PHYHIP	0.03
TRIM9	328.10	SLC46A2	0.04
ANKRD1	325.52	ZNF763	0.04
TNC	323.55	NYNRIN	0.04
NES	323.27	LINGO3	0.05
ANKRD22	309.22	P2RY13	0.05
IRG1	252.57	CD1D	0.05
CCL20	244.28	PSRC1	0.06
XIRP1	234.35	**KLHDC8B**	0.06
MMP10	192.53	**BMF**	0.07
IL36G	152.35	PROC	0.07
VGF	151.86	F2RL3	0.07
CXCL11	146.51	**TMEM37**	0.08
RRAD	145.50	ALK	0.08
MYO1B	129.57	**PDK4**	0.08

INHBA	128.09	GPRC5B	0.08
IL36RN	111.98	NHLRC4	0.08
IDO1	106.48	ANGPTL2	0.08
MMP1	106.28	P2RY8	0.08
OCSTAMP	100.88	SLC45A4	0.09
IL1RN	93.91	SLC46A1	0.09
STAC2	92.18	TMEM86A	0.09
NDP	90.45	OR2W3	0.09
ADORA2A	81.93	RHOBTB1	0.09
HEY1	81.41	RNF125	0.09
HCAR3	73.23	**RGS18**	0.09
CSF2	69.46	NHSL2	0.10
EGLN3	68.35	IGSF22	0.10
REM1	67.36	ATG4C	0.10
IL36B	62.76	TFAP4	0.11
CCL4L2	61.48	GAL3ST4	0.11
HCAR2	57.93	CABLES1	0.11
SSTR2	57.70	ST5	0.12
LIF	56.50	LPAR5	0.12
CCL7	54.30	IQCD	0.12
CCL1	53.61	LRMP	0.12
CYP7B1	48.97	LGR4	0.12
LAD1	48.40	KIAA1211L	0.12
NACAD	47.78	RAB3A	0.12
NDRG4	45.76	C15orf52	0.13
NT5E	45.27	ENC1	0.13

OVOL1	44.05	PSCA	0.13
EREG	43.60	TLR3	0.13
COL1A1	43.48	PIK3C2B	0.13
TMOD1	42.05	FLI1	0.13
EDN1	40.76	TFCP2L1	0.13
CILP2	40.49	KLF1	0.14
C1QTNF1	40.40	**FAM174B**	0.14
PTGS2	39.22	ZBTB12	0.14
RGMA	37.98	JPH4	0.14
APCDD1L	37.51	ID3	0.14
TBX21	36.91	RPP25	0.14
CCL24	35.77	OPRL1	0.14
SLAMF1	34.20	CALCRL	0.14
SLCO4A1	33.70	FAM53B	0.15
ELFN1	32.28	RGS14	0.15
C3orf52	30.92	OSGEPL1	0.15
CYP27B1	30.90	LRRC4	0.15
SCG5	30.89	**DAB2IP**	0.16
TINAGL1	29.48	CD200R1	0.16
GAL	29.22	ADCK3	0.16
KIAA1199	29.03	SERPINF2	0.16
C19orf26	28.70	FRAT1	0.16
SRSF12	27.61	**PAQR7**	0.16
ABTB2	27.36	MBP	0.16
TMEM88	26.94	CTTNBP2	0.16
TNFRSF18	26.39	**NR1D1**	0.16

GREM1	25.25	RAB11FIP1	0.16
KIAA1045	24.84	EHMT2	0.17
GBP5	24.69	GRAMD1B	0.17
MDGA1	24.55	B3GNT1	0.17
RGS16	24.47	FAM13A	0.17
GEM	24.26	ZNF589	0.17
ALDH1A2	23.21	GPBAR1	0.17
CRLF2	23.03	C19orf35	0.17
ANGPTL4	22.71	GPR34	0.17
CXCL9	22.19	ZMYM3	0.17
SERPINE1	22.17	SETDB2	0.17
SEC14L2	21.56	**SCAMP5**	0.17
SOCS1	21.13	SLC22A18AS	0.17
N4BP3	20.89	FBXO32	0.18
MMP19	20.89	THEM6	0.18
SYNGR3	20.32	FAM105A	0.18
GCNT4	20.30	TTC7A	0.18
C22orf42	20.29	FES	0.18
PRR16	20.07	**IGFBP4**	0.18
LRRC16B	19.96	SPATA12	0.18
TMEM217	19.96	TYSND1	0.18
EBI3	19.95	CLCN4	0.18
MYL9	19.76	SOX12	0.18
CSPG4	19.05	YPEL3	0.19
MYEOV	18.91	NINL	0.19
FLT1	18.29	PTCH2	0.19

FAM19A3	18.19	CREB3L4	0.19
OASL	17.88	HVCN1	0.19
RSAD2	17.57	APPL2	0.19
LRTM2	17.49	TTLL1	0.19
FERMT2	17.49	LPAR6	0.19
DUSP8	16.80	HSPBAP1	0.19
SPP1	16.70	BLNK	0.20
ESPL1	16.52	DHRS3	0.20
LAMA5	16.51	KIF17	0.20
RTN4RL2	16.40	TLR5	0.20
KIAA1644	16.34	SUOX	0.20
C6orf223	16.18	RIN1	0.20
SLC2A14	16.00	C17orf103	0.20
CAV1	15.56	PITHD1	0.20
HSPB7	15.51	**C1orf127**	0.20
PTRF	15.46	LRRC45	0.21
OLFM2	15.40	P2RY6	0.21
EGR3	15.36	PRR5L	0.21
PDCD1	15.13	TACC3	0.21
SERPINE2	15.05	XCR1	0.21
NPAS1	14.99	SPATA7	0.21
HAPLN3	14.83	ACSS1	0.21
OLIG2	14.79	PRAM1	0.21
ETV7	14.76	TK2	0.21
LTA	14.37	CARD9	0.21
HOMER1	14.28	MTUS1	0.22

SPOCD1	13.96	CDKN1C	0.22
HS3ST3A1	13.78	RASGRP4	0.22
EHD2	13.75	CEBPE	0.22
S1PR3	13.61	NAIP	0.22
IL6	13.60	SMPD3	0.22
PHLDB1	13.48	RAP1GAP2	0.22
MYBPH	13.29	DIRC2	0.22
GP1BA	13.19	RGS12	0.22
ARHGAP23	12.87	THRA	0.22
CXCL5	12.72	MBOAT1	0.22
MAMLD1	12.72	SUFU	0.22
SEPT5	12.62	XYLT2	0.23
TNFRSF9	12.61	MBNL2	0.23
IL2RA	12.39	MGAT4A	0.23
JAG1	12.30	FBXL20	0.23
XCL2	12.25	PAQR8	0.23
LAMP3	12.23	SH2D3C	0.23
RNF175	12.14	KHK	0.23
ARC	12.07	SLC7A8	0.23
SLC39A8	11.77	**S1PR1**	0.23
DUSP4	11.58	**LRP5**	0.24
IFIT2	11.58	ACSM5	0.24
CCNA1	11.39	NLRP12	0.24
IL27	11.31	ABCG1	0.24
CKB	11.30	POLB	0.24
TLE1	11.23	FN3K	0.24

GBP1	11.18	SLC40A1	0.24
SERPINB2	10.93	SLC27A1	0.24
ECE1	10.71	MCEE	0.24
CCRN4L	10.33	TIGD2	0.24
IFIT3	10.19	EEPD1	0.25
HELZ2	9.98	ZNF33B	0.25
TMEM132A	9.96	CACNA2D3	0.25
UPB1	9.60	ZHX3	0.25
IL1R2	9.59	YPEL4	0.25
TNFSF15	9.49	RAB42	0.25
BCAR1	9.36	STARD13	0.25
RHBDL3	9.27	TRIM32	0.25
P4HA3	9.25	MGME1	0.25
COL5A3	9.18	RHOBTB2	0.25
SPAG5	9.15	RAB3D	0.25
RASGRP1	9.15	SYTL3	0.25
IRF1	9.08	IFFO1	0.25
HSD11B1	9.02	CYGB	0.25
DNAJB5	8.96	ZNF331	0.25
ASPHD1	8.89	**TLR7**	0.26
C8orf56	8.68	**GPR150**	0.26
PBX4	8.61	AVPI1	0.26
DIXDC1	8.61	P2RY1	0.26
DNAAF1	8.57	ABHD15	0.26
PLAUR	8.57	CHST13	0.26
PHLDA2	8.55	ABHD8	0.26

PDLIM4	8.44	FAM212B	0.26
GZMB	8.36	C14orf159	0.26
KLF9	8.11	SNX21	0.26
MET	8.09	TBC1D24	0.26
MATK	8.01	NTHL1	0.26
VEGFA	7.87	PDK2	0.26
GRAMD1A	7.87	CDKN2C	0.26
GBP2	7.84	INPP5D	0.26
HES4	7.70	RAD51AP1	0.26
TNIP1	7.48	ARHGAP9	0.26
AMZ1	7.46	SLC16A5	0.26
B4GALT5	7.40	DHRS9	0.27
CLEC4E	7.37	NREP	0.27
CLEC5A	7.32	FAXDC2	0.27
RASSF5	7.28	MARCH1	0.27
TNFSF14	7.25	CORO2A	0.27
RGCC	7.21	NISCH	0.27
TNFAIP8L3	7.18	ADORA2B	0.27
TSC22D1	7.15	SLC45A3	0.27
GBP4	7.15	C15orf38	0.27
SHOX2	7.14	RITA1	0.27
C15orf48	7.12	PXMP4	0.27
USP12	7.10	GINS1	0.27
TIMP3	7.06	ZBED3	0.27
CST6	7.03	PEX11G	0.27
BATF3	7.02	ZNF467	0.27

ACHE	7.02	SMAD6	0.27
DDX58	6.99	CCNG2	0.27
USP18	6.98	EPOR	0.27
SIK1	6.97	AMDHD1	0.27
SLC2A6	6.95	SNX30	0.27
SHF	6.95	WDR91	0.28
SLC28A3	6.92	PPP1R21	0.28
CMPK2	6.84	MFSD3	0.28
SLC7A5	6.78	ZNF362	0.28
GFPT2	6.74	GGA2	0.28
PMAIP1	6.67	SELPLG	0.28
STARD4	6.64	JMY	0.28
GPC1	6.45	OCEL1	0.28
PAQR5	6.45	SHPK	0.28
TMEM151A	6.41	SOWAHD	0.28
REL	6.39	CBX8	0.28
POU2F2	6.38	ARMC7	0.28
PTP4A3	6.37	SNX18	0.28
ACSL4	6.33	SDCCAG3	0.29
NCS1	6.31	MARVELD1	0.29
GLIS3	6.25	TRIM58	0.29
DTX4	6.24	MFNG	0.29
PNPLA1	6.19	SLC29A1	0.29
BCL2A1	6.17	SDS	0.29
CSRNP1	6.15	SLC43A1	0.29
KLF5	6.13	BOLA1	0.29

SLC16A10	6.10	MIS18BP1	0.29
A4GALT	6.09	KLHL24	0.29
ADAMTS14	6.06	ZNF792	0.29
FSCN1	5.96	REEP4	0.29
TNFAIP8	5.96	PIK3CG	0.29
MAP2K3	5.90	TBC1D14	0.29
MYOF	5.89	HDAC5	0.29
NFKBID	5.88	NMNAT3	0.30
BATF2	5.87	SAC3D1	0.30
GOLGA7B	5.84	KLHDC3	0.30
DDIT4	5.82	ING4	0.30
PTPRE	5.81	FOXRED2	0.30
FHL2	5.80	ZNF688	0.30
INSIG1	5.78	CAMK2G	0.30
SLC41A2	5.77	TESK2	0.30
GPR153	5.70	RAP2B	0.30
MAPK8IP2	5.68	ANKZF1	0.30
ABL2	5.66	FUZ	0.30
ALCAM	5.65	LDHD	0.30
CRIM1	5.65	RTN4R	0.30
DDR1	5.64	SSH3	0.30
IL15RA	5.62	GRIN3A	0.30
FYN	5.60	AP001816.1	0.30
SOD2	5.58	TNRC6B	0.30
SLC2A1	5.58	ABCC5	0.31
DYRK3	5.57	M1AP	0.31

KCNJ2	5.55	OSBPL7	0.31
PCDHGC3	5.54	CCDC125	0.31
BTG1	5.53	**HS3ST2**	0.31
ICAM5	5.52	FUT10	0.31
PDGFA	5.52	C5orf55	0.31
STX1A	5.46	ZCCHC24	0.31
NEDD9	5.45	HAMP	0.31
GPSM1	5.43	NLRC4	0.31
LRP12	5.41	FAM50B	0.31
MPP6	5.40	KRBA1	0.31
ABCB4	5.39	MAP3K12	0.31
MTF1	5.38	MAF	0.31
TCF7L2	5.33	ASGR1	0.31
IFIT1	5.33	EPDR1	0.31
AQP9	5.32	KLHDC2	0.31
TNFSF10	5.28	KBTBD7	0.31
TTC39B	5.25	RNF44	0.31
NR4A1	5.20	SHMT1	0.31
ZHX2	5.18	PARD6A	0.31
CLCF1	5.16	PLEKHH3	0.32
UBTD2	5.16	C17orf75	0.32
MSANTD3	5.14	LRRC27	0.32
DMWD	5.12	CD180	0.32
KBTBD12	5.10	RASAL1	0.32
IFIH1	5.03	**WBSCR27**	0.32
SLC7A1	5.02	PVRL4	0.32

SGMS2	5.00	NPRL2	0.32
CTNNAL1	4.98	WDR81	0.32
CD276	4.94	RCSD1	0.32
MYO10	4.91	MIF4GD	0.32
FN1	4.89	**SH3PXD2A**	0.32
RAI14	4.88	BRI3BP	0.32
CD97	4.81	IMPA2	0.32
CNKSR3	4.81	YPEL2	0.32
PDK1	4.81	ARL4C	0.32
PTGER2	4.76	CHEK2	0.32
PIM3	4.70	TRERF1	0.32
NEU4	4.69	LXN	0.32
RUNX1	4.68	MCM6	0.33
MX1	4.67	KAT2A	0.33
AMPD3	4.66	ARRDC2	0.33
SPSB1	4.65	MERTK	0.33
OTUD7B	4.63	PCED1B	0.33
TNFRSF12A	4.61	ZNF710	0.33
STX11	4.60	ITSN1	0.33
IL3RA	4.60	SASH3	0.33
ATP8B2	4.59	SLC25A20	0.33
CD80	4.58	DOK3	0.33
HSPA2	4.57	CNNM2	0.33
MAOA	4.55	RCBTB2	0.33
APOL6	4.52	SCIMP	0.33
CEP170B	4.52	TNFRSF8	0.33

TRIM36	4.51	ELMSAN1	0.33
MN1	4.51	INPP4A	0.33
JARID2	4.50	HDDC3	0.33
PPP1R13B	4.49	GALM	0.33
TJP1	4.49	CCDC85B	0.34
AMIGO2	4.48	CYP2U1	0.34
ISG15	4.48	**KANK2**	0.34
CCL5	4.48	ZNF232	0.34
PITPNM3	4.46	FDXR	0.34
GRAMD3	4.45	CTPS2	0.34
ZP3	4.45	THAP8	0.34
ITGB3	4.43	SLC25A35	0.34
TP53INP2	4.42	GPR162	0.34
CXCL3	4.42	ZBTB4	0.34
RCAN1	4.41	MEF2C	0.34
SRRM3	4.41	TSHZ1	0.34
P2RX7	4.41	GADD45A	0.34
TNIP2	4.40	TRIM65	0.34
ARAP2	4.36	ADCK1	0.34
DFNB31	4.35	ACSF2	0.34
ITGB8	4.35	HEXDC	0.34
PTPN1	4.35	FGD3	0.34
SRC	4.35	MRPL34	0.34
DDX21	4.33	SLC9A3R1	0.34
OTUD4	4.32	CD300LF	0.34
PSTPIP2	4.31	PNMA2	0.35

LDLR	4.31	FCHO1	0.35
RAPGEF2	4.30	KLHL21	0.35
BOK	4.30	PMFBP1	0.35
NCR3LG1	4.30	TDRKH	0.35
TAP1	4.30	CLMN	0.35
MX2	4.28	TST	0.35
IGLON5	4.28	MCM5	0.35
KYNU	4.27	ARMCX1	0.35
NUMB	4.27	TMEM187	0.35
ZNF462	4.25	ZMAT5	0.35
SLAMF7	4.23	AIFM1	0.35
ARNTL2	4.23	CDCA7L	0.35
IFI44	4.22	WFS1	0.35
BCL3	4.22	ZFP14	0.35
ZBTB10	4.21	PPAPDC2	0.35
SERPINB9	4.20	JDP2	0.35
STAT4	4.20	CNRIP1	0.35
ITPRIP	4.18	ZFP64	0.35
CHST15	4.16	CNNM3	0.35
ATP13A3	4.14	PAQR4	0.35
XAF1	4.12	LRRC29	0.35
PTPN12	4.11	PGPEP1	0.35
OTUD1	4.10	DTWD2	0.35
TNFRSF10D	4.10	ABHD10	0.35
PML	4.07	UNC119	0.36
PEAK1	4.07	L3MBTL3	0.36

LCP2	4.03	RGS19	0.36
CD40	4.03	NARF	0.36
IL7	4.01	ORMDL3	0.36
GPRC5A	4.01	GPD1L	0.36
BAMBI	3.99	HMBS	0.36
DRAM1	3.99	RILPL1	0.36
SYNJ2	3.96	SLC8B1	0.36
FNDC3B	3.95	MXD4	0.36
METTL1	3.95	SGK3	0.36
LAMB3	3.94	NARS2	0.36
GPC4	3.93	HMGB2	0.36
RNF145	3.91	PCYT2	0.36
APOBEC3A	3.91	CAPN5	0.36
B4GALT1	3.89	BTN3A3	0.36
YRDC	3.88	FLOT2	0.36
FGFR1	3.88	STAG3	0.36
MLLT4	3.87	LRRC25	0.36
ARL5B	3.87	MYCL	0.36
MESDC1	3.86	GLUL	0.36
PMEPA1	3.86	ORAI3	0.36
ENO2	3.86	LRRC8D	0.36
PHOSPHO1	3.83	ZNF652	0.36
ZC3HAV1	3.83	HTR7	0.36
SLC37A3	3.83	KIAA0513	0.36
SBNO2	3.83	**FBLIM1**	0.36
CD109	3.82	HLTF	0.36

STK17A	3.82	ARHGAP27	0.36
ZCCHC2	3.80	ZSCAN2	0.37
FAM83G	3.79	HMGCL	0.37
TMEM2	3.78	COQ3	0.37
IFI44L	3.77	FYB	0.37
ACSL5	3.76	RPS6KA4	0.37
FGFRL1	3.76	NCF4	0.37
KCNN4	3.74	PINK1	0.37
PNRC1	3.72	SIRT3	0.37
CD44	3.71	RASGRP3	0.37
GFRA2	3.70	GLCE	0.37
CEBPB	3.70	AGFG2	0.37
KREMEN1	3.69	GRAMD4	0.37
MICALL1	3.68	TMEM180	0.37
FASN	3.68	FAM214A	0.37
CBLB	3.66	C4orf27	0.37
MFI2	3.65	BRD3	0.37
ISG20	3.65	AP3S2	0.37
RIPK2	3.65	KIAA1147	0.37
LPAR2	3.65	SLC35F6	0.37
PNPT1	3.64	ASB13	0.37
ARL4A	3.64	TSPAN15	0.37
FOSL2	3.64	TMEM129	0.37
HR	3.63	HEMK1	0.37
TRIM56	3.60	RAD9A	0.37
HK2	3.60	FAM217B	0.37

OGFRL1	3.60	LTB4R	0.38
ACSL1	3.59	CORO1A	0.38
TJP2	3.59	NIF3L1	0.38
BAZ1A	3.57	GCHFR	0.38
TNFRSF10A	3.57	FRMD4A	0.38
PPP1R15A	3.56	AMDHD2	0.38
HMGCS1	3.55	ARHGAP25	0.38
CLIC4	3.55	ANP32A	0.38
AGO2	3.54	C1orf162	0.38
NUP188	3.54	NUP85	0.38
SPAG9	3.54	ALDH3B1	0.38
HIP1	3.54	HAUS4	0.38
MCOLN3	3.54	MAPK14	0.38
HMGCR	3.54	NIPSNAP1	0.38
YPEL1	3.52	PLCL2	0.38
KHDRBS3	3.52	SLC1A5	0.38
SAMD9L	3.52	ST6GAL1	0.38
TRIP10	3.51	BBS2	0.38
ATN1	3.51	C17orf62	0.38
OAS2	3.50	SLC35E2B	0.38
BCL11A	3.50	ATP10D	0.38
PLEK	3.50	DENND3	0.38
BID	3.49	DHDH	0.38
ZNFX1	3.49	NIPAL3	0.38
MASTL	3.49	CMBL	0.38
ASAP1	3.48	REPS2	0.39

NFATC1	3.47	PPP2R4	0.39
CLIP2	3.47	HES6	0.39
QPCT	3.45	CKLF	0.39
ADCY6	3.43	CBY1	0.39
LTB	3.43	CLUAP1	0.39
IFIT5	3.43	ARL11	0.39
EIF2AK2	3.43	METTL7A	0.39
NFAT5	3.42	HACL1	0.39
KIAA0247	3.42	TTLL12	0.39
CCR5	3.41	GNB1L	0.39
HILPDA	3.40	WAS	0.39
IFRD1	3.39	THYN1	0.39
NXN	3.39	TEF	0.39
DGKH	3.39	CTNNBIP1	0.39
HERC5	3.38	LDB1	0.39
ARHGAP31	3.37	SEPHS2	0.39
OLIG1	3.37	HAUS1	0.39
IFNGR2	3.36	MRPL55	0.39
BCL2	3.35	MPST	0.39
ITGAV	3.35	FGD2	0.39
BTBD19	3.35	FAM115A	0.39
PIM1	3.34	NT5DC2	0.39
SRXN1	3.34	HPS4	0.39
SH2B3	3.33	TTC8	0.39
WNT5A	3.33	LYPLAL1	0.39
UAP1	3.31	SYK	0.39

GPR84	3.31	CSRP2BP	0.39
MTHFD2	3.29	TAB1	0.39
SH2B2	3.28	PRKCDBP	0.39
TRIM24	3.27	HENMT1	0.39
CHML	3.26	KLC4	0.39
PRKAG2	3.26	GALT	0.39
CPEB2	3.25	PRKACB	0.39
MLLT6	3.24	ARHGAP19	0.40
ABCE1	3.23	PPFIBP2	0.40
ANPEP	3.21	FAM78A	0.40
TSHZ3	3.21	AKIP1	0.40
SLC39A14	3.20	PCNA	0.40
CLEC4D	3.20	BTN3A1	0.40
ABCC1	3.20	NMRAL1	0.40
RDX	3.20	CORO1B	0.40
PPARD	3.20	APBB1IP	0.40
STAT1	3.19	TRAF3IP3	0.40
LRRC8B	3.18	PDLIM2	0.40
HIF1A	3.18	CATSPER1	0.40
RAPH1	3.18	DAGLB	0.40
TGM2	3.18	LYL1	0.40
IL4I1	3.17	DIRAS1	0.40
RASL11A	3.16	NCAPD2	0.40
CCNL1	3.16	CBX1	0.40
EIF4E	3.14	LY9	0.40
DDX60L	3.14	AKR1C3	0.40

ZNF654	3.14	TGFBR2	0.40
FLRT2	3.13	SLC22A5	0.40
GRASP	3.13	VPS26B	0.40
HDGFRP3	3.13	SMYD4	0.40
NABP1	3.12	MAP3K1	0.40
FOSB	3.11	SORD	0.40
HMGA1	3.11	CACFD1	0.40
CDK17	3.11	NTPCR	0.41
RELB	3.11	SPHK2	0.41
BHLHE41	3.10	EPHB2	0.41
ELOVL5	3.09	ZKSCAN4	0.41
ADAM17	3.09	**CXCR4**	0.41
FLNA	3.08	BDH1	0.41
PPAP2A	3.07	HMHA1	0.41
PLK3	3.07	KCNJ5	0.41
MYADM	3.06	RAB9A	0.41
ANKRD37	3.06	PNPO	0.41
ATAD3B	3.05	TRPS1	0.41
PNP	3.05	MLPH	0.41
NEDD4L	3.05	PFKFB2	0.41
LRIG1	3.04	SDSL	0.41
ARFGAP3	3.04	AKNA	0.41
TUBB2A	3.04	CALM2	0.41
FJX1	3.03	RB1	0.41
PHACTR2	3.03	KATNB1	0.41
FSD1L	3.03	TSPAN10	0.41

MME	3.03	GNPDA1	0.41
EMR2	3.02	RAB3IL1	0.41
JUN	3.02	SLCO2B1	0.41
HERC6	3.02	EFNA4	0.41
MED13L	3.02	CNPY4	0.41
RHOF	3.02	DIS3L	0.41
IRF7	3.02	FRMD4B	0.41
RPS6KA3	3.01	ITFG2	0.41
RASGEF1B	3.00	PRMT7	0.41
TNFSF9	3.00	CKAP2	0.41
ACTN1	3.00	STX10	0.41
PER2	3.00	FAM63A	0.41
TRAF3IP2	3.00	PFKM	0.41
GTPBP4	2.98	KIAA1467	0.42
NBN	2.98	PTPRO	0.42
TNFAIP2	2.98	ACBD4	0.42
MCL1	2.97	ABLIM3	0.42
ATF5	2.97	MYO18A	0.42
LONRF1	2.97	ARHGAP12	0.42
NRIP3	2.97	**HAGHL**	0.42
SLC25A25	2.96	PFKFB4	0.42
PLEKHM3	2.96	PLA2G15	0.42
VIM	2.96	RGAG4	0.42
PDSS1	2.96	QPRT	0.42
MTFP1	2.96	HHEX	0.42
C1orf21	2.96	TATDN3	0.42

ARAP3	2.94	FBXO10	0.42
CXCL2	2.94	C12orf76	0.42
AQP3	2.94	GSDMD	0.42
MVD	2.93	MPPE1	0.42
STARD8	2.92	TNFAIP8L2	0.42
SEMA3C	2.92	USP21	0.42
SPHK1	2.91	SGSH	0.42
NOTCH3	2.91	MIIP	0.42
AHR	2.90	ZFYVE19	0.42
FILIP1L	2.90	MNDA	0.43
RHOBTB3	2.90	LRRK2	0.43
DPYSL3	2.90	NAPRT1	0.43
FUT4	2.90	**MAPK12**	0.43
ARL10	2.90	B3GNT8	0.43
MARCH3	2.90	CBR4	0.43
FAM26F	2.89	JUP	0.43
HLX	2.89	SLC12A9	0.43
SH3BP5	2.89	MCCC1	0.43
PTP4A1	2.88	INSR	0.43
MED13	2.87	MSRB1	0.43
PKD2	2.87	EIF4EBP1	0.43
MCOLN2	2.86	PTGFRN	0.43
RC3H1	2.85	CMTM7	0.43
SLC16A6	2.85	CARD14	0.43
STRN3	2.84	EEF2K	0.43
NR1H3	2.84	TMEM173	0.43

SCML1	2.83	UBAC1	0.43
PPP1R18	2.83	ZFP36L2	0.43
TANK	2.83	BBC3	0.43
PLSCR1	2.83	TSC22D3	0.43
EML4	2.83	CAB39L	0.43
ATP10A	2.83	RNASEH2B	0.43
TRIM5	2.82	NLRX1	0.43
BACH1	2.82	NFATC3	0.43
CHSY1	2.81	GDE1	0.43
SLC16A3	2.81	MVB12A	0.43
PLEKHG2	2.80	SEMA6B	0.43
KCNA3	2.80	SLC37A4	0.43
PDE4DIP	2.79	C20orf27	0.44
BHLHE40	2.79	BAD	0.44
PLAGL2	2.79	SLC46A3	0.44
NAMPT	2.79	NBPF1	0.44
PTPRJ	2.78	UBL7	0.44
RAB39A	2.78	TMEM218	0.44
PANX1	2.78	GCDH	0.44
ZBTB46	2.78	BTBD2	0.44
DCSTAMP	2.77	OSBPL3	0.44
RASSF8	2.77	CEP68	0.44
SPAG1	2.77	MPG	0.44
ARID5B	2.76	MARCH8	0.44
KIAA0020	2.76	GALK1	0.44
PPP1R15B	2.76	SCRN1	0.44

CDKN2B	2.76	IQCE	0.44
SERPINB8	2.76	MIPEP	0.44
TXNIP	2.75	SLC48A1	0.44
NAT8L	2.75	SRGAP3	0.44
THBD	2.74	SECTM1	0.44
POLR3D	2.74	PREX1	0.44
PSD4	2.74	GMPR2	0.44
EMILIN1	2.74	CTDSP2	0.44
SMOX	2.74	PTPN18	0.44
HNRNPH1	2.74	POLR3GL	0.45
RUSC2	2.74	PRR12	0.45
BDP1	2.72	CALCOCO1	0.45
PITPNB	2.72	HN1	0.45
NOP16	2.72	RSAD1	0.45
AEBP2	2.72	TMEM80	0.45
ZBTB43	2.71	APBA1	0.45
SLC11A2	2.71	SLC36A1	0.45
ADARB1	2.71	REPIN1	0.45
BTG2	2.70	TEX264	0.45
SP110	2.69	NDUFS3	0.45
FAM210A	2.69	PDK3	0.45
ETV3	2.69	ACADS	0.45
RHBDF1	2.69	LTA4H	0.45
ZBTB17	2.68	IL17RC	0.45
TM4SF19	2.68	GALK2	0.45
LRCH1	2.68	NUDT16	0.45

PCGF5	2.67	TCEAL8	0.45
SLC43A3	2.67	HADH	0.45
B3GNT5	2.67	COMMD3	0.45
MREG	2.66	RENBP	0.45
FEM1C	2.66	FECH	0.45
RGS1	2.66	ALDH3A2	0.45
PPIF	2.65	**STMN1**	0.45
GIMAP5	2.65	ZNF358	0.45
ZFYVE16	2.65	DTNBP1	0.45
ARL8B	2.65	CDK5	0.45
NUPL1	2.65	RNF135	0.45
ICOSLG	2.65	IDH1	0.45
FAM115C	2.65	XRCC3	0.45
DSE	2.64	DOPEY2	0.45
TAF13	2.64	C20orf196	0.45
RAC2	2.64	NUPR1	0.45
MAP4K3	2.64	RPA1	0.45
ST3GAL1	2.63	PCK2	0.46
CCR7	2.63	SLA	0.46
GRB10	2.63	AKAP11	0.46
AP5B1	2.62	CASP6	0.46
HESX1	2.62	CASP9	0.46
FAM129B	2.62	ATP6V0D2	0.46
RELA	2.62	COQ2	0.46
TSPYL2	2.62	SWAP70	0.46
ACVR1	2.61	DUS2	0.46

PPRC1	2.60	CDS2	0.46
SPRED2	2.60	AP2A2	0.46
PHLPP2	2.60	CLEC2B	0.46
PEA15	2.60	PAFAH2	0.46
ST3GAL4	2.59	KCNK6	0.46
SQLE	2.59	BBS4	0.46
CFLAR	2.59	PNPLA4	0.46
LYN	2.59	TNFSF12	0.46
GDAP1	2.58	CCDC106	0.46
RAB8B	2.58	**GALNT14**	0.46
CYP51A1	2.58	DHRS1	0.46
MMP9	2.58	BTN3A2	0.46
PELI1	2.58	PYCARD	0.46
PMM2	2.58	**MAN1C1**	0.46
TSPAN33	2.57	DSN1	0.46
TICAM1	2.57	DISC1	0.46
PIM2	2.57	C9orf91	0.46
SAMD9	2.57	ITPKB	0.46
WWC2	2.56	UNG	0.46
DENND5A	2.56	AP1B1	0.46
MFSD6	2.55	DAB2	0.46
CAMSAP2	2.55	CBS	0.46
EIF2AK3	2.55	DVL2	0.46
ENPP4	2.55	C22orf29	0.46
POP1	2.55	DNASE2	0.46
TNS3	2.54	VWA5A	0.46

ATP1A1	2.54	CACYBP	0.47
CCNJ	2.54	TANGO2	0.47
MARCKSL1	2.54	ATG9A	0.47
MSMO1	2.53	CDIPT	0.47
BYSL	2.53	SPECC1	0.47
BLZF1	2.53	FAM134A	0.47
NCK2	2.53	UBE4B	0.47
AFF4	2.53	SSH2	0.47
ADPRHL2	2.53	ETV5	0.47
MFSD2B	2.53	LEPROTL1	0.47
MITF	2.52	CEBPA	0.47
ST3GAL2	2.52	DRAM2	0.47
VASP	2.52	CD33	0.47
PFKP	2.51	CCDC88C	0.47
URB2	2.51	HEBP1	0.47
METRNL	2.51	ADCK4	0.47
NAMPTL	2.51	PPM1L	0.47
KLF10	2.51	FOXO1	0.47
EIF5B	2.51	ERCC2	0.47
SLC25A32	2.50	HIRIP3	0.47
FAM101B	2.50	MKNK2	0.47
LIG4	2.50	EVA1B	0.47
RYBP	2.50	LSM10	0.47
TREM1	2.50	C11orf83	0.47
PDGFB	2.50	SMAP2	0.47
DCP1A	2.48	NT5DC1	0.47

NAA15	2.48	C11orf49	0.47
SASH1	2.47	**ST6GALNAC2**	0.47
SH3PXD2B	2.47	IDH2	0.47
IFITM1	2.47	P2RY11	0.47
BZW1	2.47	C2orf68	0.47
FNIP2	2.47	SNX2	0.47
SH3BP2	2.47	C1orf233	0.47
DTX3L	2.47	TMEM42	0.47
PURB	2.47	SMARCA2	0.47
CD300E	2.46	PPCS	0.47
RNF19A	2.46	COX18	0.47
FAM129A	2.46	MSH2	0.47
APBA3	2.45	TTC9C	0.47
MT2A	2.45	LRSAM1	0.48
FAM208B	2.45	USP30	0.48
DTX2	2.45	PPP1R9B	0.48
RCN1	2.45	DYRK1B	0.48
SLC43A2	2.45	FCHO2	0.48
CLDND1	2.44	RNASEL	0.48
BEND3	2.44	HERPUD1	0.48
JUNB	2.44	ARL3	0.48
NAA50	2.44	WIPI1	0.48
MOB3C	2.43	MAP2K5	0.48
DAGLA	2.43	**MAP4K1**	0.48
RPGR	2.43	EZH1	0.48
YWHAG	2.43	ADRBK1	0.48

LUC7L	2.42	SYNE1	0.48
PARP9	2.42	NR1D2	0.48
SCARF1	2.42	AP3M2	0.48
DHX34	2.42	VPS8	0.48
MYO1E	2.42	ARHGEF18	0.48
OAS3	2.42	C17orf59	0.48
NFKBIE	2.41	ACSS2	0.48
RIF1	2.41	TLR6	0.48
ACTG1	2.41	DHTKD1	0.48
NRP1	2.41	PSEN2	0.48
MRAS	2.41	LMBR1L	0.48
LPAR1	2.41	PDHB	0.48
LSS	2.40	ARHGAP35	0.48
DDX39B	2.40	MRPS34	0.48
TMEM63B	2.40	CLIP4	0.48
SLC25A33	2.39	ARHGEF6	0.48
TRAF2	2.39	PARP4	0.48
CD58	2.38	ACSF3	0.48
RAPGEF6	2.38	AMPD2	0.48
TEX30	2.38	C20orf194	0.48
HECTD2	2.37	H1FX	0.48
PDPN	2.37	CHKA	0.48
ERBB2IP	2.37	ZFYVE26	0.48
GPATCH4	2.37	PAAF1	0.48
SLC25A37	2.36	STK32C	0.48
TPM4	2.36	DOK1	0.48

PPP3CC	2.36	ADH5	0.48
MYO1C	2.36	CHST14	0.48
ABCA1	2.36	AHRR	0.48
PUS7	2.36	EPHB6	0.48
GIMAP8	2.36	METTL21A	0.48
KIF1B	2.35	DEF6	0.49
TRIB1	2.35	GNB4	0.49
CLDN12	2.35	TMEM53	0.49
DVL1	2.35	ABHD11	0.49
IL1RAP	2.35	ZBTB14	0.49
APOL4	2.35	C14orf119	0.49
CIRH1A	2.34	NUDT22	0.49
MMP14	2.34	NMRK1	0.49
SFPQ	2.34	RNASEH2A	0.49
STK38L	2.34	RNF166	0.49
E2F3	2.33	NBR1	0.49
ALDH1B1	2.33	METTL7B	0.49
MAK16	2.33	PSIP1	0.49
ANKLE2	2.33	DHX57	0.49
ZNF281	2.33	KIAA2013	0.49
SMAD3	2.32	C16orf54	0.49
ZNF267	2.32	ZNF616	0.49
PLEKHO1	2.32	IQSEC2	0.49
SLC12A6	2.32	HSDL2	0.49
RBM19	2.32	HDHD3	0.49
SPATA13	2.32	MANBA	0.49

TRMT6	2.32	MTAP	0.49
TRIM25	2.31	POLD1	0.49
PVR	2.31	ZNF704	0.49
KRR1	2.31	UBAC2	0.49
COL6A1	2.31	NUDT16L1	0.49
SEMA7A	2.31	PIGM	0.49
FICD	2.31	FAH	0.49
CYTIP	2.31	IVD	0.49
PAPD7	2.31	FBXL4	0.49
DDX3Y	2.30	C7orf43	0.49
NDRG1	2.30	SAMD4A	0.49
WDR4	2.30	NSD1	0.49
KLHL28	2.30	PIP4K2B	0.49
BAG3	2.30	FAM96A	0.49
OPTN	2.30	SMIM4	0.49
IL2RG	2.30	CAMKK1	0.49
PID1	2.30	SERGEF	0.49
NOC3L	2.30	CLEC10A	0.50
SLC16A1	2.30	PEX6	0.50
ZNF335	2.30	LYPLA2	0.50
TIFA	2.29	DALRD3	0.50
RHBDF2	2.29	QARS	0.50
APOL3	2.29	ENTPD6	0.50
FBRS	2.29	EVI2B	0.50
SGTB	2.29	SCRN2	0.50
MAP3K8	2.29	RCBTB1	0.50

SMG1	2.29	CYB5D2	0.50
MIER3	2.28	TLE3	0.50
IL27RA	2.28	SNRNP25	0.50
USP42	2.28	SMIM14	0.50
NFE2L2	2.28	SLC39A3	0.50
LARP1B	2.27	PAK1	0.50
NINJ1	2.27	DYRK4	0.50
ARHGAP5	2.27	OAF	0.50
GOLT1B	2.27	FAM210B	0.50
ENTPD7	2.27		
NRROS	2.27		
TDG	2.27		
MYH9	2.27		
IPO7	2.27		
NSUN2	2.27		
OPN3	2.27		
SOWAHC	2.27		
KDM7A	2.27		
CYLD	2.26		
IL6ST	2.26		
KLF6	2.26		
MAP4K5	2.26		
RICTOR	2.26		
MTRR	2.25		
TMEM158	2.25		
SEC24A	2.25		

RARG	2.24		
FLNB	2.24		
TUBB6	2.24		
VCAN	2.23		
DNAJA4	2.23		
ANXA5	2.23		
GNA13	2.23		
BCAR3	2.23		
HSP90AB1	2.22		
UXS1	2.22		
SMURF1	2.22		
FBXL5	2.22		
URB1	2.22		
IL4R	2.22		
POM121	2.22		
NFKBIB	2.21		
USP6NL	2.21		
EPT1	2.21		
TDRD7	2.21		
COQ10B	2.21		
NLRC5	2.21		
CLINT1	2.21		
SAMD8	2.21		
NR3C1	2.21		
SACS	2.21		
KCTD9	2.21		

DLGAP4	2.20		
CCNT2	2.20		
MT-ND6	2.20		
CYCS	2.20		
ZNF121	2.20		
SNX9	2.20		
C1orf198	2.20		
UGCG	2.20		
TEX10	2.19		
RILPL2	2.19		
SRSF6	2.19		
IL32	2.19		
ALAS1	2.19		
SAMD4B	2.18		
RAP1B	2.18		
PNO1	2.18		
BNIP3	2.18		
ITGA5	2.18		
MOB4	2.17		
NANOS1	2.17		
DCUN1D4	2.17		
GCLM	2.17		
OSGIN1	2.17		
RASAL2	2.17		
PSD3	2.17		
CSRNP2	2.17		

EIF1	2.17		
EIF5	2.17		
EZH2	2.16		
LMTK2	2.16		
SRFBP1	2.16		
RHOC	2.16		
UPP1	2.16		
RAP2C	2.16		
GPR68	2.16		
PVRL2	2.16		
NAB1	2.16		
MAPKAPK2	2.16		
FMNL3	2.16		
NFYA	2.15		
BTBD3	2.15		
SEH1L	2.15		
GLS	2.15		
CHORDC1	2.15		
CD300LB	2.15		
KRAS	2.15		
RAB20	2.15		
SLC35F5	2.14		
ASH1L	2.14		
SRSF5	2.14		
TRAF3	2.14		
TAB3	2.14		

PPARG	2.14		
TSC22D2	2.13		
EPSTI1	2.13		
UGDH	2.13		
DMTF1	2.13		
TRIM16	2.13		
FGR	2.13		
GSPT1	2.13		
VPS37C	2.13		
TAB2	2.12		
CPEB4	2.12		
ANKRD28	2.12		
ZNF800	2.12		
ZBTB7A	2.12		
TCERG1	2.12		
ACO1	2.12		
MAP4K4	2.12		
RBPJ	2.12		
CDC42SE1	2.12		
UFM1	2.11		
LDHA	2.11		
OXSR1	2.11		
SCAF4	2.11		
ISOC1	2.11		
UBE2Z	2.11		
MTMR9	2.11		

NAA30	2.10		
C3	2.10		
JAK1	2.10		
RNF11	2.10		
CD82	2.10		
UBE2E1	2.10		
FAM126B	2.09		
COL6A2	2.09		
ANKRD12	2.09		
CHERP	2.08		
N4BP1	2.08		
PTPN7	2.08		
CSNK1G1	2.08		
S1PR2	2.08		
SIRPA	2.08		
ZNF318	2.07		
EPG5	2.07		
PIK3AP1	2.07		
LMNB1	2.07		
ZNF202	2.07		
SLC39A13	2.07		
USP15	2.07		
MAPK6	2.07		
TBC1D9	2.06		
NOM1	2.06		
FYTTD1	2.06		

UBE2S	2.06		
C15orf39	2.06		
FAM107B	2.06		
SRF	2.05		
AHCTF1	2.05		
DCUN1D3	2.05		
GRWD1	2.05		
NDEL1	2.05		
PPP4R1L	2.05		
SRRM2	2.05		
TET2	2.05		
TOP1	2.05		
AHDC1	2.04		
AMMECR1L	2.04		
BCL6	2.04		
SLC25A28	2.04		
RRS1	2.03		
FAM57A	2.03		
RLF	2.03		
FAIM	2.03		
PPTC7	2.03		
CHST11	2.03		
FBXO30	2.03		
IER5	2.03		
FZD1	2.03		
INTS6	2.03		

WBP4	2.02		
ZNF579	2.02		
PDZD8	2.02		
SKIL	2.02		
SCAF8	2.02		
DUSP1	2.02		
MAML2	2.02		
EIF3J	2.01		
NIFK	2.01		
DAXX	2.01		
PIK3R5	2.01		
UBALD2	2.01		
AFTPH	2.01		
KMT2E	2.01		
REXO1	2.01		
MAP7	2.01		
ST3GAL6	2.01		
PSMA6	2.00		
INF2	2.00		
IL6R	2.00		
DHX15	2.00		

Notes: In bold are reported genes differentially modulated at either 4 and 20 h. FC = Fold Change.

Table II. Genes modulated by anti-CCL2 Ab at 20 h in MDMs

Upregulated		Downregulated	
Gene Symbol	**FC**	**Gene Symbol**	**FC**
MT1E	33.31	F13A1	0.09
CA12	31.58	KLHL30	0.14
MT1M	26.03	METTL7B	0.15
ANKRD22	22.29	TPPP3	0.17
MT1L	22.26	LPPR3	0.19
TNC	21.57	**DAB2IP**	0.19
CXCL9	19.12	**TLR7**	0.20
TNFRSF18	18.72	GNG7	0.20
EBI3	18.47	LILRA4	0.23
OLIG2	16.64	SPTBN1	0.27
C1QTNF1	16.12	DTX1	0.27
MT1F	14.91	TPSAB1	0.27
PTGES	13.53	GAS6	0.29
MYEOV	13.47	**LRP5**	0.29
MT1X	13.01	S100A13	0.29
ANKRD1	12.71	**STMN1**	0.29
IDO1	11.90	TPSB2	0.30
GGT5	11.53	RP11-598F7.3	0.30
CCND1	10.75	**PAQR7**	0.31
ADAMTS14	9.94	PKD2L1	0.31
RP11316P17.2	9.32	PNPLA7	0.31
CCL7	9.00	IGF1	0.32

INHBA	8.37	HSF4	0.32
CXCL10	7.67	MYO1A	0.32
CYP27B1	7.65	COBLL1	0.33
CXCL11	7.25	**SCAMP5**	0.33
CCL13	6.91	ROR2	0.33
CLEC5A	6.81	HPSE	0.33
ETV7	6.59	CTSV	0.33
IFI44L	6.54	SLC39A10	0.33
C1R	6.48	**KLHDC8B**	0.34
TNFRSF9	6.42	ZDHHC1	0.34
TMEM132A	6.42	AIG1	0.34
GPR84	6.28	CTSF	0.34
SERPINE1	6.13	**RGS18**	0.34
MME	6.10	RBP7	0.34
GJA3	6.10	CEBPD	0.34
DCSTAMP	5.96	RP111018N14.5	0.35
MMP19	5.95	TUBB4A	0.35
RSAD2	5.58	SORL1	0.35
PTX3	5.54	PVALB	0.35
S100A12	5.36	**GPR150**	0.36
PROCR	5.12	**SH3PXD2A**	0.36
CRISPLD2	4.95	ANG	0.36
DUSP4	4.85	DACT1	0.36
AQP9	4.76	**S1PR1**	0.36
IFIT3	4.65	CHCHD6	0.37
C1S	4.59	GPX3	0.37

ARNTL2	4.51	**SMAD3**	0.37
RP13-452N2.1	4.41	NFATC2	0.37
STAT1	4.41	GNG2	0.38
FCAR	4.35	BAALC	0.38
ISG15	4.34	NGFRAP1	0.38
NCS1	4.29	CRHBP	0.38
IL4I1	4.26	AZU1	0.38
OASL	4.20	DPEP2	0.38
LINC00996	4.20	SLC18B1	0.38
TLE1	4.11	**C1orf127**	0.38
GBP1	4.01	AMICA1	0.38
CCL2	3.90	NFIA	0.38
CMPK2	3.88	CERS4	0.38
KCNN4	3.81	SERPINF1	0.39
TNFRSF4	3.80	APOC1	0.39
GCH1	3.79	EPB41L1	0.39
GCAT	3.76	**GALNT14**	0.39
LAMB3	3.72	FOLR2	0.39
CSF1	3.71	RNASE1	0.40
HAPLN3	3.56	**WBSCR27**	0.40
MEI1	3.52	BIRC7	0.40
CLU	3.50	GADD45B	0.41
DUSP6	3.49	FXYD6	0.41
MREG	3.46	PCED1B-AS1	0.41
SEMA3A	3.45	PRLR	0.42
ETV5	3.45	RCN3	0.42

SLC22A4	3.41	SLC47A1	0.42
COL6A2	3.35	OTOA	0.42
XAF1	3.33	**PDK4**	0.43
PVRL4	3.30	**NR1D1**	0.43
HELZ2	3.25	ZSCAN16-AS1	0.43
TSPAN33	3.25	ANKH	0.43
MATK	3.22	LSR	0.43
ALCAM	3.21	RARRES1	0.43
PLEKHA7	3.15	FABP3	0.44
ZSWIM4	3.11	**BMF**	0.44
CCL5	3.07	**MAPK12**	0.44
CTTN	3.07	EGFL7	0.44
OLIG1	3.07	ZNF395	0.44
IL15RA	3.06	**HAGHL**	0.44
CD38	3.06	**IGFBP4**	0.45
QPCT	3.00	GS1-358P8.4	0.45
VDR	3.00	ALK	0.45
IL1RN	2.96	RP11-368J21.3	0.45
SNX10	2.93	FCGR2B	0.45
MGST1	2.87	**FAM174B**	0.45
C17orf96	2.87	**HS3ST2**	0.45
IL1R2	2.84	CTD-2337J16.1	0.45
PSME2	2.83	MYO1D	0.45
OSM	2.83	ATP8A1	0.46
MAOA	2.83	SAT1	0.46
LPL	2.83	PIK3IP1	0.46

C1RL	2.75	RP11-67L2.2	0.46
TGM2	2.71	**KANK2**	0.46
DDX60	2.71	CDC42EP3	0.46
COL6A1	2.70	GPNMB	0.46
SPHK1	2.68	**TMEM37**	0.47
MYOF	2.68	RP11-65J3.1	0.47
NOTCH3	2.68	**MAP4K1**	0.48
USP18	2.67	CSF3R	0.48
FFAR2	2.67	**ST6GALNAC2**	0.48
ANPEP	2.65	**MAN1C1**	0.48
ACVRL1	2.62	AP001007.1	0.48
RTN1	2.60	**FBLIM1**	0.48
TNIK	2.60	STAB1	0.48
IL2RG	2.58	SRPX	0.49
BATF2	2.57	SIDT1	0.49
IRF7	2.56	RNASET2	0.49
COLEC12	2.55	**CXCR4**	0.50
EPSTI1	2.51		
PCSK6	2.51		
PAPLN	2.51		
NR1H3	2.49		
C3	2.45		
CD40	2.44		
SAMD9L	2.43		
TYMP	2.43		
IFI44	2.42		

CD44	2.41		
METTL1	2.41		
SPRED2	2.41		
ADM	2.39		
CYBB	2.36		
IFI35	2.35		
MX2	2.35		
SLC11A1	2.35		
EMILIN1	2.32		
HERC6	2.32		
FAIM	2.31		
RDX	2.30		
APOL3	2.30		
ATF5	2.28		
KMO	2.27		
EIF2AK2	2.27		
OLFML2B	2.26		
PHLDA1	2.25		
MMP14	2.25		
APOBEC3A	2.25		
DDX58	2.22		
SPRED1	2.22		
PRKCA	2.21		
CISH	2.21		
TAP2	2.21		
S100A9	2.20		

CDK14	2.20		
PLSCR1	2.20		
IKBKE	2.20		
MTF1	2.20		
LILRB1	2.19		
GSN	2.17		
ZMIZ1-AS1	2.16		
NRIP3	2.14		
SLC8A1	2.14		
GBP5	2.14		
SIGLEC10	2.14		
LILRA3	2.12		
ACSL5	2.11		
EML4	2.11		
WARS	2.10		
CD82	2.10		
NFE2L3	2.09		
PLAUR	2.08		
STEAP3	2.08		
ENPP2	2.07		
TGFBI	2.07		
FBP1	2.06		
PARP12	2.06		
TAP1	2.06		
PDPN	2.05		
ITGB7	2.03		

IFIH1	2.03		
SLC30A1	2.03		
BCL2A1	2.02		
GIMAP8	2.01		
IL21R	2.00		
LYN	2.00		

Notes: In bold are reported genes differentially modulated at either 4 and 20 h. FC = Fold Change.

Table III. Functional annotation clustering by GOrilla of the 1002 genes upregulated by anti-CCL2 Ab at 4 h in MDMs

Category	Term	count	pvalue	FDR
GO:0034612	response to tumor necrosis factor	12	2.92E-9	2.02E-5
GO:0071356	cellular response to tumor necrosis factor	11	1.65E-8	5.71E-5
GO:0072676	lymphocyte migration	7	1.86E-7	4.29E-4
GO:0048247	lymphocyte chemotaxis	7	5.35E-7	9.23E-4
GO:0071347	cellular response to interleukin-1	9	9.91E-7	1.37E-3
GO:0071346	cellular response to interferon-gamma	8	1.64E-6	1.89E-3
GO:0034341	response to interferon-gamma	9	2.71E-6	2.68E-3
GO:0070555	response to interleukin-1	9	3.36E-6	2.91E-3
GO:0051239	regulation of multicellular organismal process	70	4.48E-6	3.44E-3
GO:0007186	G-protein coupled receptor signaling pathway	23	7.08E-6	4.89E-3
GO:0043270	positive regulation of ion transport	17	1.27E-5	7.97E-3
GO:0044702	single organism reproductive process	15	1.83E-5	1.05E-2
GO:0032101	regulation of response to external stimulus	36	1.96E-5	1.04E-2
GO:0010817	regulation of hormone levels	13	2.49E-5	1.23E-2
GO:0022414	reproductive process	16	2.94E-5	1.36E-2
GO:0060326	cell chemotaxis	16	3.26E-5	1.41E-2
GO:0030595	leukocyte chemotaxis	8	3.29E-5	1.34E-2
GO:0044700	single organism signaling	19	3.77E-5	1.45E-2
GO:0007267	cell-cell signaling	12	4.94E-5	1.8E-2
GO:0032103	positive regulation of response to external stimulus	22	4.97E-5	1.72E-2
GO:0023052	signaling	19	5.41E-5	1.78E-2

GO:0008283	cell proliferation	55	5.62E-5	1.77E-2
GO:1903531	negative regulation of secretion by cell	12	6.18E-5	1.86E-2
GO:0051048	negative regulation of secretion	12	6.18E-5	1.78E-2
GO:0019221	cytokine-mediated signaling pathway	29	6.84E-5	1.89E-2
GO:0033993	response to lipid	21	7.19E-5	1.91E-2
GO:0044060	regulation of endocrine process	5	7.33E-5	1.88E-2
GO:0006952	defense response	86	7.8E-5	1.93E-2
GO:0071674	mononuclear cell migration	8	8.05E-5	1.92E-2
GO:0002548	monocyte chemotaxis	8	8.05E-5	1.86E-2
GO:0006954	inflammatory response	23	8.54E-5	1.9E-2
GO:0048545	response to steroid hormone	9	8.78E-5	1.9E-2
GO:0006935	chemotaxis	19	1.03E-4	2.16E-2
GO:0042330	taxis	19	1.03E-4	2.09E-2
GO:0071396	cellular response to lipid	11	1.11E-4	2.19E-2
GO:0002685	regulation of leukocyte migration	10	1.14E-4	2.19E-2
GO:0070098	chemokine-mediated signaling pathway	9	1.18E-4	2.2E-2
GO:0009725	response to hormone	13	1.2E-4	2.19E-2
GO:0009914	hormone transport	6	1.32E-4	2.33E-2
GO:0050729	positive regulation of inflammatory response	11	1.35E-4	2.33E-2
GO:0031960	response to corticosteroid	7	1.39E-4	2.34E-2
GO:0050900	leukocyte migration	11	1.52E-4	2.51E-2
GO:0007166	cell surface receptor signaling pathway	119	1.61E-4	2.58E-2
GO:0032846	Positive regulation of homeostatic process	10	2.04E-4	3.2E-2
GO:0071407	cellular response to organic cyclic compound	10	2.06E-4	3.16E-2

GO:0071345	cellular response to cytokine stimulus	11	2.07E-4	3.11E-2
GO:0043207	response to external biotic stimulus	81	2.14E-4	3.15E-2
GO:0003006	developmental process involved in reproduction	12	2.16E-4	3.11E-2
GO:0046879	hormone secretion	5	2.19E-4	3.08E-2
GO:0051968	positive regulation of synaptic transmission. glutamatergic	3	2.55E-4	3.53E-2
GO:0030593	neutrophil chemotaxis	5	2.7E-4	3.66E-2
GO:1990266	neutrophil migration	5	2.7E-4	3.59E-2
GO:0046887	positive regulation of hormone secretion	5	2.74E-4	3.57E-2
GO:0023061	signal release	6	2.74E-4	3.51E-2
GO:0051240	positive regulation of multicellular organismal process	41	2.85E-4	3.58E-2
GO:0043269	regulation of ion transport	36	2.87E-4	3.54E-2
GO:0021879	forebrain neuron differentiation	2	3.16E-4	3.84E-2
GO:0021773	striatal medium spiny neuron differentiation	2	3.16E-4	3.77E-2
GO:0046883	regulation of hormone secretion	7	3.36E-4	3.94E-2
GO:0032689	negative regulation of interferon-gamma production	3	3.39E-4	3.91E-2
GO:1903530	regulation of secretion by cell	36	3.76E-4	4.26E-2
GO:0051046	regulation of secretion	36	3.76E-4	4.19E-2
GO:0002687	positive regulation of leukocyte migration	9	3.89E-4	4.26E-2
GO:0070372	regulation of ERK1 and ERK2 cascade	23	4.26E-4	4.6E-2
GO:0072678	T cell migration	2	4.34E-4	4.62E-2
GO:0007399	nervous system development	12	4.53E-4	4.74E-2
GO:2000833	positive regulation of steroid hormone secretion	3	4.6E-4	4.75E-2

GO:2000831	regulation of steroid hormone secretion	3	4.6E-4	4.68E-2
GO:0044057	regulation of system process	14	4.92E-4	4.93E-2
GO:0007154	cell communication	13	5.06E-4	5.00E-02
GO:0050710	negative regulation of cytokine secretion	9	5.08E-4	4.94E-2
GO:0010466	negative regulation of peptidase activity	18	5.11E-4	4.91E-2
GO:0010951	negative regulation of endopeptidase activity	18	5.11E-4	4.84E-2
GO:0006955	immune response	71	5.14E-4	4.8E-2
GO:0071621	granulocyte chemotaxis	5	5.65E-4	5.2E-2
GO:0097530	granulocyte migration	5	5.65E-4	5.14E-2
GO:0002376	immune system process	108	5.74E-4	5.15E-2
GO:0042127	regulation of cell proliferation	137	5.86E-4	5.19E-2
GO:0060740	prostate gland epithelium morphogenesis	3	5.93E-4	5.19E-2
GO:0009605	response to external stimulus	157	6.01E-4	5.19E-2
GO:0007600	sensory perception	7	6.11E-4	5.21E-2
GO:0030072	peptide hormone secretion	5	6.11E-4	5.15E-2
GO:0052548	regulation of endopeptidase activity	28	6.22E-4	5.18E-2
GO:0014070	response to organic cyclic compound	14	6.56E-4	5.4E-2
GO:0051384	response to glucocorticoid	6	7.28E-4	5.92E-2
GO:0010033	response to organic substance	33	7.47E-4	6.01E-2
GO:0007610	behavior	13	8.64E-4	6.87E-2
GO:0052547	regulation of peptidase activity	30	9.81E-4	7.7E-2

Notes: FDR = False discovery rate.

Table IV. Functional annotation clustering by DAVID of the 808 genes downregulated by anti-CCL2 Ab at 4 h in MDMs

Category	Term	count	pvalue	FDR
UP_KEYWORDS	Mitochondrion	77	6.66E-07	9.22E-04
GOTERM_CC_DIRECT	GO:0005759~mitochondrial matrix	34	1.33E-06	0.002
UP_KEYWORDS	Kinase	56	1.65E-06	0.002
UP_KEYWORDS	Transit peptide	45	1.69E-06	0.002
UP_KEYWORDS	ATP-binding	86	1.05E-05	0.015
UP_SEQ_FEATURE	nucleotide phosphate-binding region:ATP	68	9.15E-06	0.016

Notes: FDR = False discovery rate.

Table V. Functional annotation clustering by DAVID of the 184 genes upregulated by anti-CCL2 Ab at 20 h in MDMs

Category	Term	count	pvalue	FDR
UP_KEYWORDS	Immunity	33	3.47E-20	4.52E-17
UP_KEYWORDS	Innate immunity	21	1.05E-13	1.37E-10
UP_KEYWORDS	Secreted	51	5.71E-13	7.44E-10
GOTERM_CC_DIRECT	GO:0005576~extracellular region	45	6.54E-11	8.08E-08
UP_KEYWORDS	Inflammatory response	14	7.57E-10	9.87E-07
UP_SEQ_FEATURE	signal peptide	64	1.04E-09	1.56E-06
UP_KEYWORDS	Disulfide bond	62	5.23E-09	6.81E-06
UP_SEQ_FEATURE	disulfide bond	57	6.93E-09	1.04E-05
UP_KEYWORDS	Signal	68	5.04E-08	6.57E-05
GOTERM_BP_DIRECT	GO:0045087~innate immune response	20	1.04E-07	1.71E-04
KEGG_PATHWAY	hsa04060:Cytokine-cytokine receptor interaction	17	1.74E-07	2.15E-04
UP_KEYWORDS	Cadmium	5	6.61E-07	8.61E-04
UP_SEQ_FEATURE	glycosylation site:N-linked (GlcNAc...)	67	6.91E-07	0.001
UP_KEYWORDS	Glycoprotein	69	8.58E-07	0.001
GOTERM_BP_DIRECT	GO:0050729~positive regulation of inflammatory response	9	9.71E-07	0.002
GOTERM_CC_DIRECT	GO:0005615~extracellular space	33	1.35E-06	0.002
UP_KEYWORDS	Chemotaxis	9	2.18E-06	0.003
INTERPRO	IPR018064:Metallothionein. vertebrate. metal binding site	5	2.38E-06	0.003
UP_SEQ_FEATURE	region of interest:Beta	5	4.02E-06	0.006
UP_SEQ_FEATURE	region of interest:Alpha	5	4.02E-06	0.006

UP_KEYWORDS	Metal-thiolate cluster	5	5.07E-06	0.007
INTERPRO	IPR001811:Chemokine interleukin-8-like domain	7	4.97E-06	0.007
INTERPRO	IPR001811:Chemokine interleukin-8-like domain	7	4.97E-06	0.007
GOTERM_BP_DIRECT	GO:0006935~chemotaxis	10	4.89E-06	0.008
UP_SEQ_FEATURE	metal ion-binding site:Divalent metal cation; cluster A	5	5.59E-06	0.008
UP_SEQ_FEATURE	metal ion-binding site:Divalent metal cation; cluster B	5	5.59E-06	0.008
SMART	SM00199:SCY	7	8.28E-06	0.009
SMART	SM00199:SCY	7	8.28E-06	0.009
INTERPRO	IPR023587:Metallothionein domain. vertebrate	5	7.05E-06	0.010
INTERPRO	IPR017854:Metallothionein domain	5	7.05E-06	0.010
INTERPRO	IPR003019:Metallothionein superfamily. eukaryotic	5	7.05E-06	0.010
INTERPRO	IPR000006:Metallothionein. vertebrate	5	7.05E-06	0.010
GOTERM_MF_DIRECT	GO:0008009~chemokine activity	7	9.87E-06	0.014
GOTERM_MF_DIRECT	GO:0008009~chemokine activity	7	9.87E-06	0.014
UP_KEYWORDS	Copper	7	2.09E-05	0.027
GOTERM_BP_DIRECT	GO:0071276~cellular response to cadmium ion	5	1.76E-05	0.029
GOTERM_CC_DIRECT	GO:0005887~integral component of plasma membrane	31	2.37E-05	0.029
UP_KEYWORDS	Host-virus interaction	14	3.23E-05	0.042

Notes: FDR = False discovery rate.

Bibliography

(1) Deeks SG, Lewin SR, Ross AL, Ananworanich J, Benkirane M, Cannon P, et al. International AIDS Society global scientific strategy: towards an HIV cure 2016. Nat Med 2016 Aug;22(8):839-850.

(2) Engelman A, Cherepanov P. The structural biology of HIV-1: mechanistic and therapeutic insights. Nat Rev Microbiol 2012 Mar 16;10(4):279-290.

(3) Fanales-Belasio E, Raimondo M, Suligoi B, Butto S. HIV virology and pathogenetic mechanisms of infection: a brief overview. Ann Ist Super Sanita 2010;46(1):5-14.

(4) Mogensen TH, Melchjorsen J, Larsen CS, Paludan SR. Innate immune recognition and activation during HIV infection. Retrovirology 2010 Jun 22;7:54-4690-7-54.

(5) Maartens G, Celum C, Lewin SR. HIV infection: epidemiology, pathogenesis, treatment, and prevention. Lancet 2014 Jul 19;384(9939):258-271.

(6) Lackner AA, Lederman MM, Rodriguez B. HIV pathogenesis: the host. Cold Spring Harb Perspect Med 2012 Sep 1;2(9):a007005.

(7) Nasi M, De Biasi S, Gibellini L, Bianchini E, Pecorini S, Bacca V, et al. Ageing and inflammation in patients with HIV infection. Clin Exp Immunol 2016 May 20.

(8) Koppensteiner H, Brack-Werner R, Schindler M. Macrophages and their relevance in Human Immunodeficiency Virus Type I infection. Retrovirology 2012 Oct 4;9:82-4690-9-82.

(9) Murray PJ, Wynn TA. Protective and pathogenic functions of macrophage subsets. Nat Rev Immunol 2011 Oct 14;11(11):723-737.

(10) Abbas W, Tariq M, Iqbal M, Kumar A, Herbein G. Eradication of HIV-1 from the macrophage reservoir: an uncertain goal? Viruses 2015 Mar 31;7(4):1578-1598.

(11) Gartner S, Markovits P, Markovitz DM, Kaplan MH, Gallo RC, Popovic M. The role of mononuclear phagocytes in HTLV-III/LAV infection. Science 1986 Jul 11;233(4760):215-219.

(12) Wiley CA, Schrier RD, Nelson JA, Lampert PW, Oldstone MB. Cellular localization of human immunodeficiency virus infection within the brains of acquired immune deficiency syndrome patients. Proc Natl Acad Sci U S A 1986 Sep;83(18):7089-7093.

(13) Koenig S, Gendelman HE, Orenstein JM, Dal Canto MC, Pezeshkpour GH, Yungbluth M, et al. Detection of AIDS virus in macrophages in brain tissue from AIDS patients with encephalopathy. Science 1986 Sep 5;233(4768):1089-1093.

(14) Salahuddin SZ, Rose RM, Groopman JE, Markham PD, Gallo RC. Human T lymphotropic virus type III infection of human alveolar macrophages. Blood 1986 Jul;68(1):281-284.

(15) Takahashi K, Wesselingh SL, Griffin DE, McArthur JC, Johnson RT, Glass JD. Localization of HIV-1 in human brain using polymerase chain reaction/in situ hybridization and immunocytochemistry. Ann Neurol 1996 Jun;39(6):705-711.

(16) Wang TH, Donaldson YK, Brettle RP, Bell JE, Simmonds P. Identification of shared populations of human immunodeficiency virus type 1 infecting microglia and tissue macrophages outside the central nervous system. J Virol 2001 Dec;75(23):11686-11699.

(17) Zalar A, Figueroa MI, Ruibal-Ares B, Bare P, Cahn P, de Bracco MM, et al. Macrophage HIV-1 infection in duodenal tissue of patients on long term HAART. Antiviral Res 2010 Aug;87(2):269-271.

(18) Orenstein JM, Fox C, Wahl SM. Macrophages as a source of HIV during opportunistic infections. Science 1997 Jun 20;276(5320):1857-1861.

(19) Honeycutt JB, Wahl A, Baker C, Spagnuolo RA, Foster J, Zakharova O, et al. Macrophages sustain HIV replication in vivo independently of T cells. J Clin Invest 2016 Apr 1;126(4):1353-1366.

(20) Graziano F, Vicenzi E, Poli G. Immuno-Pharmacological Targeting of Virus-Containing Compartments in HIV-1-Infected Macrophages. Trends Microbiol 2016 Jul;24(7):558-567.

(21) Sattentau QJ, Stevenson M. Macrophages and HIV-1: An Unhealthy Constellation. Cell Host Microbe 2016 Mar 9;19(3):304-310.

(22) Cassol E, Cassetta L, Rizzi C, Alfano M, Poli G. M1 and M2a polarization of human monocyte-derived macrophages inhibits HIV-1 replication by distinct mechanisms. J Immunol 2009 May 15;182(10):6237-6246.

(23) Cassol E, Cassetta L, Alfano M, Poli G. Macrophage polarization and HIV-1 infection. J Leukoc Biol 2010 Apr;87(4):599-608.

(24) Campbell JH, Hearps AC, Martin GE, Williams KC, Crowe SM. The importance of monocytes and macrophages in HIV pathogenesis, treatment, and cure. AIDS 2014 Sep 24;28(15):2175-2187.

(25) Jia X, Zhao Q, Xiong Y. HIV suppression by host restriction factors and viral immune evasion. Curr Opin Struct Biol 2015 Apr;31:106-114.

(26) Simon V, Bloch N, Landau NR. Intrinsic host restrictions to HIV-1 and mechanisms of viral escape. Nat Immunol 2015 Jun;16(6):546-553.

(27) Koning FA, Newman EN, Kim EY, Kunstman KJ, Wolinsky SM, Malim MH. Defining APOBEC3 expression patterns in human tissues and hematopoietic cell subsets. J Virol 2009 Sep;83(18):9474-9485.

(28) Sheehy AM, Gaddis NC, Choi JD, Malim MH. Isolation of a human gene that inhibits HIV-1 infection and is suppressed by the viral Vif protein. Nature 2002 Aug 8;418(6898):646-650.

(29) Feng Y, Baig TT, Love RP, Chelico L. Suppression of APOBEC3-mediated restriction of HIV-1 by Vif. Front Microbiol 2014 Aug 26;5:450.

(30) Malim MH, Bieniasz PD. HIV Restriction Factors and Mechanisms of Evasion. Cold Spring Harb Perspect Med 2012 May;2(5):a006940.

(31) Aguiar RS, Lovsin N, Tanuri A, Peterlin BM. Vpr.A3A chimera inhibits HIV replication. J Biol Chem 2008 Feb 1;283(5):2518-2525.

(32) Bishop KN, Holmes RK, Sheehy AM, Davidson NO, Cho SJ, Malim MH. Cytidine deamination of retroviral DNA by diverse APOBEC proteins. Curr Biol 2004 Aug 10;14(15):1392-1396.

(33) Peng G, Greenwell-Wild T, Nares S, Jin W, Lei KJ, Rangel ZG, et al. Myeloid differentiation and susceptibility to HIV-1 are linked to APOBEC3 expression. Blood 2007 Jul 1;110(1):393-400.

(34) Berger G, Durand S, Fargier G, Nguyen XN, Cordeil S, Bouaziz S, et al. APOBEC3A is a specific inhibitor of the early phases of HIV-1 infection in myeloid cells. PLoS Pathog 2011 Sep;7(9):e1002221.

(35) Mohanram V, Skold AE, Bachle SM, Pathak SK, Spetz AL. IFN-alpha induces APOBEC3G, F, and A in immature dendritic cells and limits HIV-1 spread to CD4+ T cells. J Immunol 2013 Apr 1;190(7):3346-3353.

(36) Koning FA, Goujon C, Bauby H, Malim MH. Target cell-mediated editing of HIV-1 cDNA by APOBEC3 proteins in human macrophages. J Virol 2011 Dec;85(24):13448-13452.

(37) Greenwell-Wild T, Vazquez N, Jin W, Rangel Z, Munson PJ, Wahl SM. Interleukin-27 inhibition of HIV-1 involves an intermediate induction of type I interferon. Blood 2009 Aug 27;114(9):1864-1874.

(38) Cassetta L, Kajaste-Rudnitski A, Coradin T, Saba E, Della Chiara G, Barbagallo M, et al. M1 polarization of human monocyte-derived macrophages restricts pre and postintegration steps of HIV-1 replication. AIDS 2013 Jul 31;27(12):1847-1856.

(39) Graziano F, Vicenzi E, Poli G. Plastic restriction of HIV-1 replication in human macrophages derived from M1/M2 polarized monocytes. J Leukoc Biol 2016 Nov;100(5):1147-1153.

(40) Wang Y, Schmitt K, Guo K, Santiago ML, Stephens EB. Role of the single deaminase domain APOBEC3A in virus restriction, retrotransposition, DNA damage and cancer. J Gen Virol 2016 Jan;97(1):1-17.

(41) Warren CJ, Xu T, Guo K, Griffin LM, Westrich JA, Lee D, et al. APOBEC3A functions as a restriction factor of human papillomavirus. J Virol 2015 Jan;89(1):688-702.

(42) Suspene R, Aynaud MM, Guetard D, Henry M, Eckhoff G, Marchio A, et al. Somatic hypermutation of human mitochondrial and nuclear DNA by APOBEC3 cytidine

deaminases, a pathway for DNA catabolism. Proc Natl Acad Sci U S A 2011 Mar 22;108(12):4858-4863.

(43) Landry S, Narvaiza I, Linfesty DC, Weitzman MD. APOBEC3A can activate the DNA damage response and cause cell-cycle arrest. EMBO Rep 2011 May;12(5):444-450.

(44) Land AM, Law EK, Carpenter MA, Lackey L, Brown WL, Harris RS. Endogenous APOBEC3A DNA cytosine deaminase is cytoplasmic and nongenotoxic. J Biol Chem 2013 Jun 14;288(24):17253-17260.

(45) Ballana E, Este JA. SAMHD1: at the crossroads of cell proliferation, immune responses, and virus restriction. Trends Microbiol 2015 Nov;23(11):680-692.

(46) Schmidt S, Schenkova K, Adam T, Erikson E, Lehmann-Koch J, Sertel S, et al. SAMHD1's protein expression profile in humans. J Leukoc Biol 2015 Jul;98(1):5-14.

(47) Hrecka K, Hao C, Gierszewska M, Swanson SK, Kesik-Brodacka M, Srivastava S, et al. Vpx relieves inhibition of HIV-1 infection of macrophages mediated by the SAMHD1 protein. Nature 2011 Jun 29;474(7353):658-661.

(48) Laguette N, Sobhian B, Casartelli N, Ringeard M, Chable-Bessia C, Segeral E, et al. SAMHD1 is the dendritic- and myeloid-cell-specific HIV-1 restriction factor counteracted by Vpx. Nature 2011 May 25;474(7353):654-657.

(49) Lahouassa H, Daddacha W, Hofmann H, Ayinde D, Logue EC, Dragin L, et al. SAMHD1 restricts the replication of human immunodeficiency virus type 1 by depleting the intracellular pool of deoxynucleoside triphosphates. Nat Immunol 2012 Feb 12;13(3):223-228.

(50) White TE, Brandariz-Nunez A, Valle-Casuso JC, Amie S, Nguyen LA, Kim B, et al. The retroviral restriction ability of SAMHD1, but not its deoxynucleotide triphosphohydrolase activity, is regulated by phosphorylation. Cell Host Microbe 2013 Apr 17;13(4):441-451.

(51) Cribier A, Descours B, Valadao AL, Laguette N, Benkirane M. Phosphorylation of SAMHD1 by cyclin A2/CDK1 regulates its restriction activity toward HIV-1. Cell Rep 2013 Apr 25;3(4):1036-1043.

(52) Yang Z, Greene WC. A new activity for SAMHD1 in HIV restriction. Nat Med 2014 Aug;20(8):808-809.

(53) Haller O. Dynamins are forever: MxB inhibits HIV-1. Cell Host Microbe 2013 Oct 16;14(4):371-373.

(54) Kane M, Yadav SS, Bitzegeio J, Kutluay SB, Zang T, Wilson SJ, et al. MX2 is an interferon-induced inhibitor of HIV-1 infection. Nature 2013 Oct 24;502(7472):563-566.

(55) Goujon C, Moncorge O, Bauby H, Doyle T, Ward CC, Schaller T, et al. Human MX2 is an interferon-induced post-entry inhibitor of HIV-1 infection. Nature 2013 Oct 24;502(7472):559-562.

(56) Haller O, Staeheli P, Schwemmle M, Kochs G. Mx GTPases: dynamin-like antiviral machines of innate immunity. Trends Microbiol 2015 Mar;23(3):154-163.

(57) Hattlmann CJ, Kelly JN, Barr SD. TRIM22: A Diverse and Dynamic Antiviral Protein. Mol Biol Int 2012;2012:153415.

(58) Doyle T, Goujon C, Malim MH. HIV-1 and interferons: who's interfering with whom? Nat Rev Microbiol 2015 Jul;13(7):403-413.

(59) Arts EJ, Hazuda DJ. HIV-1 antiretroviral drug therapy. Cold Spring Harb Perspect Med 2012 Apr;2(4):a007161.

(60) Clutter DS, Jordan MR, Bertagnolio S, Shafer RW. HIV-1 drug resistance and resistance testing. Infect Genet Evol 2016 Aug 29.

(61) Marzolini C, Gibbons S, Khoo S, Back D. Cobicistat versus ritonavir boosting and differences in the drug-drug interaction profiles with co-medications. J Antimicrob Chemother 2016 Jul;71(7):1755-1758.

(62) Woollard SM, Kanmogne GD. Maraviroc: a review of its use in HIV infection and beyond. Drug Des Devel Ther 2015 Oct 1;9:5447-5468.

(63) Margolis AM, Heverling H, Pham PA, Stolbach A. A review of the toxicity of HIV medications. J Med Toxicol 2014 Mar;10(1):26-39.

(64) Cihlar T, Fordyce M. Current status and prospects of HIV treatment. Curr Opin Virol 2016 Jun;18:50-56.

(65) Badowski ME, Perez SE, Biagi M, Littler JA. New Antiretroviral Treatment for HIV. Infect Dis Ther 2016 Sep;5(3):329-352.

(66) Marier JF, Trinh M, Pheng LH, Palleja SM, Martin DE. Pharmacokinetics and pharmacodynamics of TBR-652, a novel CCR5 antagonist, in HIV-1-infected, antiretroviral treatment-experienced, CCR5 antagonist-naive patients. Antimicrob Agents Chemother 2011 Jun;55(6):2768-2774.

(67) Lalezari J, Gathe J, Brinson C, Thompson M, Cohen C, Dejesus E, et al. Safety, efficacy, and pharmacokinetics of TBR-652, a CCR5/CCR2 antagonist, in HIV-1-infected, treatment-experienced, CCR5 antagonist-naive subjects. J Acquir Immune Defic Syndr 2011 Jun 1;57(2):118-125.

(68) Thompson M, Saag M, DeJesus E, Gathe J, Lalezari J, Landay AL, et al. A 48-week randomized phase 2b study evaluating cenicriviroc versus efavirenz in treatment-naive HIV-infected adults with C-C chemokine receptor type 5-tropic virus. AIDS 2016 Mar 27;30(6):869-878.

(69) Massanella M, Fromentin R, Chomont N. Residual inflammation and viral reservoirs: alliance against an HIV cure. Curr Opin HIV AIDS 2016 Mar;11(2):234-241.

(70) Wong JK, Hezareh M, Gunthard HF, Havlir DV, Ignacio CC, Spina CA, et al. Recovery of replication-competent HIV despite prolonged suppression of plasma viremia. Science 1997 Nov 14;278(5341):1291-1295.

(71) Finzi D, Hermankova M, Pierson T, Carruth LM, Buck C, Chaisson RE, et al. Identification of a reservoir for HIV-1 in patients on highly active antiretroviral therapy. Science 1997 Nov 14;278(5341):1295-1300.

(72) Chun TW, Stuyver L, Mizell SB, Ehler LA, Mican JA, Baseler M, et al. Presence of an inducible HIV-1 latent reservoir during highly active antiretroviral therapy. Proc Natl Acad Sci U S A 1997 Nov 25;94(24):13193-13197.

(73) Murray AJ, Kwon KJ, Farber DL, Siliciano RF. The Latent Reservoir for HIV-1: How Immunologic Memory and Clonal Expansion Contribute to HIV-1 Persistence. J Immunol 2016 Jul 15;197(2):407-417.

(74) Paiardini M, Lichterfeld M. Follicular T helper cells: hotspots for HIV-1 persistence. Nat Med 2016 Jul 7;22(7):711-712.

(75) Wong JK, Yukl SA. Tissue reservoirs of HIV. Curr Opin HIV AIDS 2016 Jul;11(4):362-370.

(76) Barton K, Winckelmann A, Palmer S. HIV-1 Reservoirs During Suppressive Therapy. Trends Microbiol 2016 May;24(5):345-355.

(77) Kimata JT, Rice AP, Wang J. Challenges and strategies for the eradication of the HIV reservoir. Curr Opin Immunol 2016 Oct;42:65-70.

(78) Delagreverie HM, Delaugerre C, Lewin SR, Deeks SG, Li JZ. Ongoing Clinical Trials of Human Immunodeficiency Virus Latency-Reversing and Immunomodulatory Agents. Open Forum Infect Dis 2016 Oct 7;3(4):ofw189.

(79) Margolis DM, Garcia JV, Hazuda DJ, Haynes BF. Latency reversal and viral clearance to cure HIV-1. Science 2016 Jul 22;353(6297):aaf6517.

(80) Barouch DH, Deeks SG. Immunologic strategies for HIV-1 remission and eradication. Science 2014 Jul 11;345(6193):169-174.

(81) Chun TW, Moir S, Fauci AS. HIV reservoirs as obstacles and opportunities for an HIV cure. Nat Immunol 2015 Jun;16(6):584-589.

(82) Paiardini M, Muller-Trutwin M. HIV-associated chronic immune activation. Immunol Rev 2013 Jul;254(1):78-101.

(83) Appay V, Sauce D. Immune activation and inflammation in HIV-1 infection: causes and consequences. J Pathol 2008 Jan;214(2):231-241.

(84) Klatt NR, Chomont N, Douek DC, Deeks SG. Immune activation and HIV persistence: implications for curative approaches to HIV infection. Immunol Rev 2013 Jul;254(1):326-342.

(85) Younas M, Psomas C, Reynes J, Corbeau P. Immune activation in the course of HIV-1 infection: Causes, phenotypes and persistence under therapy. HIV Med 2016 Feb;17(2):89-105.

(86) Tincati C, Douek DC, Marchetti G. Gut barrier structure, mucosal immunity and intestinal microbiota in the pathogenesis and treatment of HIV infection. AIDS Res Ther 2016 Apr 11;13(1):19.

(87) Valverde-Villegas JM, Matte MC, de Medeiros RM, Chies JA. New Insights about Treg and Th17 Cells in HIV Infection and Disease Progression. J Immunol Res 2015;2015:647916.

(88) Vieillard V, Gharakhanian S, Lucar O, Katlama C, Launay O, Autran B, et al. Perspectives for immunotherapy: which applications might achieve an HIV functional cure? Oncotarget 2016 Jun 21;7(25):38946-38958.

(89) Cochran BH, Reffel AC, Stiles CD. Molecular cloning of gene sequences regulated by platelet-derived growth factor. Cell 1983 Jul;33(3):939-947.

(90) Deshmane SL, Kremlev S, Amini S, Sawaya BE. Monocyte chemoattractant protein-1 (MCP-1): an overview. J Interferon Cytokine Res 2009 Jun;29(6):313-326.

(91) Yadav A, Saini V, Arora S. MCP-1: chemoattractant with a role beyond immunity: a review. Clin Chim Acta 2010 Nov 11;411(21-22):1570-1579.

(92) Sanseverino I, Rinaldi AO, Purificato C, Cortese A, Millefiorini E, Gessani S, et al. CCL2 induction by 1,25(OH)2D3 in dendritic cells from healthy donors and multiple sclerosis patients. J Steroid Biochem Mol Biol 2014 Oct;144 Pt A:102-105.

(93) Fantuzzi L, Canini I, Belardelli F, Gessani S. IFN-beta stimulates the production of beta-chemokines in human peripheral blood monocytes. Importance of macrophage differentiation. Eur Cytokine Netw 2001 Oct-Dec;12(4):597-603.

(94) Ansari AW, Bhatnagar N, Dittrich-Breiholz O, Kracht M, Schmidt RE, Heiken H. Host chemokine (C-C motif) ligand-2 (CCL2) is differentially regulated in HIV type 1 (HIV-1)-infected individuals. Int Immunol 2006 Oct;18(10):1443-1451.

(95) Ansari AW, Heiken H, Meyer-Olson D, Schmidt RE. CCL2: a potential prognostic marker and target of anti-inflammatory strategy in HIV/AIDS pathogenesis. Eur J Immunol 2011 Dec;41(12):3412-3418.

(96) Covino DA, Sabbatucci M, Fantuzzi L. The CCL2/CCR2 Axis in the Pathogenesis of HIV-1 Infection: A New Cellular Target for Therapy? Curr Drug Targets 2016;17(1):76-110.

(97) Fantuzzi L, Canini I, Belardelli F, Gessani S. HIV-1 gp120 stimulates the production of beta-chemokines in human peripheral blood monocytes through a CD4-independent mechanism. J Immunol 2001 May 1;166(9):5381-5387.

(98) Fantuzzi L, Spadaro F, Purificato C, Cecchetti S, Podo F, Belardelli F, et al. Phosphatidylcholine-specific phospholipase C activation is required for CCR5-dependent, NF-kB-driven CCL2 secretion elicited in response to HIV-1 gp120 in human primary macrophages. Blood 2008 Apr 1;111(7):3355-3363.

(99) Fantuzzi L, Spadaro F, Vallanti G, Canini I, Ramoni C, Vicenzi E, et al. Endogenous CCL2 (monocyte chemotactic protein-1) modulates human immunodeficiency virus type-1 replication and affects cytoskeleton organization in human monocyte-derived macrophages. Blood 2003 Oct 1;102(7):2334-2337.

(100) Eugenin EA, Osiecki K, Lopez L, Goldstein H, Calderon TM, Berman JW. CCL2/monocyte chemoattractant protein-1 mediates enhanced transmigration of human immunodeficiency virus (HIV)-infected leukocytes across the blood-brain barrier: a potential mechanism of HIV-CNS invasion and NeuroAIDS. J Neurosci 2006 Jan 25;26(4):1098-1106.

(101) Tan S, Duan H, Xun T, Ci W, Qiu J, Yu F, et al. HIV-1 impairs human retinal pigment epithelial barrier function: possible association with the pathogenesis of HIV-associated retinopathy. Lab Invest 2014 Jul;94(7):777-787.

(102) Vicenzi E, Alfano M, Ghezzi S, Gatti A, Veglia F, Lazzarin A, et al. Divergent regulation of HIV-1 replication in PBMC of infected individuals by CC chemokines: suppression by RANTES, MIP-1alpha, and MCP-3, and enhancement by MCP-1. J Leukoc Biol 2000 Sep;68(3):405-412.

(103) Campbell GR, Spector SA. CCL2 increases X4-tropic HIV-1 entry into resting CD4+ T cells. J Biol Chem 2008 Nov 7;283(45):30745-30753.

(104) Rollenhagen C, Asin SN. Enhanced HIV-1 replication in ex vivo ectocervical tissues from post-menopausal women correlates with increased inflammatory responses. Mucosal Immunol 2011 Nov;4(6):671-681.

(105) Kelder W, McArthur JC, Nance-Sproson T, McClernon D, Griffin DE. Beta-chemokines MCP-1 and RANTES are selectively increased in cerebrospinal fluid of patients with human immunodeficiency virus-associated dementia. Ann Neurol 1998 Nov;44(5):831-835.

(106) Spudich S, Gisslen M, Hagberg L, Lee E, Liegler T, Brew B, et al. Central nervous system immune activation characterizes primary human immunodeficiency virus 1 infection even in participants with minimal cerebrospinal fluid viral burden. J Infect Dis 2011 Sep 1;204(5):753-760.

(107) Weiss L, Si-Mohamed A, Giral P, Castiel P, Ledur A, Blondin C, et al. Plasma levels of monocyte chemoattractant protein-1 but not those of macrophage inhibitory protein-1alpha and RANTES correlate with virus load in human immunodeficiency virus infection. J Infect Dis 1997 Dec;176(6):1621-1624.

(108) Miller AP, Feng W, Xing D, Weathington NM, Blalock JE, Chen YF, et al. Estrogen modulates inflammatory mediator expression and neutrophil chemotaxis in injured arteries. Circulation 2004 Sep 21;110(12):1664-1669.

(109) Pulliam L, Sun B, Rempel H. Invasive chronic inflammatory monocyte phenotype in subjects with high HIV-1 viral load. J Neuroimmunol 2004 Dec;157(1-2):93-98.

(110) Van den Bergh R, Florence E, Vlieghe E, Boonefaes T, Grooten J, Houthuys E, et al. Transcriptome analysis of monocyte-HIV interactions. Retrovirology 2010 Jun 14;7:53-4690-7-53.

(111) Duskova K, Nagilla P, Le HS, Iyer P, Thalamuthu A, Martinson J, et al. MicroRNA regulation and its effects on cellular transcriptome in human immunodeficiency virus-1 (HIV-1) infected individuals with distinct viral load and CD4 cell counts. BMC Infect Dis 2013 May 30;13:250-2334-13-250.

(112) Monteiro de Almeida S, Letendre S, Zimmerman J, Kolakowski S, Lazzaretto D, McCutchan JA, et al. Relationship of CSF leukocytosis to compartmentalized changes in MCP-1/CCL2 in the CSF of HIV-infected patients undergoing interruption of antiretroviral therapy. J Neuroimmunol 2006 Oct;179(1-2):180-185.

(113) Weiss JM, Downie SA, Lyman WD, Berman JW. Astrocyte-derived monocyte-chemoattractant protein-1 directs the transmigration of leukocytes across a model of the human blood-brain barrier. J Immunol 1998 Dec 15;161(12):6896-6903.

(114) Williams DW, Byrd D, Rubin LH, Anastos K, Morgello S, Berman JW. CCR2 on CD14(+)CD16(+) monocytes is a biomarker of HIV-associated neurocognitive disorders. Neurol Neuroimmunol Neuroinflamm 2014 Oct 9;1(3):e36.

(115) Bernasconi S, Cinque P, Peri G, Sozzani S, Crociati A, Torri W, et al. Selective elevation of monocyte chemotactic protein-1 in the cerebrospinal fluid of AIDS patients with cytomegalovirus encephalitis. J Infect Dis 1996 Nov;174(5):1098-1101.

(116) Cinque P, Vago L, Mengozzi M, Torri V, Ceresa D, Vicenzi E, et al. Elevated cerebrospinal fluid levels of monocyte chemotactic protein-1 correlate with HIV-1 encephalitis and local viral replication. AIDS 1998 Jul 30;12(11):1327-1332.

(117) Christo PP, Vilela Mde C, Bretas TL, Domingues RB, Greco DB, Livramento JA, et al. Cerebrospinal fluid levels of chemokines in HIV infected patients with and without opportunistic infection of the central nervous system. J Neurol Sci 2009 Dec 15;287(1-2):79-83.

(118) Chang CC, Omarjee S, Lim A, Spelman T, Gosnell BI, Carr WH, et al. Chemokine levels and chemokine receptor expression in the blood and the cerebrospinal fluid of HIV-infected patients with cryptococcal meningitis and cryptococcosis-associated immune reconstitution inflammatory syndrome. J Infect Dis 2013 Nov 15;208(10):1604-1612.

(119) Ansari AW, Kamarulzaman A, Schmidt RE. Multifaceted Impact of Host C-C Chemokine CCL2 in the Immuno-Pathogenesis of HIV-1/M. tuberculosis Co-Infection. Front Immunol 2013 Oct 4;4:312.

(120) Ansari AW, Schmidt RE, Shankar EM, Kamarulzaman A. Immuno-pathomechanism of liver fibrosis: targeting chemokine CCL2-mediated HIV:HCV nexus. J Transl Med 2014 Dec 10;12:341-014-0341-8.

(121) Allers K, Fehr M, Conrad K, Epple HJ, Schurmann D, Geelhaar-Karsch A, et al. Macrophages accumulate in the gut mucosa of untreated HIV-infected patients. J Infect Dis 2014 Mar 1;209(5):739-748.

(122) Fantuzzi L, Borghi P, Ciolli V, Pavlakis G, Belardelli F, Gessani S. Loss of CCR2 expression and functional response to monocyte chemotactic protein (MCP-1) during the differentiation of human monocytes: role of secreted MCP-1 in the regulation of the chemotactic response. Blood 1999 Aug 1;94(3):875-883.

(123) Federico M, Percario Z, Olivetta E, Fiorucci G, Muratori C, Micheli A, et al. HIV-1 Nef activates STAT1 in human monocytes/macrophages through the release of soluble factors. Blood 2001 Nov 1;98(9):2752-2761.

(124) Sparacio S, Pfeiffer T, Schaal H, Bosch V. Generation of a flexible cell line with regulatable, high-level expression of HIV Gag/Pol particles capable of packaging HIV-derived vectors. Mol Ther 2001 Apr;3(4):602-612.

(125) Negri DR, Michelini Z, Baroncelli S, Spada M, Vendetti S, Buffa V, et al. Successful immunization with a single injection of non-integrating lentiviral vector. Mol Ther 2007 Sep;15(9):1716-1723.

(126) Negri DR, Bona R, Michelini Z, Leone P, Macchia I, Klotman ME, et al. Transduction of human antigen-presenting cells with integrase-defective lentiviral vector enables functional expansion of primed antigen-specific CD8(+) T cells. Hum Gene Ther 2010 Aug;21(8):1029-1035.

(127) Durand S, Nguyen XN, Turpin J, Cordeil S, Nazaret N, Croze S, et al. Tailored HIV-1 vectors for genetic modification of primary human dendritic cells and monocytes. J Virol 2013 Jan;87(1):234-242.

(128) Mochizuki H, Schwartz JP, Tanaka K, Brady RO, Reiser J. High-titer human immunodeficiency virus type 1-based vector systems for gene delivery into nondividing cells. J Virol 1998 Nov;72(11):8873-8883.

(129) Weiss S, Konig B, Muller HJ, Seidel H, Goody RS. Synthetic human tRNA(UUULys3) and natural bovine tRNA(UUULys3) interact with HIV-1 reverse transcriptase and serve as specific primers for retroviral cDNA synthesis. Gene 1992 Feb 15;111(2):183-197.

(130) Liszewski MK, Yu JJ, O'Doherty U. Detecting HIV-1 integration by repetitive-sampling Alu-gag PCR. Methods 2009 Apr;47(4):254-260.

(131) Reigadas S, Andreola ML, Wittkop L, Cosnefroy O, Anies G, Recordon-Pinson P, et al. Evolution of 2-long terminal repeat (2-LTR) episomal HIV-1 DNA in raltegravir-treated patients and in in vitro infected cells. J Antimicrob Chemother 2010 Mar;65(3):434-437.

(132) Trapnell C, Pachter L, Salzberg SL. TopHat: discovering splice junctions with RNA-Seq. Bioinformatics 2009 May 1;25(9):1105-1111.

(133) Anders S, Pyl PT, Huber W. HTSeq--a Python framework to work with high-throughput sequencing data. Bioinformatics 2015 Jan 15;31(2):166-169.

(134) Love MI, Huber W, Anders S. Moderated estimation of fold change and dispersion for RNA-seq data with DESeq2. Genome Biol 2014;15(12):550.

(135) Bischof D, Cornetta K. Flexibility in cell targeting by pseudotyping lentiviral vectors. Methods Mol Biol 2010;614:53-68.

(136) Federico M. HIV-protease inhibitors block the replication of both vesicular stomatitis and influenza viruses at an early post-entry replication step. Virology 2011 Aug 15;417(1):37-49.

(137) Finkelshtein D, Werman A, Novick D, Barak S, Rubinstein M. LDL receptor and its family members serve as the cellular receptors for vesicular stomatitis virus. Proc Natl Acad Sci U S A 2013 Apr 30;110(18):7306-7311.

(138) Zack JA, Arrigo SJ, Weitsman SR, Go AS, Haislip A, Chen IS. HIV-1 entry into quiescent primary lymphocytes: molecular analysis reveals a labile, latent viral structure. Cell 1990 Apr 20;61(2):213-222.

(139) Sloan RD, Wainberg MA. The role of unintegrated DNA in HIV infection. Retrovirology 2011 Jul 1;8:52-4690-8-52.

(140) Thielen BK, McNevin JP, McElrath MJ, Hunt BV, Klein KC, Lingappa JR. Innate immune signaling induces high levels of TC-specific deaminase activity in primary monocyte-derived cells through expression of APOBEC3A isoforms. J Biol Chem 2010 Sep 3;285(36):27753-27766.

(141) Taya K, Nakayama EE, Shioda T. Moderate restriction of macrophage-tropic human immunodeficiency virus type 1 by SAMHD1 in monocyte-derived macrophages. PLoS One 2014 Mar 5;9(3):e90969.

(142) Dragin L, Nguyen LA, Lahouassa H, Sourisce A, Kim B, Ramirez BC, et al. Interferon block to HIV-1 transduction in macrophages despite SAMHD1 degradation and high deoxynucleoside triphosphates supply. Retrovirology 2013 Mar 11;10:30-4690-10-30.

(143) Goujon C, Schaller T, Galao RP, Amie SM, Kim B, Olivieri K, et al. Evidence for IFNalpha-induced, SAMHD1-independent inhibitors of early HIV-1 infection. Retrovirology 2013 Feb 25;10:23-4690-10-23.

(144) Tasker C, Ding J, Schmolke M, Rivera-Medina A, Garcia-Sastre A, Chang TL. 17beta-estradiol protects primary macrophages against HIV infection through induction of interferon-alpha. Viral Immunol 2014 May;27(4):140-150.

(145) Stopak KS, Chiu YL, Kropp J, Grant RM, Greene WC. Distinct patterns of cytokine regulation of APOBEC3G expression and activity in primary lymphocytes, macrophages, and dendritic cells. J Biol Chem 2007 Feb 9;282(6):3539-3546.

(146) Chen H, Wang LW, Huang YQ, Gong ZJ. Interferon-alpha induces high expression of APOBEC3G and STAT-1 in vitro and in vivo. Int J Mol Sci 2010 Sep 20;11(9):3501-3512.

(147) Sarkis PT, Ying S, Xu R, Yu XF. STAT1-independent cell type-specific regulation of antiviral APOBEC3G by IFN-alpha. J Immunol 2006 Oct 1;177(7):4530-4540.

(148) Mehta HV, Jones PH, Weiss JP, Okeoma CM. IFN-alpha and lipopolysaccharide upregulate APOBEC3 mRNA through different signaling pathways. J Immunol 2012 Oct 15;189(8):4088-4103.

(149) Sauter D, Kirchhoff F. IFITMs: Important Factors In Trans-Mission of HIV-1. Cell Host Microbe 2016 Oct 12;20(4):407-408.

(150) Morales DJ, Lenschow DJ. The antiviral activities of ISG15. J Mol Biol 2013 Dec 13;425(24):4995-5008.

(151) Ranganath N, Sandstrom TS, Fadel S, Cote SC, Angel JB. Type I interferon responses are impaired in latently HIV infected cells. Retrovirology 2016 Sep 9;13(1):66-016-0302-9.

(152) Zaritsky LA, Gama L, Clements JE. Canonical type I IFN signaling in simian immunodeficiency virus-infected macrophages is disrupted by astrocyte-secreted CCL2. J Immunol 2012 Apr 15;188(8):3876-3885.

(153) Vazquez-Perez JA, Ormsby CE, Hernandez-Juan R, Torres KJ, Reyes-Teran G. APOBEC3G mRNA expression in exposed seronegative and early stage HIV infected individuals decreases with removal of exposure and with disease progression. Retrovirology 2009 Mar 2;6:23-4690-6-23.

(154) Kourteva Y, De Pasquale M, Allos T, McMunn C, D'Aquila RT. APOBEC3G expression and hypermutation are inversely associated with human immunodeficiency virus type 1 (HIV-1) burden in vivo. Virology 2012 Aug 15;430(1):1-9.

(155) Jin X, Brooks A, Chen H, Bennett R, Reichman R, Smith H. APOBEC3G/CEM15 (hA3G) mRNA levels associate inversely with human immunodeficiency virus viremia. J Virol 2005 Sep;79(17):11513-11516.

(156) Ulenga NK, Sarr AD, Hamel D, Sankale JL, Mboup S, Kanki PJ. The level of APOBEC3G (hA3G)-related G-to-A mutations does not correlate with viral load in HIV type 1-infected individuals. AIDS Res Hum Retroviruses 2008 Oct;24(10):1285-1290.

(157) Biasin M, Piacentini L, Lo Caputo S, Kanari Y, Magri G, Trabattoni D, et al. Apolipoprotein B mRNA-editing enzyme, catalytic polypeptide-like 3G: a possible role in the resistance to HIV of HIV-exposed seronegative individuals. J Infect Dis 2007 Apr 1;195(7):960-964.

(158) Reddy K, Winkler CA, Werner L, Mlisana K, Abdool Karim SS, Ndung'u T, et al. APOBEC3G expression is dysregulated in primary HIV-1 infection and polymorphic

variants influence CD4+ T-cell counts and plasma viral load. AIDS 2010 Jan 16;24(2):195-204.

(159) Cho SJ, Drechsler H, Burke RC, Arens MQ, Powderly W, Davidson NO. APOBEC3F and APOBEC3G mRNA levels do not correlate with human immunodeficiency virus type 1 plasma viremia or CD4+ T-cell count. J Virol 2006 Feb;80(4):2069-2072.

(160) Katsounas A, Frank AC, Lempicki RA, Polis MA, Asmuth DM, Kottilil S. Differential Specificity of Interferon-alpha Inducible Gene Expression in Association with Human Immunodeficiency Virus and Hepatitis C Virus Levels and Declines in vivo. J AIDS Clin Res 2015;6(1):1000410.

Ringraziamenti

Vorrei ringraziare il mio corso di dottorato, in particolare il Prof. Stefano D'Amelio per la sua disponibilità e la Prof.ssa Miriam Licthner per aver preso visione di questa tesi e i suoi consigli.

In modo particolare ringrazio la Dott.ssa Laura Fantuzzi per avermi seguito in questo percorso e per il suo prezioso aiuto nella scrittura di questa tesi. In questi anni con la sua disponibilità, i suoi consigli e la sua pazienza è stata più di una Tutor, è stata semplicemente "Laura". La ringrazio per aver creduto in me e per avermi aiutato ad affrontare cose per me impensabili prima d'ora, come scrivere un abstract o parlare ad un congresso.

Ringrazio la Dott.ssa Cristina Purificato per i suoi consigli, il suo aiuto nella parte sperimentale e per essere stata la mia piccola maestra. Ringrazio la Dott.ssa Laura Catapano per la sua disponibilità, il suo aiuto e per avermi fatto capire cose che non sapevo nemmeno io di sapere. Ringrazio la Dott.ssa Cristina Gauzzi per i suoi consigli nella stesura di questa tesi e per essere sempre pronta ad ascoltare le mie domande. Ringrazio la Dott.ssa Michela Sabbatucci per il suo aiuto nella parte sperimentale e il suo contributo nella realizzazione di questo studio.

Ringrazio il Dott. Mauro Andreotti, la Dott.ssa Alessandra Mallano e la Dott.ssa Tina Galluzzo per la loro collaborazione nella parte relativa alla quantizzazione del DNA virale e nello studio ex vivo sui campioni dei pazienti.

Ringrazio il Dott. Maurizio Federico per il suo contributo nella preparazione dei virus (VSV-G)-HIV-1 e delle VLPs, e i Dott. Roberta Bona e Andrea Cara per la loro collaborazione nella preparazione dei LV/Vpx.

Ringrazio i Dott. Matteo Pellegrini, Jing liu e Arturo Rinaldi per la loro collaborazione per gli studi di RNAseq e per l'analisi bioinformatica dei dati.

Ringrazio il Dott. Stefano Vella per aver contribuito a stabilire un contatto con la Tobira Therapeutics. Ringrazio la Tobira Therapeutics per la loro collaborazione e per averci fornito i campioni di pazienti arruolati nello Studio 202.

Ringrazio la Dott.ssa Sandra Gessani per avermi gentilmente accolto nel suo laboratorio di Immunoregolazione e tutte le persone del reparto che ho avuto modo di conoscere per essersi mostrate sempre disponibili.

Ringrazio le colleghe che nel frattempo sono diventate le "Amiche di Lab" per allietare le giornate con scambi quotidiani di consigli, battute e risate.

Un ringraziamento speciale va alla mia famiglia, ai miei genitori e mio fratello, per esserci sempre, perché è proprio vero che nei momenti di difficoltà si capiscono le cose importanti, quelle vere.

Ringrazio Matteo e la sua famiglia, per il loro sostegno e per farmi sentire a casa pur essendo lontano dalla mia.

Ringrazio le mie amiche, quelle di sempre, che con un messaggio, una video-chiamata, da Morra, Roma, Milano, Torino non fanno mai mancare la loro presenza.